ABSTRACT

Title of Document: INVESTIGATING TWO-DIMENSIONAL BEHAVIOR OF ANTIOXIDANT ADDITIVES AND MIGRATION FROM FOOD CONTACT POLYMERS

Wendy Marie Heiserman, Doctor of Philosophy, 2008

Directed By: Professor Robert A. Walker
Department of Chemistry and Biochemistry

Research described in this thesis examines the surface and bulk behavior of analytes in food contact polymers. Irganox 1076 (IN1076) and Irganox 1010 (IN1010), phenol containing species often used as antioxidant additives in food packaging polymers, have both hydrophilic and hydrophobic functional groups. Consequently these additives are likely to absorb to surfaces where their free energy is minimized. Surface pressure isotherms show that repeated compression of films formed from IN1076 and IN10101 at the air/water interfaces leads to continued irreversible loss of molecules and that on a per molecule basis, this loss is more pronounced for IN1076 than for IN1010. Differences in the surface properties of these two antioxidant additives are interpreted based on differences in molecular structure. Surface specific vibrational measurements of these organic films show very little conformational order, implying that even when closely packed, both antioxidant species have little affinity for forming highly organized domains.

A second study examined the temperature dependent permeation of different dichloroethylene (DCE) isomers through commercially available low density polyethylene (LDPE). Initial experiments measured migration rates of DCE isomers from neat liquids through the LDPE film into Miglyol. The isomers consisted of 1,1-dichloroethylene (1,1-DCE), cis-1,2-dichloroethylene (c1,2-DCE) and trans-1,2-dichloroethylene (t1,2-DCE). Despite having equivalent masses, the three isomers migrated through LDPE with rates that varied by up to a factor of three. Migration data were used to calculate permeation coefficients. Permeation coefficients did not correlate with calculated molecular sizes. The temperature dependence of the permeation coefficients was used to calculate effective permeation activation energies. Subsequent experiments examined DCE migration through LDPE from dilute solutions (1% v/v) of c1,2-DCE and t1,2-DCE isomers in Miglyol. The permeation rates slowed at lower concentrations with the permeation coefficient of c1,2-DCE decreasing by an order of magnitude. The permeation activation energy increased, by factors of ~3, for both isomers.

INVESTIGATING TWO-DIMENSIONAL BEHAVIOR OF ANITOXIDANT ADDITIVES AND MIGRATION THROUGH FOOD CONTACT POLYMERS

By

Wendy Marie Heiserman

Dissertation submitted to the Faculty of the Graduate School of the
University of Maryland, College Park, in partial fulfillment
of the requirements for the degree of
Doctor of Philosophy
2008

Advisory Committee:
Professor Robert A. Walker, Chair
Professor Neil Blough
Professor Robert M. Briber
Professor Amy Mullin
Professor Andrei Vedernikov

Dedicated in loving memory of my pop-pop, Leo Joseph Ebner, the single greatest man I've ever met.

Acknowledgements

I would first like to thank the person who is responsible for both the beginning and end of my journey as a graduate student, Dr. Robert Walker. Through his patience and guidance, I have become the scientist that I am today. I appreciate the support and guidance that I received throughout my research career, as well as granting me the ability to pursue teaching as a career possibility.

I would like to thank the members of my committee, Drs Neil Blough, Robert Briber, Doug English, Amy Mullin, and Andrei Vedernikov, for their support.

During my graduate tenure, I have interacted with many graduate students. My group members both past and present have been the source of stimulating scientific conversations, as well as comforting advice. I'd like to thank Drs. Bill Steel, Okan Esenturk, Carmen Huffman, Mike Pomfret and Süleyman Can, for their encouragement and motivation. Current graduate students, Mike Brindza, Debjani Roy, Bryan Eigenbrodt, and Charles Murphy for providing intellectual discussions. A special thanks to Tony Dylla for help with TGA measurements, Renee Siler for her willingness to read endless drafts of my thesis chapters and for making long endless days in the lab more tolerable. I'd like to add a second thanks to Dr. Süleyman Can for help with VSFS measurements. I'd also like to thank former graduate students Drs. Amy Grimes and Amy Finch, for their support and inspiration through the thesis writing process.

I owe many thanks to people from the FDA for guidance and research expertise, particularly Tim Begley, Dr. William Limm, and Dr. Kim Morehouse. Without your help, the majority of this thesis would not be possible.

Finally I'd like to thank Nick Young, for providing support through a stressful time and always believing in me.

Most importantly, I'd like to thank my extremely supportive family. I have grown to admire my mother, sister and nana as strong women in their own ways, and I aspire to have some of these qualities. I wouldn't be here today if it weren't for my family's endless support and unfailing belief in me. They've never set limits and always allowed me to grow.

Table of Contents

List of Tables

List of Figures

List of Abbreviations

Π	surface pressure
$\chi^{(2)}$	second order susceptibility tensor
$\chi^{(2)}_{NR}$	non resonant contribution to $\chi^{(2)}$
$\chi^{(2)}_{R}$	resonant contribution to $\chi^{(2)}$
G_{part}	free energy of partitioning
H_{vap}	enthalpy of vaporization
ω_{ir}	infrared frequency
ω_{sf}	sum frequency
ω_{vis}	visible frequency
A	interfacial area
A	molecular area
A_{cs}	cross sectional area of exposed film
BHT	2,6-bis(1,1-dimethylethyl)-4-methylphenol
BPA	bisphenol-A
BPF	bisphenol-F
C	subsurface concentration
c1,2-DCE	cis-1,2-dichloroethylene
C^{bulk}	bulk concentration outside of a film
C^{s}	isothermal compressibility
D	diffusion coefficient
d^{-}	methylene asymmetric stretch
d^{+}	methylene symmetric stretch
D_0	preexponential factor
DCE	dichloroethylene
E_D	diffusion activation energy
E_P	permeation activation energy
EPA	United States Environmental Protection Agency
F	flux

FT	Fourier transform
GC	gas chromatography
GC-MSD	gas chromatography with mass spectrometry detection
HPLC	high performance liquid chromatography
HS	headspace
IF168	Irgafos 168
I_{ir}	intensity of infrared light
IN1010	Irganox 1010
IN1076	Irganox 1076
I_{sf}	intensity of sum frequency light
I_{vis}	intensity of visible light
k_B	Boltzmann's constant
K^s	inverse of isothermal compressibility
L	lag time
l	thickness of the polymer film
LDPE	low-density polyethylene
MSD	mass spectrometry detection
N	number of molecules
n	number of sheets
Nd:YAG	neodymium-yttrium-aluminum garnet
p	external vapor pressure
P	permeation coefficient
$P^{(2)}$	surface nonlinear polarization
P_0	preexponential factor
PCB	polychlorinated biphenols
PFOA	ammonium perfluorooctonate
P_{ir}	P polarized infrared light
PTFE	polytetrafluroethylene
Q_t	time dependent amount migrated
r^-	methyl asymmetric stretch
r	radius

R	universal gas constant
r^+	methyl symmetric stretch
S	solubility constant
SF	sum frequency
SFG	sum frequency generated
S_{sf}	S polarized sum frequency signal
S_{vis}	S polarized visible light
T	temperature
t	time
t1,2-DCE	trans-1,2-dichloroethylene
TGA	thermogravimetric analysis
VdWr	van der Waals radius
VSFS	vibrational sum frequency spectroscopy

Chapter 1 Introduction

Nearly every American uses food contact polymers in one form or another during daily life. They will drink from plastic bottles or a Nalgene thermos. Lunch is packed in Tupperware or wrapped in plastic wrap. A takeout meal is served in a plastic bowl with a plastic drinking cup. Our exposure to plastics has increased dramatically over the years, and in turn, more than 30% of all plastic used in the U.S. now gets recycled.[1] Some of these recycled products initially were food contact polymers that were recycled back into food contact polymers. Other recycled plastics first served to package non-consumable products. The widespread use of new and recycled plastics, especially plastic packaging, raises concerns regarding the migration of additives and contaminants from plastics into the materials they surround. Increased use of plastics has led to high profile reports regarding safety of the nation's food supply.[2-5] This thesis will discuss two main concerns salient to the subject of secondary substances in food contact polymers. The first section will examine the surface behavior of common antioxidant additives used to stabilize food contact polymers. The surface behaviors of antioxidant additives are measured at the air/water interface through the use of surface tension measurements and vibrational sum frequency spectroscopy (VSFS, a surface specific non-linear optics technique). The second section will explore questions related to pollutant migration through food contact polymers. These later studies probe the role played by molecular structure (rather than simply molecular mass) in controlling migration rates. Migration rates are measured using both Raman spectroscopy as well as headspace gas chromatography with mass spectrometry detection (GC-MSD). Migration through

polymer films appears to be governed primarily by analyte solubility in the polymer film and molecular size.

All polymers used for food packaging contain a wide variety of additives. Some additives absorb UV light. Other additives act as antimicrobial agents. A third type of additive is intended to prevent polymer oxidation and degradation.[6] Antioxidant additives fall into different families based on shared structural motifs. The functional groups on the additives generally determine their purpose in the polymer, as well as the antioxidant mechanisms used by the additives to preserve the polymer. Phenolic antioxidants can be identified based on their sterically hindered phenol groups. Irganox 1010, and BHT (2,6-bis(1,1-dimethylethyl)-4-methylphenol) are some sterically hindered phenols, that hinder oxidation by acting as hydrogen donors.[7] Phenols are the most commonly used antioxidant additives, as shown in Table 1.1. Phosphites, such as Irgafos 168, are another type of antioxidant additive that act as hydroperoxide decomposers.[8, 9] Phenols and phosphites are usually combined as processing stabilizers.[10] Together, the phenols and phosphites increase the stability of polymers against oxidation during the high heats and pressures required for processing polymers from resins into sheets or molds. Structures of the above mentioned antioxidant additives are shown in Figure 1.1.

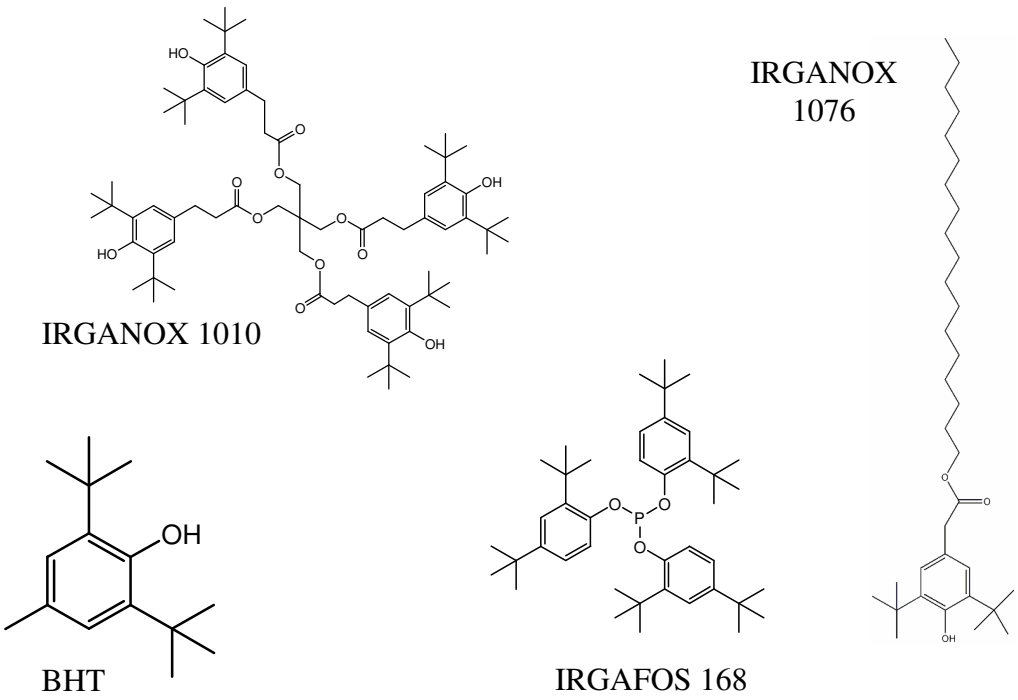

Figure 1.1. Structures of some common antioxidant additives.

Antioxidant additives are essential components for the plastics industry. As shown in Table 1.1, The United States is one of the primary consumers of antioxidant additives. Typically antioxidant additives are used in combination. As many as three antioxidant additives can be used collectively in a given polymer, with additive concentrations of 0.05-1% by mass. This statistic means that the use of phenolic additives in 1997 stabilized ~100 million tons of polymer world wide, and ~30 million tons of polymer just in the United States alone. Once in polymers, antioxidant additives can do one of three things. If the additives remain in the polymer, they can perform their designated function. However, if additives are mobile, they can accumulate at the polymer interface or partition into the food. Additives that remain at the packaging food interface can be investigated through surface specific techniques at the air/water interface. The air/water interface serves as a mimic for many interfaces of polar/nonpolar boundaries such as polymer/alcohol or

polymer/water interfaces.[11-14] Due to the widespread use of additives in polymers, migration of additives from food contact materials into foodstuffs has become an active area of research over the past years.[15-25]

antioxidant additive type	North America	Europe	Asia/ Pacific	Global total
phenolic	31.4	30.0	36.0	116.4
organo-phosphites	19.1	15.0	21.4	63.5
thioesters	5.9	5.0	6.4	19.3
others	1.1	4.0	0.2	7.3
total	57.5	54.0	64.0	206.5

Table 1.1. Global consumption of antioxidant additives (in 1000 tons) in 1997[6]

The majority of research into the behavior of antioxidant additives has focused on the loss of antioxidant additives from food contact polymers into food simulants, as determined by extraction methods, diffusion, and/or partitioning coefficients.[16, 18, 26-28] Some groups have acknowledged the ability of the solvent in contact with the polymer to affect migration, with more polar molecules exhibiting higher migration in polar solvents like water.[18, 27] Many large antioxidants exhibit little migration, due to their large masses and poor flexibility and low mobility. Although these migration and partitioning experiments determine the amount of antioxidant loss from a food contact polymer, they neglect analyte surface activity and adsorption to the interface as another pathway that can deplete antioxidant in the

bulk population. High surface activity of antioxidant additives could lead to enhanced population at polymer/aqueous interfaces. Such surface excess, in turn, could drive aggregation and "surface blooming," a term used to describe the precipitation of additives in the polymer bulk or at the polymer surface.[28, 29] These gradients would lead to non uniform diffusion, resulting in unpredictable losses of additive from the polymer.

Chapter three of this thesis focuses on the surface activity of two antioxidant additives, Irganox 1010 (IN1010), and Irganox 1076 (IN1076). Since IN1010 and IN1076 have both hydrophilic and hydrophobic functional groups, these additives are likely to adsorb to surfaces where their free energy is minimized. These interfaces can include a packaging/aqueous food interface. Consequences of surface activity could lead to reduced antioxidant activity in the polymer itself.

The two-dimensional phase behaviors of IN1076 and IN1010 films adsorbed to the air/water interface are studied using surface tensiometry and surface specific VSFS. A noticeable feature of these two additives adsorbed to the air/water interface is the continued irreversible loss of molecules from the film when the film is repeatedly compressed and expanded. Comparing the loss of molecules from IN1010 films and IN1076 films on a per molecule basis shows a more pronounced loss for IN1076. However, if this loss is scaled according to the number of hydroxyl groups on the molecules (four for IN1010, one for IN1076) then this functional group loss is equivalent within the limits of experimental uncertainty. To get a clearer idea of the interactions and possible molecular orientation at the air/water interface of the IN1010 and IN1076 films, VSFS spectra were acquired. Polarization dependent

spectra show very little conformational order, for both loose and closely packed monolayers, implying little affinity for the formation of highly organized domains.

Additive migration is another area of concern in the food packaging industry. These same concerns also apply to the transport of external contaminants through food packaging into the food. The study of external contaminant permeability has typically been limited to applications of protective clothing, or chemical waste containers.[30-32] Saleem, et al. investigated the diffusion of xylene isomers through low-density polyethylene (LDPE), with diffusion coefficients of similar values for the isomers, with the largest difference in coefficients being ~20%.[33] This difference in isomer migration is much lower than the results discussed in Chapter 4, which can be as large as 100% at some temperatures for molecules that have essentially the same size. This thesis intends to expand the investigation of the effects of molecular structure on migration. The migration barrier in our studies will not be chemical protective clothing or waste container. Rather, experiments discussed in this thesis examine the migration of different isomers through the commonly used food contact polymer LDPE. Exposure estimates of toxins migrating out of food contact polymers are determined typically by using empirical models.[10, 34-36] The only property of the migrant considered in these models is the molecular weight –structure is largely ignored. The aim of the migration studies is to explore the differences molecular structure can have on migration and that models predicting migration solely based on molecular weights may need to be amended.

Chapters 4 and 5 discuss the migration of dichloroethylene (DCE) isomers through commercially available (LDPE) into a common fatty food simulant,

Miglyol.[37-43] It is noted here that both Chapters (4 and 5) are being submitted for publication so some repetition may exist. Miglyol 812 is a fatty acid triglyceride that is composed of capric and caprilic acids. The relative solubilities of the DCE isomers in LDPE are discussed in Chapter 2, with cis-1,2-dichloroethylene (c1,2-DCE) being the most soluble in LDPE. Since these molecules are commonly used as refrigerants, exposure of food contact packaging to these solutions is possible in the event of chemical spills or leaks. All three isomers have exposure estimates that are regulated by the EPA. Possible side effects of exposure range from minor skin irritation and seizures to neurological damage and cancer.[44, 45]

Migration of neat DCE liquids through LDPE into Miglyol is investigated in Chapter 4. The migration of DCE through LDPE is quantified through permeation. Permeation is a function of both diffusion - how fast an analyte travels through a film - and solubility, how soluble an analyte is in a film. At a single temperature, the permeation of the three isomers is markedly different. Differences in DCE permeation rates do not scale with the molecular volume or molecular cross section for a given isomer. Differences in permeation of DCE isomers persisted over a range of temperatures. An Arrhenius analysis of the temperature dependent permeation data imply that differences in solubility are responsible for the different transport rates. Collectively, results from these studies show that molecular structure plays a significant role in analyte transport through food contact polymers. The results from these permeation studies should be considered in the development of more accurate migration models to include considerations of migrant properties beyond molecular mass.[10, 34-36]

Dilute DCE (1% DCE in Miglyol by volume) investigates how transport properties change as a function of migrant concentration. Chapter 5 discusses the dilute transport of c1,2-DCE and trans-1,2-dichloroethylene (t1,2-DCE) in 1% by volume solutions in Miglyol migrating through LDPE into clean Miglyol. The goal of Chapter 5 is to determine if the migration properties of neat c1,2-DCE compared to neat t1,2-DCE persist at low concentrations when the solubility effects are no longer emphasized. At a single temperature, t1,2-DCE permeates ~3 times faster than c1,2-DCE. Compared to the neat migration results, migration rates decreased at lower concentration values. Typically migration decreases with decreasing concentration.[46] Temperature dependent permeation studies allowed for an Arrhenius treatment to determine a permeation activation energy for dilute migration. These values were higher than those observed for the neat permeation studies discussed in Chapter 4.

References

1. Municipal Solid Waste (MSW): Recycling. (July 14, 2008),

2. Eilperin, J., Compound in Teflon A 'Likely Carcinogen'. *The Washington Post. Washington, D.C.* Jun 29, 2005, 2005, p A.04.

3. Grossman, E., Chemicals May Play Role in Rise in Obesity. *The Washington Post* March 12, 2007, 2007, p A06.

4. Eliperin, J., Harmful Teflon Chemical To Be Eliminated by 2015. *Washington Post* January 26, 2006, p A01.

5. Mishori, R., The Plastics Revolution: It Changed Our World. But Are We Trading Convenience for Safety? *The Wahsington Post* April 22, 2008, 2008, p HE01.

6. Zweifel, H., *Plastics Additives Handbook*. 5th ed.; Hanser: Cincinnati, 2001.

7. Zweifel, H. In *Polymer Durability*, American Chemical Society, Washington, 1996; R. L. Clough, K. T. G., N. C. Billingham, Ed. Washington, 1996.

8. Schwetlick, K., *Pure and Applied Chemistry* **1983,** 55, 1634.

9. Schwetlick, K.; Konig, T.; Ruger, C.; Pointeck, J.; Habicher, W. D., *Polymer Degradation and Stability* **1986,** 55, (97).

10. *Plastic Packaging Materials for Food: Barrier Function, Mass Transport, Quality Assurance and Legislation*. Wiley-VCH: New York, 2000.

11. Mao, G.; Desai, J.; Flach, C. R.; Mendelsohn, R., Structural characterization of the monolayer-multilayer transition in a pulmonary surfactant model: IR studies of films transferred at continuously varying surface pressures. *Langmuir* **2008,** 24, (5), 2025-2034.

12. Sakai, K.; Umezawa, S.; Tamura, M.; Takamatsu, Y.; Tsuchiya, K.; Torigoe, K.; Ohkubo, T.; Yoshimura, T.; Esumi, K.; sakai, H.; Abe, M., Adsorption and micellization behavior of novel gluconamide-type gemini surfactants. *Journal of Colloid and Interface Science* **2008,** 318, 440-448.

13. Kosaka, O.; Iida, S.; Sehgal, P.; Doe, H., Solubilization of endocrine disruptors in micellar media. *Colloid Polymer Science* **2008,** 286, 545-551.

14. Kosaka, O.; Sehgal, P.; Doe, H., Behavior of cationic surfactants micellar solution solubilizing an endocrine disruptor bisphenol A. *Food Hydrocolloids* **2008,** 22, (1), 144-149.

15. Bradley, E. L.; Read, W. A.; Castle, L., Investigation into the migration potential of coating materials from cookware products. *Food Additives and Contaminants* **2007,** 24, (3), 326-335.

16. Bradley, E. L.; Speck, D. R.; Read, W. A.; Castle, L., Method of test and survey of caprolactam migration into foods packaged in nylon-6. *Food Additives and Contaminants* **2004,** 21, (12), 1179-1185.

17. Choi, J. O.; Jitsunari, F.; Asakawa, F.; Lee, D. S., Migration of styrene monomer, dimers and trimers from polystyrene to food simulants. *Food Additives and Contaminants* **2005,** 22, (7), 693-699.

18. Garde, J. A.; Catala, R.; Gavara, R.; Hernandez, R. J., Characterizing the migration of antioxidants from polypropylene into fatty food simulants. *Food Additives and Contaminants* **2001,** 18, (8), 750-762.

19. Limm, W.; Begley, T. H.; Lickly, T.; Hentges, S. G., Diffusion of limonene in polyethylene. *Food Additives and Contaminants* **2006,** 23, (7), 738-746.

20. O'Brien, A.; Cooper, I., Polymer additive migration to foods -- a direct comparison of experimental data and values calculated from migration models for polypropylene. *Food Additives and Contaminants* **2001,** 18, (4), 343-355.

21. Begley, T., Biles, J., Cunningham, C., Pringer, O. , Migration of a UV stabilizer from polyethylene terephthalate (PET) into food simulants. *Food Additives and Contaminants* **2004,** 21, 1007-1014.

22. Dopico-Garcia, M. S., Lopez-Vilarino, J. M., Gonzalez-Rodriguez, M. V. , Effect of temperature and type of food simulant on antioxidant stability. *Journal of Applied Polymer Science* **2006,** 100, 656-663.

23. Helmroth, I. E., Dekker, M., Hankemeier, T., Additive Diffusion from LDPE Slabs into Contacting Solvents as a Function of Solvent Absorption. *Journal of Applied Polymer Science* **2003,** 90, 1609-1617.

24. Limm, W., Hollifield. H. C. , Effects of temperature and mixing on polymer adjuvant migration to corn oil and water. *Food Additives and Contaminants* **1995,** 12, 609-624.

25. Vitrac, O., Mougharbel, A., Feigenbaum, A. , Interfacial mass transport properties which control the migration of packaging constituents into foodstuffs. *Journal of Food Engineering* **2007, 79**, (3), 1048-1064.

26. O'Brien, A.; Cooper, I., Polymer additive migration into foods -- a direct comparison of experimental data and values calculated from migration models for polypropylene. *Food Additives and Contaminants* **2001,** 18, (4), 343-355.

27. Lundback, M.; Hedenqvist, M. S.; Mattozzi, A.; Geede, U. W., Migration of phenolic antioxidants from linear and branched polyethylene. *Polymer Degradation and Stability* **2006,** 91, 1571-1580.

28. Rawls, A. S.; Hirt, D. E.; Havens, M. R.; Roberts, W. P., Evaluation of surface concentration of erucamide in LLDPE films. *Journal of Vinyl and Additive Technology* **2002,** 8, 130-138.

29. Spatafore, R.; Pearson, L. T., *Polymer Engineering and Science* **1991,** 31, 1610-1617.

30. Schwope, A. D.; Goydan, R.; Reid, R. C.; Krishnamurthy, S., Sate-of-the-Art Review of Permeation Testing and the Interpretation of Its Results. *American Industrial Hygiene Association Journal* **1988,** 49, (11), 557-565.

31. O'Callaghan, K.; Fredericks, P. M.; Bromwich, D., Evaulation of Chemical Protective Clothing by FT-IR/ATR Spectroscopy. *Applied Spectroscopy* **2001,** 55, (5), 555-562.

32. Britton, L. N.; Ashman, R. B.; Aminabhavi, T. M.; Cassidy, P. E., Permeation and Diffusion of Enviornmental Pollutants through Flexible Polymers. *Journal of Applied Polymer Science* **1989,** 38, 227-236.

33. Saleem, M.; Asfour, A.-F. A.; Kee, D. D., Diffusion of Organic Penetrants through Low Density Polyethylene (LDPE) Films: Effect of Size and Shape of the Penetrant Molecules. *Journal of Applied Polymer Science* **1989,** 37, 617-625.

34. Begley, T. H.; Castle, L.; Feigenbaum, A.; Franz, R.; Hinrichs, K.; Lickley, T.; Mercea, P.; Milana, M.; O'Brien, A.; Rebre, S.; Rijk, R.; Piringer, O., Evaluation of migration models that might be used in support of regulations for food-contact plastics. *Food Additives and Contaminants* **2005,** 22, (1), 73-90.

35. Brandsch, J.; Mercea, P.; Ruter, M.; Tosa, V.; Piringer, O., Migration modeling as a tool for quality assurance of food packaging. *Food Additives and Contaminants* **2002,** 19, (Supplement), 29-41.

36. Stoffers, N. H.; Brandsch, R.; Bradley, E. L.; Cooper, I.; Dekker, M.; Stormer, A.; Franz, R., Feasibility study for the development of certified reference materials for specific migration testing: Part 2: Estimation of diffusion parameters and

comparison of experimental and predicted data. *Food Additives and Contaminants* **2005,** 22, (2), 173-184.

37. Begley, T. H.; Hsu, W.; Noonan, G.; Diachenko, G., Migration of fluorochemical paper additives from food-contact paper into foods and food simulants. *Food Additives and Contaminants* **2007,** 25, (3), 384-392.

38. Begley, T. H.; White, K.; Honigfort, P.; Twaroski, M. L.; Neches, R.; Walker, R. A., Perfluorochemicals: Potential sources of and migration from food packaging. *Food Additives and Contaminants* **2005,** 22, (10), 1023-1031.

39. Begley, T. H.; Gay, M. L.; Hollifield, H. C., Determination of the migrants in and migration from nylon food packaging. *Food Additives and Contaminants* **1995,** 12, 671-676.

40. Biles, J. E.; McNeal, T. P.; Begley, T. H.; Hollifield, H. C., Determination of bisphenol A in reusable polycarbonate food-contact plastics and migration to food-simulating liquids. *Journal of Agricultural and Food Chemistry* **1997,** 45, 3541-3544.

41. Brede, C.; Fjeldal, P.; Skjevrak, I.; Herikstad, H., Increased migration levels of bisphenol A from polycarbonate baby bottles after dishwashing, boiling and brushing. *Food Additives and Contaminants* **2003,** 20, 684-689.

42. Franz, R.; Welle, F., Migration measurement and modeling from poly(ethylene terephthalate) (PET) into soft drinks and fruit juices in comparison with food simulants. *Food Additives and Contaminants* **2008,** 25, (8), 1033-1046.

43. Begley, T. H.; Biles, J. E.; Cunningham, C.; Piringer, O., Migration of a UV stabilizer from polyethylene terephthalate (PET) into food simulants. *Food Additives and Contaminants* **2004,** 21, 1007-1014.

44. Consumer Factsheet on: 1,2-dichloroethylene.

http://www.epa.gov/OGWDW/dwh/c-voc/12-dich2.html (Febuary 28th, 2008),

45. Consumer Factsheet on: 1,1-dichloroethylene.

http://www.epa.gov/safewater/dwh/c-voc/11-dichl.html (Febuary 28th, 2008),

46. Huang, J.-C.; Liu, H.; Liu, Y., Diffusion in Polymers with Concentration Dependent Diffusivity. *International Journal of Polymeric Material* **2001,** 49, 15-24.

Chapter 2 Experimental

2.1 Surface Tension Experiments

2.1.1 Materials

IN1076 and IN1010 (98.0%, and 99.4% purity, respectively) were obtained from Ciba Specialty Chemicals Corp. and used as received. Antioxidant additives were dissolved in a hexane (HPLC grade) spreading solvent. Typical spreading solvent concentrations were between 0.7 - 1.0 mg antioxidant additive/mL hexanes. IN1010 solutions were sonicated for 5 minutes to facilitate dissolution. The water used in these experiments came from an ultra-pure Millipore, Milli-Q filtration system (18 MΩ·cm) and had a measured surface tension of 72.6 0.6 mN/m. The pH of the subphase was ~5.5, meaning that the films themselves should have consisted of neutral monomers (assuming a phenol pK_a of ~10).[1] All measurements were carried out at room temperature (23 1°C).

2.1.2 Isotherm Studies

A standard Langmuir trough was used for the isotherm studies (300 cm^2, Nima Technology, 302LL) as shown in Figure 2.1. A paper Wilhelmy plate was left in contact with the water for 3 minutes (to allow the plate to be fully wetted) before the tension of the pure water was tested for cleanliness. No discernable difference was observed between isotherms acquired with a paper plate and those acquired with a platinum plate. The water surface was considered pure when the initial tension was 72.6 0.6 mN/m and the change in pressure ($\Delta\Pi$) was less than 0.5 mN/m for a complete surface compression (250 cm^2 to 20 cm^2 at a speed of 100 cm^2/min). In the

event that $\Delta\Pi$ was greater than 0.5 mN/m th,e water surface was aspirated before another isotherm was acquired. This procedure was repeated until the water surface was sufficiently clean. Following preparation of the clean water surface, monolayers were formed by depositing ~15 μL of a spreading solvent onto the clean water surface. After allowing the spreading solvent to evaporate (~10 min), monolayer compressions were carried out with constant barrier speeds reducing the trough area by 30 cm^2/min. The resolution of the isotherm varied with the speed of the compression, with resolution depending inversely on speed. Compression speeds of 20 cm^2/min and 30 cm^2/min showed no discernable differences in the resulting isotherms.

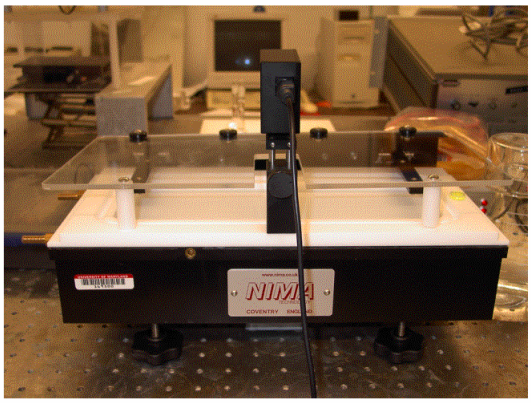

Figure 2.1. Langmuir trough used for dynamic surface tension measurements.

2.1.3 VSFS Measurements

The molecular structure of IN1076 and IN1010 monolayers at their equilibrium spreading pressures were compared based on surface specific, vibrational spectra acquired using broadband VSFS.[2,3] Experiments were carried out with assistance from Dr. Süleyman Can. Briefly, this technique requires that visible and infrared optical fields with respective frequencies of ω_{vis} and ω_{ir} be overlapped

temporally and spatially on the interface being studied. These two fields couple together through the second order susceptibility, $\chi^{(2)}$, to produce a new field (ω_{sf}) equal in energy to the sum of ω_{vis} and ω_{ir}. Because $\chi^{(2)}$ is a third rank tensor, its elements necessarily change sign upon inversion. Consequently, all elements of the $\chi^{(2)}$ tensor vanish in isotropic media. Only at surfaces where interfacial anisotropy breaks the center of symmetry found in bulk liquids can the $\chi^{(2)}$ tensor assume nonzero values.

The intensity of the sum frequency signal is proportional to the square of the surface nonlinear polarization, $P^{(2)}$ induced by the incident infrared and visible beams as shown in Equation 2.1.[4]

$$I_{sf} \propto \left|P^{(2)}\right|^2 \propto \left|\chi_{NR}^{(2)} + \sum_v \left|\chi_{R_v}^{(2)}\right| e^{i\gamma_v}\right|^2 I_{vis} I_{ir} \qquad (2.1)$$

where χ_{NR} and χ_R are the nonresonant and resonant terms of the second order susceptibility, γ_v is the relative phase of the v^{th} vibrational mode, I_{vis} and I_{ir} are the intensities of the incoming visible and infrared light, respectively, as shown in Figure 2.2. For the systems studied in this work, the nonresonant component of the $\chi^{(2)}$ tensor is quite small compared to the resonant contributions.

Details about the broad band sum frequency spectrometer used in these studies can be found in previous reports.[2,6] Spectra presented in this work result from S polarized VSF signal created by S polarized visible and P polarized IR. These $S_{sf}S_{vis}P_{ir}$ conditions sample vibrational modes having a net out-of-plane component of IR allowed vibrational transitions.

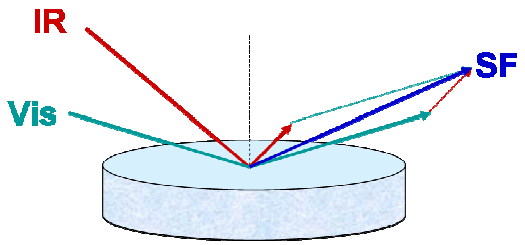

Figure 2.2. Illustration of incoming IR and visible frequencies, and the reflected sum frequency collected in an VSFG measurement.[5]

2.2 Permeation Experiments

2.2.1 Materials

1,1-dichloroethylene (99.90 % stabilized with 4-methoxyphenol) and cis-1,2-dichloroethylene (97 % stabilized with 4-methoxyphenol) were obtained from Acros Organics. 1,1-DCE was stored in a refrigerator kept between 0 and 4 °C. Cis-1,2-dichloroethylene (97 %) was also obtained from Aldrich Chemical Company. Trans-1,2-dichloroethylene (98 % stabilized with 4-methoxyphenol) was obtained from Aldrich Chemical Company and Alfa Aesar. The physical properties of the isomers are summarized in Table 2.1. Miglyol 812 was obtained from Sasol Germany (distributed by Warner Graham Company). Toluene (HPLC grade) was obtained from Fisher Scientific. All chemicals were used as received. Headspace vials (22 mL), with Teflon-faced silicon septa, and aluminum crimp seals were purchased from Shamrock Glass Co.

	1,1-DCE	t1,2-DCE	c1,2-DCE
bp (^{o}C)[7]	31.6	48.7	60.1
MW (g/mol)[7]	96.94	96.94	96.94
density (g/mL)[7]	1.213	1.2565	1.2837
(D)[8,9]	1.34	0	1.85
Viscosity[10] (cP)	0.358	0.444	0.317

Table 2.1. Properties of DCE isomers. Viscosities for c1,2-DCE and t1,2-DCE at 25 ^{o}C, for 1,1-DCE at 20 ^{o}C.

Diffusion cells (0.9 mm orifice diameter, 3.4 mL volume, Figure 2.3) were purchased from PermeGear, Inc (Hellertown, PA, USA). Cells were thermally regulated to within 0.3 ^{o}C with a water bath and both sides of a cell were stirred with H-series stir bars. The side-bi-side cells were cleaned for 25-60 minutes by sonication then placed in an acid bath (50 % Nitric Acid/ 50 % sulfuric acid) for >1 hour before use in experiments. Stirrers and Teflon caps were cleaned by sonicating for >20 minutes.

2.2.2 Assembly Procedures

The diffusion cells were prepared by assembling the cells with a piece of commercially available LDPE (76.2 m thick, 0.83 g/cm^3 density) between the cells with a Teflon gasket on each side of the LDPE, the cells were then connected to a temperature controlled water circulator and the appropriate amount of time passed until the cells came to temperature. After allowing the cells to reach the required temperature the right side of the cell was filled with Miglyol 812 the left side was filled with a known concentration of DCE. At specific times 0.1-0.05 mL aliquots of the Miglyol on the right side of the cells were withdrawn and replaced with pure

Miglyol — with the change in concentration accounted for in the data analysis. The aliquot (0.1 mL) for the cells with pure DCE on the left side was typically tested using Raman spectroscopy with the parameters described below. Aliquots (0.05 mL) for the cells with dilute (≤ 1% by volume) concentrations of DCE were tested using headspace GC-MSD, with the parameters described below.

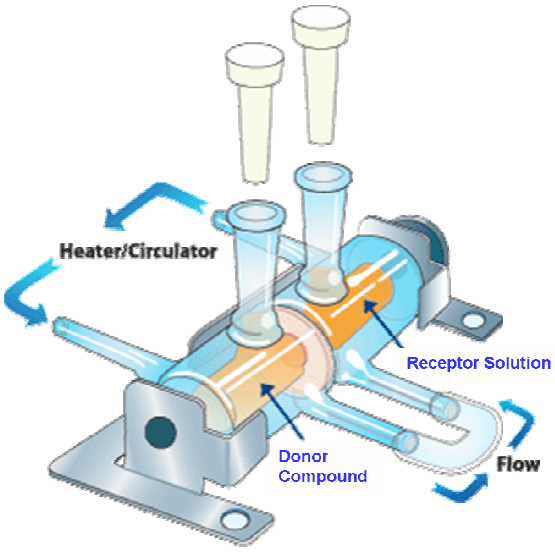

Figure 2.3. Diffusion cell set up (reproduced with permission from PermeGear, Inc.). In all experiments the receptor solution is Miglyol 812. Saturated experiments have pure DCE as the donor compound, dilute experiments have DCE in Miglyol 812 as donor compound.

2.2.3 Raman Spectroscopy

Aliquots were analyzed using a Nicolet FT-Raman spectrometer. Samples were excited using 1.336 W of 1064 nm light produced by a continuous wave Nd:YAG laser. Spectra resulted from 256 scans of the interferometer operating with a spectral resolution of 8 cm^{-1}. The absolute intensity of the Raman scattered signal depends on many experimental parameters, but with the same experimental conditions and an accurate calibration curve, concentrations can be measured to

within 1 % by volume, using the intensity of the DCE-CH symmetric stretch near 3075 cm^{-1}. This band was chosen because of its clear signal free of interference from Miglyol.

Concentrations of migrants were determined based on quantitative Raman vibrational spectra. Prior to performing a migration measurement, calibration plots were measured to correlate the vibrational intensity of the DCE-CH symmetric stretch with DCE concentration. These samples were created by serially diluting a stock solution of 50 % by volume DCE in Miglyol. A representative Raman spectrum and the resulting calibration plot are shown in Figure 2.4. As expected, vibrational intensity depended linearly on concentration. Typical R^2 agreement was ≥ 0.990. The reproducibility of individual experiments can be seen by comparing the data presented in Figure 2.5.

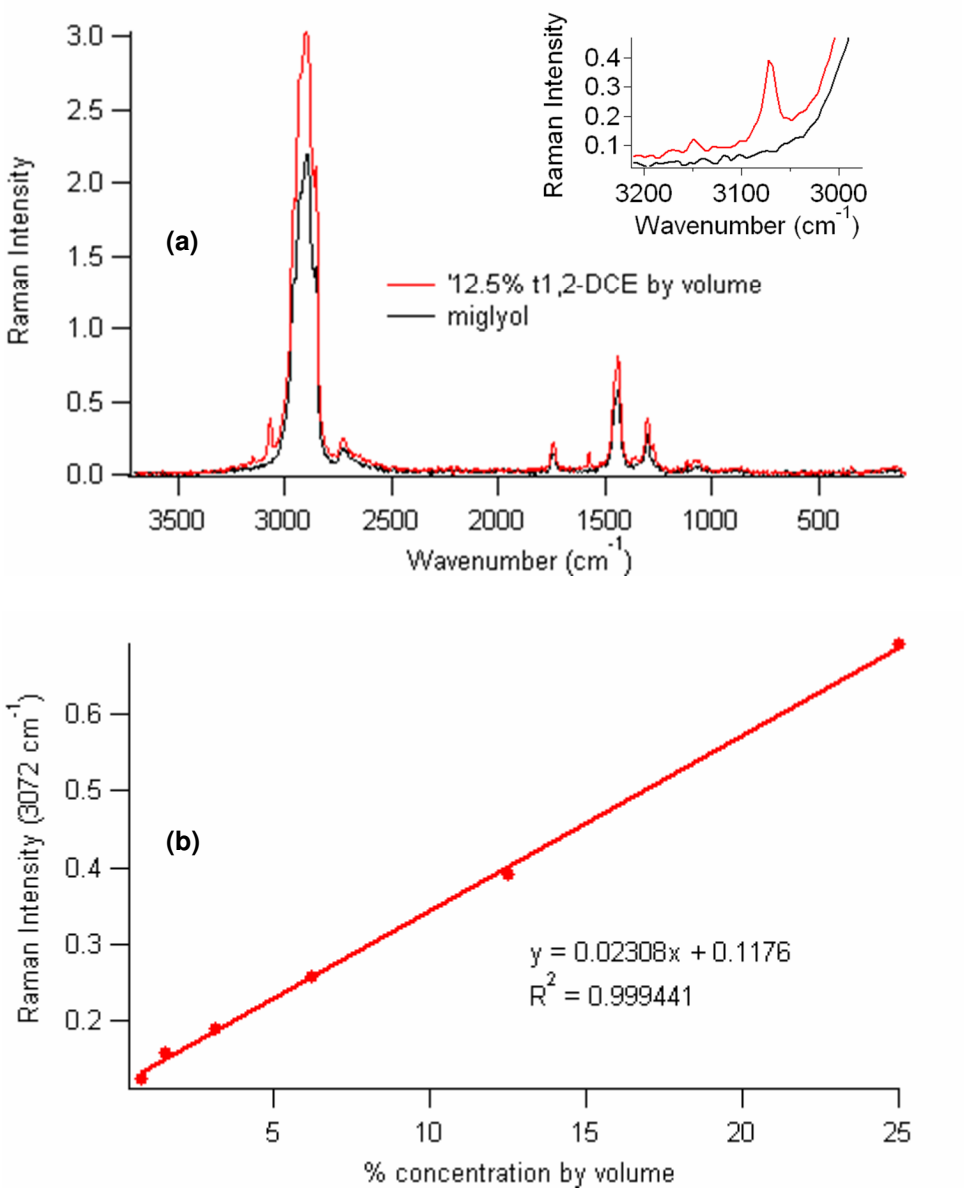

Figure 2.4. (a) t1,2-DCE and Miglyol Raman spectrum with an insert showing the peak used for calibration. (b) calibration of t1,2-DCE using the 3072 cm^{-1} DCE-CH symmetric stretch peak.

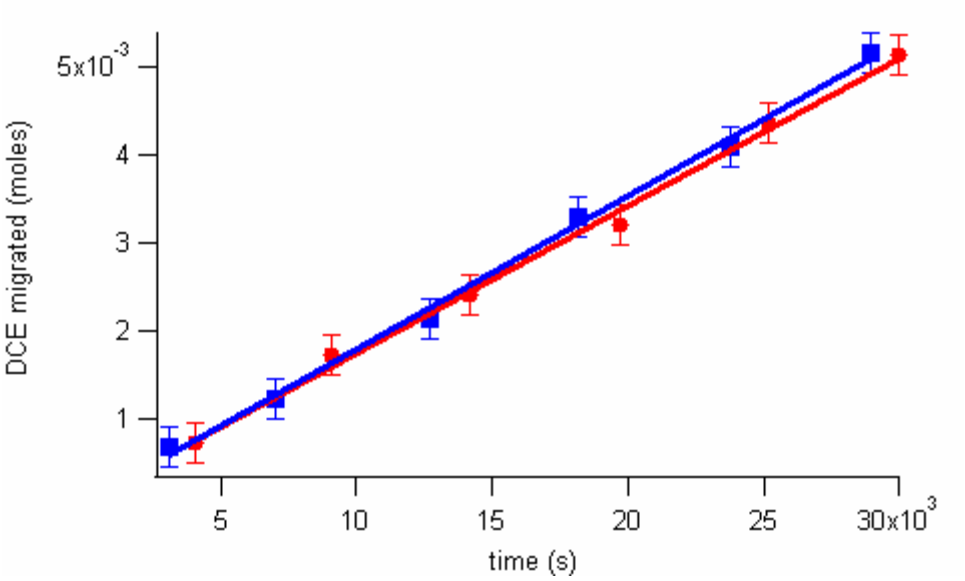

Figure 2.5. Graph of t1,2-DCE diffusion at the same temperature (25 °C) from two different days showing repeatability of measurements, line between points provided as guide to the eye.

2.2.4 TGA

Thermogravimetric Analysis (TGA) Measurements were taken using a Thermal Advantage Q500 Thermal Gravimetric Analyzer to determine if the DCE isomers were significantly soluble in the LDPE films, a property that could lead to plasticization. Plasticization occurs when films come into contact with a soluble solute and undergo structural change due to absorption of the solute. Dissolution of the solute in the film can change a film's structural properties and its permeability. The solubility of the DCE isomers were compared to isooctane, which is a known plasticizing agent. The LDPE films were soaked in the solvent for 48 hours before TGA analysis. All TGA measurements were run with a temperature ramp of 3 °C/min, experiments were then held at a constant temperature for a defined amount of time based on the molecules vaporization temperature (at 1 atm). 1,1-DCE was held at 80 °C for 2 hours, t1,2-DCE was held at 100 °C for 3 hours, c1,2-DCE was

held at 120 °C for 3 hours, and isooctane was held at 120 °C for 4 hours. Figure 2.6 shows a representative TGA analysis. Notice that the LDPE films soaked in isooctane lost significantly more mass (~3%) than any soaked in the DCE isomers. The most significant mass loss observed for the DCE isomers was that of the film soaked in c1,2-DCE. This film lost ~ 0.3% of its mass. Films soaked in 1,1-DCE and t1,2-DCE did not show any mass loss outside the limits of detection around 0.1%.

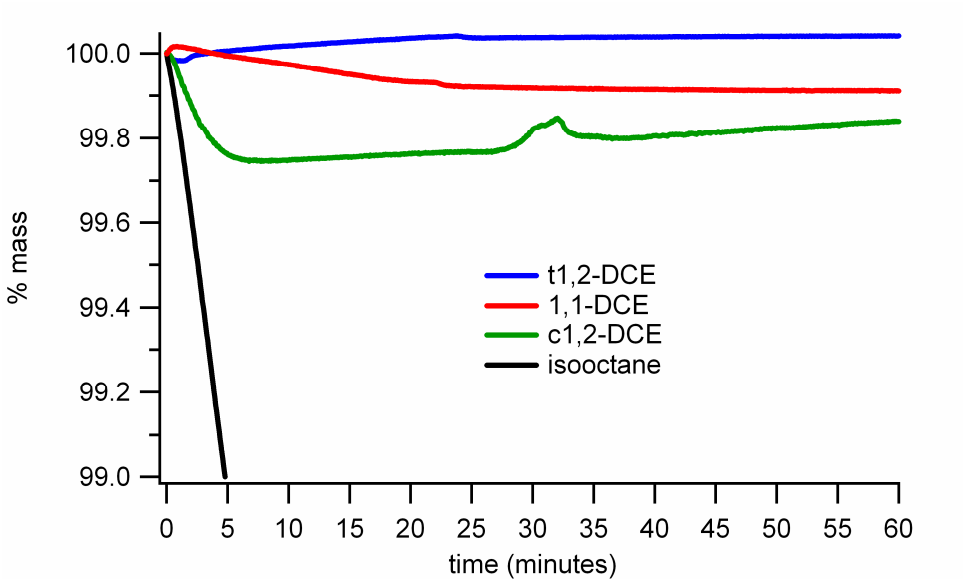

Figure 2.6. TGA analysis of DCE isomers and isooctane.

2.2.5 Headspace GC-MSD

Aliquots removed (0.05mL) from the receptor side of the cell were immediately diluted with 10.00 mL of HPLC grade toluene, and sealed in headspace (HS) vials. Aliquots were analyzed using a HS GC-MSD. The system used an Agilent 7694 Headspace Autosampler with a 2-mL sample loop, attached to an Agilent Technologies 6890 gas chromatograph with a 5973N mass selective detector. The column used was a HP-PLOT Q capillary column (30m × 0.32mm I.D., with a 20 m film thickness) The HS operating conditions were, 100 °C needle, 150 °C transfer

line, 60 °C oven; 30 minutes thermal equilibration with shaker on; 0.50 min pressurization, 0.2min injection with vial pressurized to 20 psi; 0.2 min withdrawl; 7.03 psi column head pressure. The GC-MS operating conditions were 50 ° to 250 °C at 10 °C/min and hold 30 min; injector temp 200 °C; split ratio 1:1; constant column flow 1.5 mL/min. MSD parameters were: auto tuned with perfluorotributylamine, 70eV electron impact ionization in full scan mode from *m/z* 30 to *m/z* 150, 225 °C transfer line, 230 °C source and 150 °C quadrupole, scan rate of 4.1 scans/second. The GC of the DCE isomers had good baseline resolution with a difference of about a minute in retention time for each of the isomers. As shown in Figure 2.7 1,1-DCE eluded at about 12.25min, t1,2-DCE 13.4 min and c1,2-DCE 14.3 min. A mass spectrum analysis for 1,1-DCE is shown in Figure 2.8, mass spectrum for cis and trans DCE are similar. Ion 96 was used for the calibration curves to determine DCE concentration. The reproducibility of individual experiments is demonstrated by the data presented in Figure 2.9.

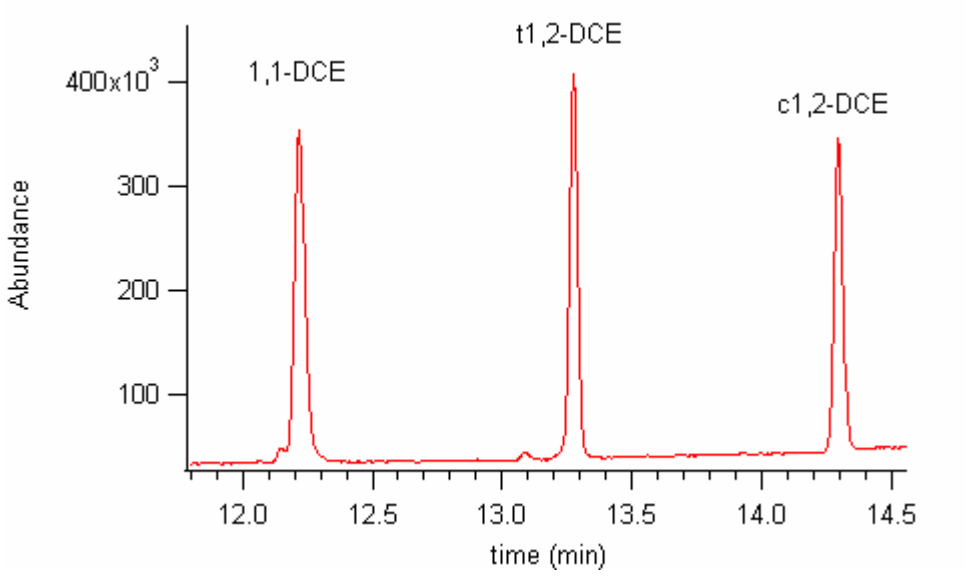

Figure 2.7. Gas chromatograph of a mixture composed of 0.05% by volume in Miglyol of each of the DCE isomers.

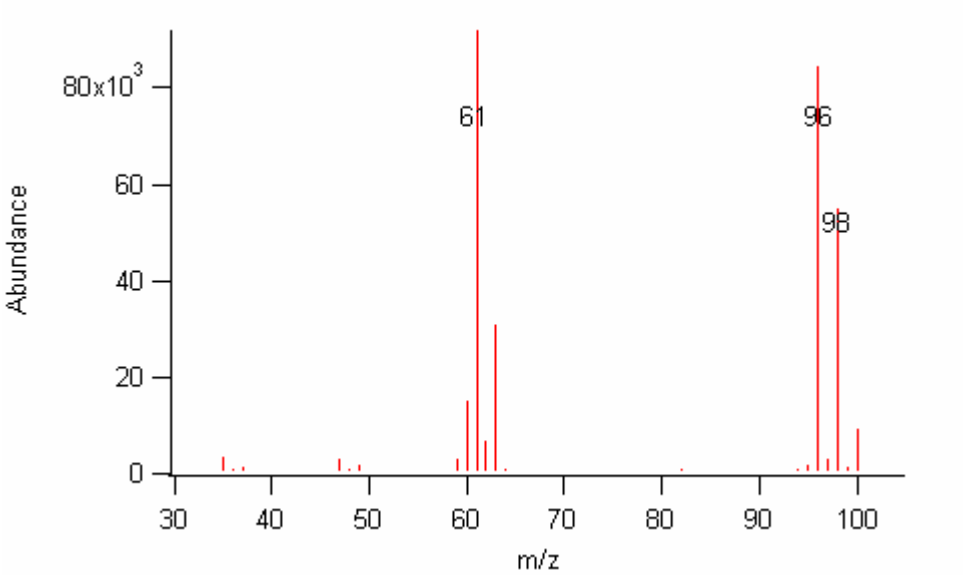

Figure 2.8. Mass spectrum of 1,1-DCE

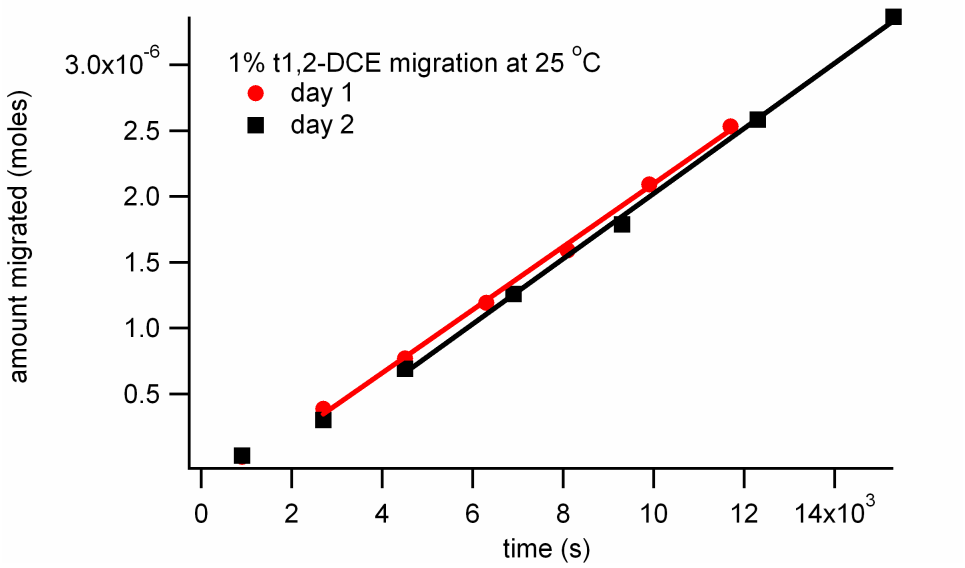

Figure 2.9. Graph of 1% by volume t1,2-DCE in Miglyol migration through LDPE into Miglyol taken at 25 °C on different days under identical experimental conditions.

References

1. Grossman, R. B., *The Art of Writing Reasonable Organic Reaction Mechanisms*. Second ed.; Springer: New York, 2003.

2. Esenturk, O.; Walker, R. A., Surface Structure at hexadecane and Halo-hexadecane Liquid/Vapor Interfaces. *Journal of Physical Chemistry B* **2004,** 108, (30), 10631-10635.

3. Richter, L. J.; Petralli-Mallow, T. P.; Stephenson, J. C., Vibrationally resolved sum-frequency generation with broad-bandwidth infrared pulses *Optics Letters* **1998,** 23, 1594-1596.

4. Richmond, G. L., Molecular bonding and interactions at aqueous surfaces as probed by vibrational sum frequency spectroscopy. *Chemical Reviews* **2002,** 102, (8), 2693-2724.

5. Can, S. Molecular Structure and Organization in Organic Monolayers at Aqueous/Vapor Interfaces. PhD, University of Maryland, College Park, 2008.

6. Can, S. Z.; Mago, D. D.; Walker, R. A., Structure and Organization of Hexadecanol Isomers. *Langmuir* **2006, 22**, 8043-8049.

7. *CRC Handbook of Chemistry and Physics*. 77 ed.; CRC Press, Inc.: New York, 1996.

8. Beyer, H.; Walter, W., *Organic Chemistry: A Comprehensive Degree Text and Source Book*. Albion Publishers: Chichester, 1997.

9. Howe, J. A.; Flygare, W. H., Strong Field Stark Effect. *The Journal of Chemical Physics* **1962,** 36, (3), 650-652.

10. *Lange's Handbook of Chemistry*. 15 ed.; McGraw-Hill, Inc.: New York, 1999.

Chapter 3 Interfacial Behavior of Common Food Contact Polymer Additives

3.1 Introduction

Additives are commonly introduced during polymer processing and production to prevent loss of mechanical properties and discoloration caused by the oxidation of polymers.[1, 2] One specific use of additives is in the production of food packaging material. Typically food packaging polymers contain one to three different types of additives to suit specific applications. For example, some additives serve as processing stabilizers, others as antioxidants, UV absorbers, antimicrobial agents, and pigments.[2] After the food has been sealed in its packaging, additives in the packaging polymer can remain in the polymer, partition to the polymer/food or polymer/air interface, or migrate from the polymer into the food. The latter pathways diminish the efficiency of antioxidants in polymers by reducing antioxidant additive concentration in the polymer itself. A fourth possible fate for antioxidant additives is phase separation, a phenomenon known commonly as blooming.[3, 4] Typically blooming results from poor mixing of the polymer resin and the antioxidant during production.

Although antioxidants are known to stabilize polymers, surprisingly little is known about their mobility and behavior at interfaces, including polymer/food and polymer/air interfaces. Often, migration rates and partitioning behaviors are predicted from models based on Fickian diffusion.[5-8] However, corresponding experimental studies to verify model accuracy are often lacking. Such quantitative information about chemical migration is important for developing accurate exposure

estimates for the general population. For example, ammonium perfluorooctonate (PFOA) is a processing aid in the production of polytetrafluroethylene (PTFE), and has been determined to migrate from PTFE into other substances, including foods. PTFE has been so widely used that the elderly American population has an average concentration of almost 40 nM PFOA in their blood.[9] Until recently PFOA was categorized as a "suggested" carcinogen but was recently reclassified as a "likely" carcinogen by the EPA, meaning that federal regulation of PFOA processing is now necessary.[10] Fortunately, antioxidants generally react to form harmless substances such as phenoxyl radicals and phosphates.[2, 11-13] Nevertheless migration of antioxidant additives out of a polymer and into food is an area of concern especially for the small population with known toxic susceptibility. Furthermore, the long term effects of persistent exposure are still not well determined. Therefore, the subject of antioxidant additive migration remains an active area of research.[5, 14-24]

Polymer additive aggregation at the packaging/food interface is also of concern. In general, antioxidants are present in polymers at concentrations of 0.05 - 1% by mass.[2] The antioxidants are added to the polymer with the assumption that molecules act independently and do not aggregate in the polymer matrix. However, an affinity for the package/food interface can lead to higher surface concentrations of antioxidants compared to concentrations in the bulk polymer or the bulk food. Such activity can promote formation of dimers, trimers or higher aggregates resulting in the reduction of antioxidant additive activity in the packaging material. In general, the affinity of additives for different surfaces and the tendency of adsorbed additives to aggregate will depend sensitively on a balance between

hydrophobic and hydrophilic functional groups as well as the overall structure of the additive monomers themselves.

Antioxidant additives fall into different families based on shared structural motifs. Antioxidants in the Irganox family have a 2,6-bis(1,1-dimethylethyl)-4-methylphenol group in one or more locations on the molecule. Two particular antioxidants from the Irganox family are the subjects of studies described below. Irganox 1010 (IN1010) and Irganox 1076 (IN1076) are both phenolic antioxidants (Figure 3.1) and are used to stabilize polymers during long term, high temperature exposure. Initially, the phenol groups react with molecular oxygen to form phenoxyl radicals that subsequently undergo additional oxidation to further protect the polymer.[25, 26] IN1076 shares many of the features associated with simple alkyl surfactants (i.e. 1-octanol) including polar head groups and large hydrophobic extensions. IN1010 looks less like a traditional surfactant although it does have multiple phenol groups coupled with bulky hydrophobic substituents. The combination of phenol and alkyl groups make IN1010 and IN1076 candidates to adsorb preferentially to boundaries between hydrophobic and hydrophilic media such as those found between a polymer packaging material and aqueous foods. Pronounced surface activities can lead to higher concentrations of antioxidant additives at an interface and eventually to aggregate formation.

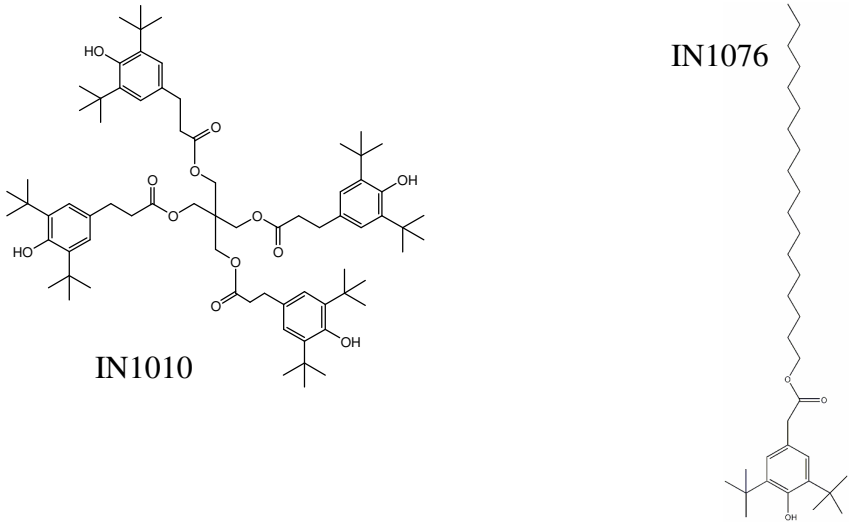

Figure 3.1. IN1010 and IN1076 structures.

Surface tension studies can provide insight into the surface properties of these antioxidants. Experiments described in this chapter examine the two-dimensional phase behavior of IN1076 and IN1010 at the air/water interface by measuring surface pressure isotherms of molecular films. Surface tension data show that sequential compressions of the antioxidant films lead to irreversible loss of monomers from the surface, suggesting a tendency for these amphiphiles to form aggregates. On a molecule for molecule basis more IN1076 is lost with each compression relative to IN1010. However when one considers that IN1010 has four phenolic groups per monomer, the number of these subunits lost per compression appears to be equivalent to within experimental uncertainty.

These films are also examined using Vibrational Sum Frequency Spectroscopy (VSFS), a surface specific vibrational spectroscopy capable of probing structure and organization within the monolayers adsorbed to the air/water interface.

Results show that differences in structure between high and low coverage of IN1010 films on water, but not for IN1076. In the case of IN1076, spectral band intensities suggest that monomer headgroups adopt a more horizontal geometry with the aromatic rings aligned approximately normal to the surface. This proposed structure correlates well with the initial collapse area of IN1076 monolayers. The phenolic groups of IN1010 monomers also appear to assume a horizontal structure at the surface with ~2-3 segments in contact with the aqueous phase, but the structural complexity of the monomer itself makes conclusions more tentative.

3.2 Results and Discussion

3.2.1 Surface Activity

Sequential Π-A isotherms for both IN1076 an IN1010 are shown in Figures 3.2 and 3.3. The IN1076 monolayer starts at a pressure of 0 mN/m at the beginning of the first compression. Eventually the isotherm shows a lift-off where the pressure begins to rise. For the initial compression, lift-off occurs at an area of 101 $Å^2$/molecule. The pressure rises linearly with a slope of -0.19 mN*molecule/$Å^2$*m, before collapsing at a surface pressure of 7.2 mN/m. Following re-expansion, the surface pressure measures slightly less than zero and does not change even after allowing the film to sit for a half hour undisturbed. The 96 $Å^2$/molecule area at lift-off for the second compression is 5% smaller than for the first compression and the collapse pressure of 6.9mN/m is also slightly lower than for the first compression.

Subsequent compressions result in similar functional forms of each isotherm with the initial surface pressure and the lift-off areas continuing to decrease. Figure 3.2b shows representative hysteresis loops that track the surface pressure

during expansion as well as during compression. One readily sees that the expansion isotherms following collapse track closely the isotherm for the subsequent compressions. This behavior proves quite general regardless of how much the collapsed monolayer is further compressed as well as how much time elapses between the cessation of a compression and the start of the subsequent expansion. The origin of the increasingly negative surface pressure at the start of each new compression in a sequence remains a mystery. A negative surface pressure means that the balance is measuring a greater forcer than it does when the plate is in contact with pure water. One possible explanation of this effect would involve increasing the amounts of surfactant sticking to the plate with each successive compression. However, registering a change in force equivalent to the eventual ~ -0.7 mN/m drop in surface pressure (between first and final compression of a sequence) would require accumulating more than one thousand times more surfactant than is deposited on the surface in the first place. We note that after successive compressions and expansions (~4-5) the expanded film showed evidence of irreversible aggregate formation as indicated by irregularly shaped patches of the aqueous surface having a different refractive index. Furthermore, these "oily" patches did not disperse uniformly over the entire area of the trough, but rather remained localized near the plate at the trough's center. How – or even if – this phenomenon leads to the increasingly negative surface pressures observed in compression sequence is unclear, but the observations have proven remarkably durable despite wide variation in compression and expansion conditions.

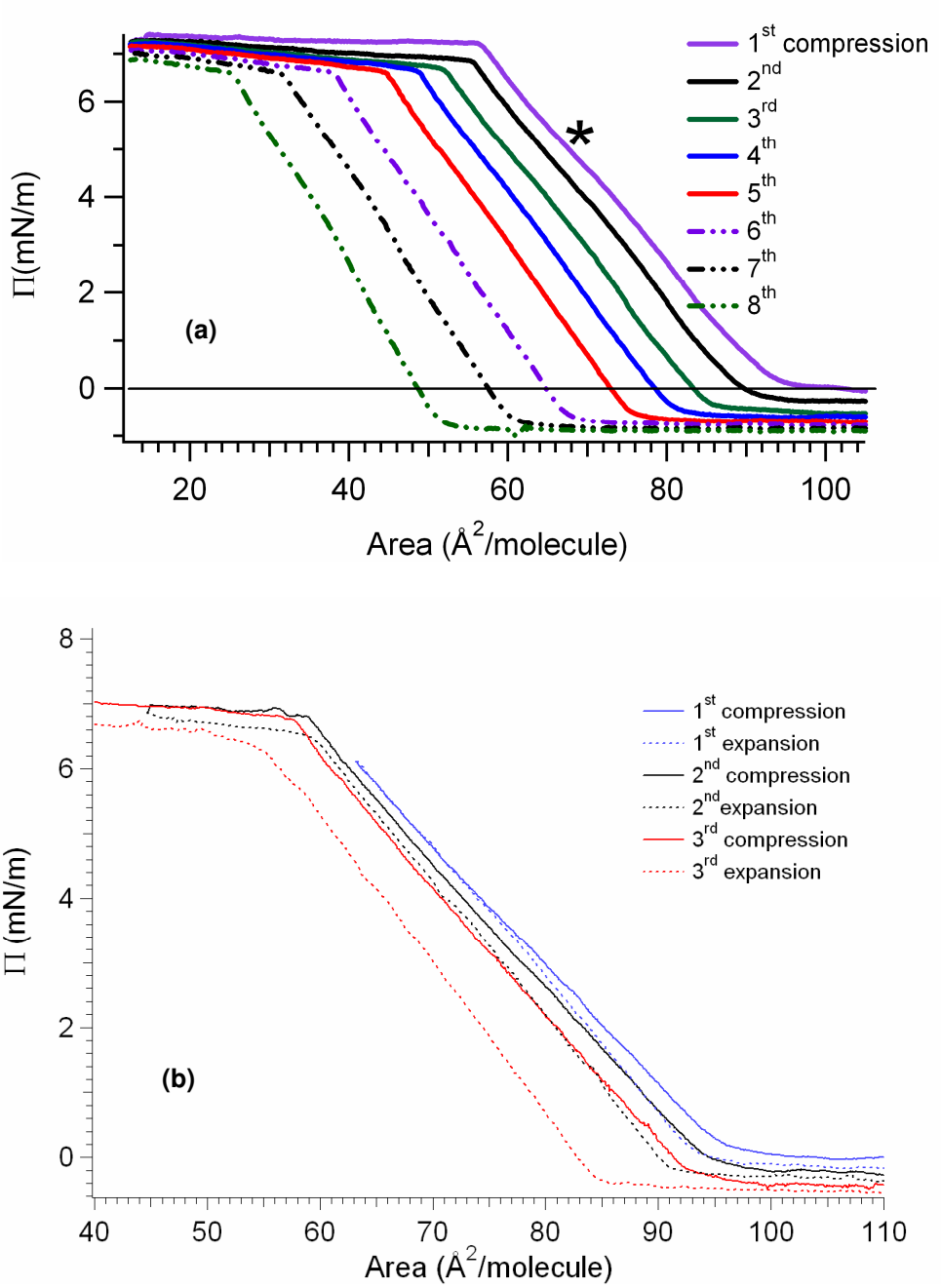

Figure 3.2. (a) IN1076 Π-A isotherms resulting from successive compressions, with an asterisk marking the conditions under which VSFS measurements were taken. (b) Hysteresis loop of IN1076

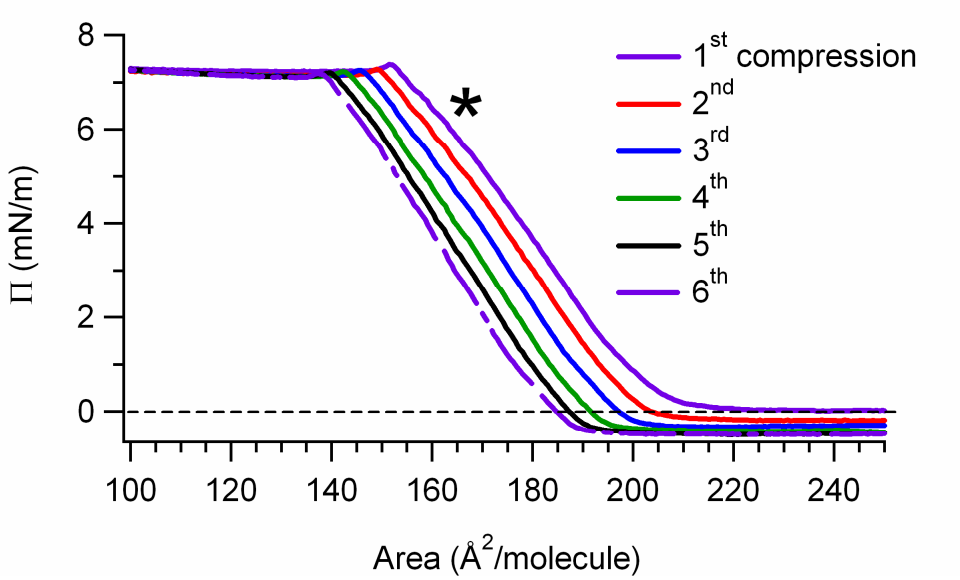

Figure 3.3. IN1010 Π-A isotherm resulting from successive compressions, with an asterisk marking the conditions under which VSFS measurements were taken.

Π-A isotherms for IN1010 (Figure 3.3) show behavior similar to those of IN1076. The first compression has a lift-off area of 215 Å^2/molecule or more than twice the lift-off area for IN1076. Considering the molecular size of IN1010 compared to IN1076, this result can be anticipated since the lift off area is directly proportional to the size of the antioxidant additive monomers. The isotherm rises with a slope of approximately -0.14 mN*molecule/Å^2*m until 7.3mN/m when the film collapses. After the first compression, the film is re-expanded. Similar to what was observed with IN1076, the lift-off area of IN1010 decreases to 208 Å^2/molecule, a small but statistically significant 3% change. The collapse pressure remains the same to within experimental uncertainty. Subsequent compressions of the IN1010 monolayer show hysteresis effects similar to those observed for IN1076 monolayer.

At first glance, the isotherms for IN1076 and IN1010 share qualitative similarities and quantitative differences. Both show linear -A behavior following

lift off and repeated film collapse leads to systematic changes in both the initial surface pressure and subsequent lift off areas. However, the slope of the IN1076 isotherms is generally 25% greater than that observed for IN1010. In addition, the IN1010 isotherms lift off at areas approximately 2-3 times as great as the IN1076 lift off areas (depending on the specific compression of a sequence). To compare the isotherms from these two additives in a more direct way, one can compare the IN1010 and IN1076 films in terms of their respective surface compressional moduli:[27]

$$K^s = -A(\partial \Pi / \partial A)_T \qquad (3.1)$$

where K^s is the inverse of the isothermal compressibility (C^s) and is an intensive property of monolayer films. The average K^s values for IN1076 vary between 13 mN/m at the beginning and 18 mN/m at the end of the linear range of the first isothermal compression. IN1010 had average values ranging from 20 mN/m to 29 mN/m. Considering that the slope for IN1010 is 25% smaller than that of IN1076, but lifts off at areas a factor of two greater than IN1076, one would expect that IN1010 would have K^s values that were approximately two-fold larger than those of IN1076.

The low pressure data from IN1076 and IN1010 isotherms can be analyzed using a two-dimensional ideal gas:

$$N = (A\Pi)/(k_B T) \qquad (3.2)$$

where N is the number of molecules on the surface, A is the molecular area, k_B is Boltzmann's constant, Π is the surface pressure (the difference between the surface tension of the neat water/vapor interface and the surface tension of the water/vapor

interface in the presence of the monolayer), and T is the temperature in degrees Kelvin. Implicit in our use of the 2-dimensional ideal gas equation of state the molecules do not interact with each other at low surface pressures. A consequence of this assumption is that if the gas is not behaving ideally, the number of molecules may be underestimated. Despite the assumption associated with this simple expression, our analysis leads to two observations worth noting. First, the lift-off area for subsequent compressions of the monolayers is smaller than the first compression. Second, the surface pressure at the start of each compression continues to decrease (from 0) meaning that the surface tension of the fully expanded monolayer continues to increase following successive compressions. Since k_B and T are constant, a decreasing surface pressure (Π) at the same area (A) likely means that the number of "molecules" at the water/vapor interface is changing. This observation could result from solubilization of monomers in the bulk – an unlikely result given the insoluble nature of the monomer itself – or the irreversible formation of aggregates following film collapse. The smaller lift-off areas could be caused by the irreversible loss of molecules to form stable aggregates, a hypothesis that can be tested using Brewster angle microscopy[28-31] or similar techniques to test the surface tension data. Such experiments however are beyond the scope of the experiments described in this work.

Using the known antioxidant concentration in spreading solutions along with the deposition volume, one calculates the number of antioxidant molecules initially spread upon the water surface. Similarly, the number of molecules for any given isotherm is calculated using specific A and Π values. Through these calculations one readily determines that an initial loss of molecules is required to account for the lift-

off area of the first compression. The initial losses of molecules, (4.15 0.06)×10^{15} for IN1010 and (14.7 0.11)×10^{15} for IN1076, are remarkably consistent for eight or more, independent experiments. This initial loss of molecules is attributed to the adsorption of a finite number of molecules to the syringe, plate and trough walls before a series of compressions is begun.

Determining the number of surface species with Equation 3.2, one can look at the loss of molecules as a function of compression sequence. Using the change in area at constant pressure (Figure 3.4) one can calculate dN from the following:

$$dN = (\Pi/k_BT)*dA \qquad (3.3)$$

Figure 3.5 shows ΔN as a function of the change in the number of compressions (Δcomp) for both IN1076 and IN1010. ΔN is the total number of molecules lost between each compression, starting with the number of molecules present initially during the first compression. (Δcomp) is found by taking the difference in the compression number, again starting with the first compression. For example, the ΔN value resulting from comparison of the first compression to the third compression describes the difference in the number of "molecules" present at the start of the first compression and the start of the third compression. For this comparison Δcomp has a value of 2 (or 3-1). If each compression (after the first) led to a constant number of molecules "lost" the data in Figure 3.5 would show linear behavior. Figure 3.5 supports this picture for both the IN1076 and the IN1010 films within the limits of experimental uncertainty. In addition, the loss observed in the IN1076 monolayer is approximately four times as great as that for each IN1010 compression when compared on a molecule by molecule basis as shown in Figure 3.5. If one compares

the data based on the number of phenolic groups lost per cycle, one sees that for every phenolic group lost from the IN1076 film the IN1010 loses four. This scaling of ΔN based on the number of phenolic groups per monomer shows the functional group losses from the IN1010 system to be similar to the values observed for the IN1076 monolayer film.

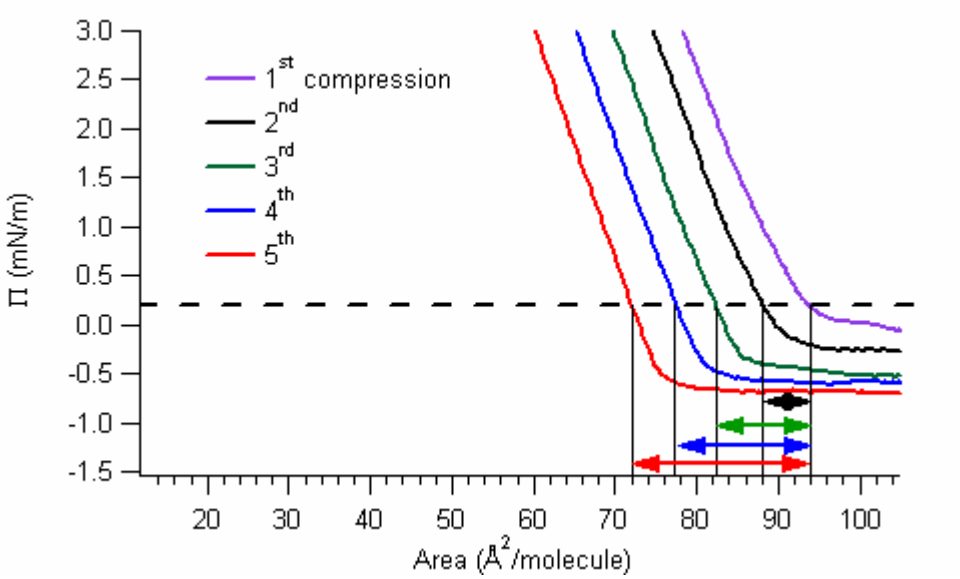

Figure 3.4. IN1076 isotherm illustrating how A values were determined.

The smaller ΔN values for subsequent compressions of IN1010 compared to IN1076 is reasonable given their respective structures. Considering the tendencies of IN1076 and IN1010 to self assemble spontaneously, one can envision that at close range, the long octadecyl tails of IN1076 can interact cohesively through extensive Van der Waals interactions. The t-butyl groups should prevent the formation of well ordered alkyl domains, but these interactions still could very well prevent the molecules from separating upon expansion. Aggregates are known to form in monolayers after collapse, and are a possible explanation for the hysteresis observed in the isotherms.[28-32] The short aromatic arms that comprise IN1010 molecule will pack together less efficiently than the alkyl chains of IN1076.

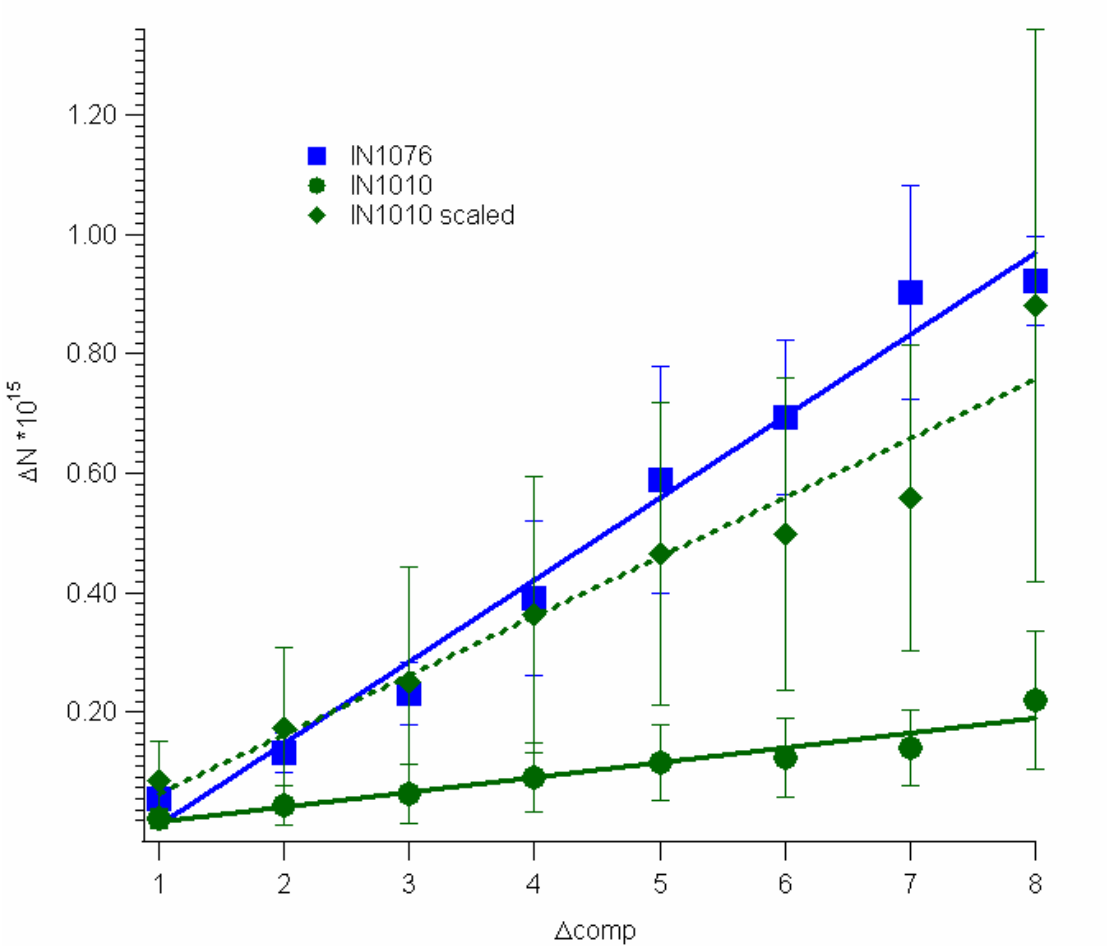

Figure 3.5. Comparison of average number of molecules lost from IN1076 and IN1010 after subsequent compressions. IN1010 scaled represents the molecules of IN1010 lost scaled to the amount of phenolic groups on IN1010.

Frequently, one would like to draw comparisons between behavior of molecules having similar functional-group composition. In this respect, the Irganox species studied in this work bear some resemblance to a family of calixarenes studied extensively by Esker, et al.[33, 34] The structures of this macrocycle is shown in Figure 3.6. Both the Irganox and calixarenes have multiple phenol groups and attached hydrophobic, alkyl segments. Furthermore, monolayers of both species exhibit a linear dependence of surface pressure on area and similar collapse pressures. However, the structure of the Irganox monomers – especially IN1010 – and the

calixarene monomers studied in references 33 and 34 are markedly different. Calixarenes in contact with water will orient themselves so that all the hydroxyl groups on the phenols are in contact with the subphase leading to strong intramolecular interactions. In fact, Esker, et al. note that these strong interactions are likely responsible for shifting the pK_a of individual hydroxyl groups by more than 9-10 units from values typical of p-alkylphenols.[33] Such intramolecular interactions are not possible with the Irganox species studied in this work. For the IN1076 monolayers, t-butyl groups will prevent the –OH groups on individual monomers from interacting strongly with each other. Similar considerations apply to the (four) hydroxyl groups on IN1010 monomers.

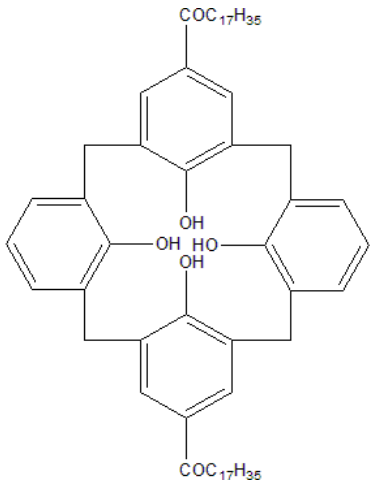

Figure 3.6. Structure of p-dioctadecanoylcalix[4]arene.

Another clear example that surface behavior depends on molecular structure and not simply functional group composition comes from comparing the collapse pressures of the species in question. During the first compression, IN1076 collapses at a molecular area of 57 $Å^2$/molecule, IN1010 at an area of 153 $Å^2$/molecule and the calixarenes in references 33 and 34 at an area of 78 $Å^2$/molecule. Based on similarities in collapse areas (and pressures), one might be tempted to draw

comparisons between IN1076 and the p-dioctadecanoylcalix[4]arene monolayers, but doing so would overlook the fact that IN1076 monolayers have only a single hydroxyl group interacting with the aqueous subphase while the calixarene monomers have four hydroxyl groups capable of hydrogen bonding to the water (although the authors of references 33 and 34 note that some of the hydroxyl groups of the calixarenes are likely hydrogen bonded to each other). The presence of the two t-butyl groups adjacent to the hydroxyl group in IN1076 will inhibit hydrogen bonding between the surfactant and the subphase meaning that the phenol group is unlikely to adopt an orientation perpendicular to the interface. Were the phenol group to assume a horizontal orientation relative to the interface, each IN1076 monomer would be able to enjoy hydrogen bonding between the phenolic hydroxyl group and the water as well as favorable interactions between water dipoles and the pi-electron system of the aromatic ring. Such a horizontal geometry is supported by the vibrational studies of the IN1076 and IN1010 films presented below.

A final point worth noting is that the collapse area of the initial IN1010 compression (of 153 $Å^2$/molecule) corresponds to ~2.5 times the area occupied by a single IN1076 monomer at its monolayer collapse pressure (3D structure of IN1010 shown in Figure 3.7.a). These results coincide with simple molecular area considerations based on forcing IN1010 hydroxyl groups to lie in the same plane (nominally that of the aqueous subphase) and then calculating the resulting projected area. An IN1010 monomer with two of its arms hydrogen bonded to the water is the other two arms directed away from the interface occupies an area of ~135 $Å^2$/molecule (shown in Figure 3.7.b). Monomers with one and three arms

hydrogen bonded to the water/vapor interface occupy an equivalent area of 275 $Å^2$ (shown in Figure 3.7.c). Forcing all four arms to interact with the water requires that the IN1010 monomer adopt a conformation that is energetically unreasonable (at kT) and would require molecular areas in excess of 300 $Å^2$/molecule. Given that the observed collapse areas lies in between the two and (one or three) phenol limit and is equal to approximately 2.5 times the collapse area of the IN1076 monolayer, we conclude that the phenolic groups of IN1010 adopt similar orientations at the air/water interface as those of IN1076 and that each IN1010 monomer interacts with the aqueous subphase with either two or three of its arms.

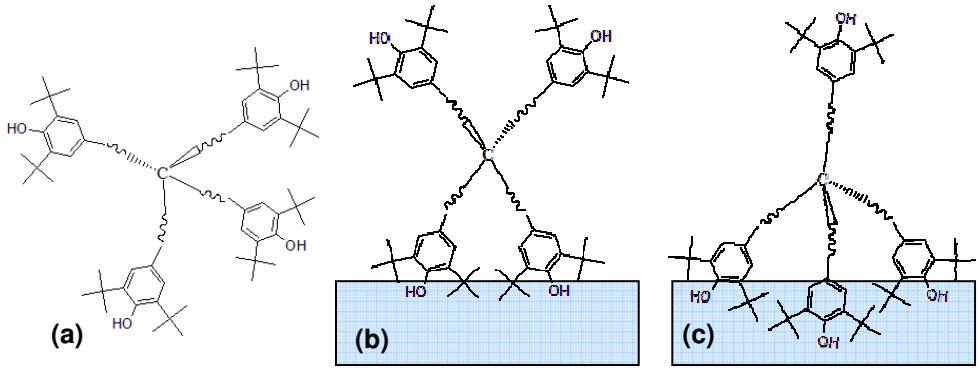

Figure 3.7. (a) IN1076 schematic showing tetrahedral geometry from central carbon, (b) IN1076 schematic with two arms oriented towards the subphase (blue box), (c) IN1076 schematic with three arms oriented towards the subphase (blue box).

3.2.2 Vibrational Structure

The behavior of IN1076 and IN1010 films at the air/water interface raises questions about the degree of molecular organization within the films themselves. To probe film structure, several samples were examined using VSFS. Films were prepared by depositing a well defined quantity of surfactant (in a spreading solvent) on a water surface, measuring the surface pressure and then probing the surface with

a combination of visible and infrared optical fields. As described in the Experimental Section, VSFS measures vibrational spectra of molecules at surfaces. In our studies of IN1076 and IN1010 films, we employed a combination of polarizations that sampled those vibrational transitions that had their IR transition moments aligned along the surface normal, perpendicular to the interface. The first samples of IN1076 and IN1010 had measured surface pressures of 6.1 mN/m corresponding to molecular areas of 68 $Å^2$/molecule and 165 $Å^2$/molecule, respectively. These conditions are marked with asterisks on the isotherms shown in Figures 3.2 and 3.3. Subsequent samples were prepared to examine the effect of excess surfactant on film structure.

Figure 3.8 shows the VSF spectra of IN1076 adsorbed to the air/water interface in both the full monolayer and excess limits. The spectra themselves are quite similar in appearance and in absolute intensity, meaning that the ~8 fold excess surfactant added to the full monolayer has very little effect on overall organization within the film. The monolayer spectrum, although noisy, shows several distinct features that can be assigned to stretching motion of various -CH functional groups.[35] Chief among these are the $-CH_2$ symmetric stretch (d^+) at 2845 cm^{-1}, the $-CH_3$ symmetric stretch (r^+) at 2870 cm^{-1}, and a broad, partially resolved feature centered at 2930 cm^{-1} that contains contributions from the $–CH_2$ asymmetric stretch (d^-), a Fermi resonance coupling between the $–CH_2$ symmetric stretch and an overtone of –CH bending motion, and the $–CH_3$ asymmetric stretch (near 2953 cm^{-1}, r^-). Given the weak intensity observed in the $–CH_3$ symmetric stretch, we do not anticipate significant intensity arising from a $–CH_3$ Fermi resonance (near 2940 cm^{-1}). The

spectrum begins to acquire broad, featureless intensity above 3100 cm^{-1} that is assigned to the coupled –OH stretching motion of the underlying water subphase.[36]

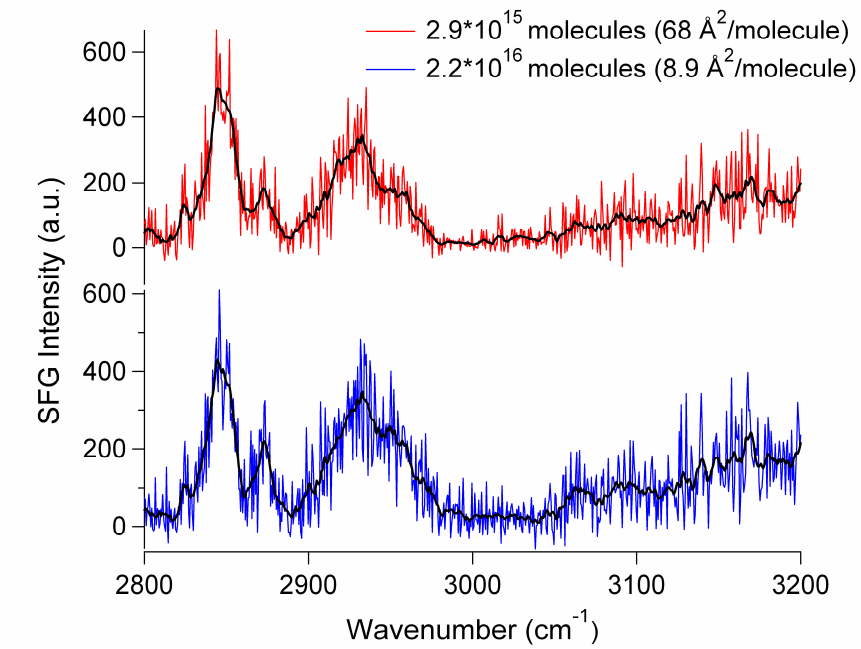

Figure 3.8. SFG spectra of IN1076 films. Spectra were acquired detecting S polarized signal resulting from S polarized visible and P polarized IR light.

A common measure of orientational order in alkyl monolayers is the r^+/d^+ ratio. For alkyl chains possessing a high degree of conformational order spectra acquired under SSP polarization conditions show a strong r^+ response (due to the out-of-plane alignment of the $–CH_3$ C_3 axis) and a weak d^+ response. For well-ordered, linear alkyl surfactants (such as *n*-hexadecanol), the r^+/d^+ ratio can exceed 20.[37] In the case of the IN1076 monolayer, r^+/d^+ is quite low – approximately ~0.25. In principle, one might expect a much stronger r^+ response given the relatively high surface coverage of $–CH_3$ groups. (Each IN1076 monomer includes a total of seven methyl groups – six from the pair of t-butyl groups and a terminal methyl group on the alkyl chain.) However, should the hydrophilic end of the surfactant adopt a

"horizontal" geometry due to competition of the attractive hydrogen bonding interactions of the phenol hydroxyl group counterbalanced by the hydrophobic effects of the adjacent t-butyl groups, then the t-butyl methyl groups will keep their symmetric stretch transition moments aligned parallel to the surface and not appear in the spectra acquired with $S_{sum}S_{vis}P_{IR}$ polarization conditions. Furthermore given that the IN1076 surface concentration at full monolayer coverage (1.6×10^{14} molecules/cm^2) is approximately 1/3 that of tightly packed, linear alkyl chains ($\sim 5 \times 10^{14}$ molecules/cm^2) the observed disorder from the alkyl chain (as significant intensity in d^+ and d^-) should not be surprising. A horizontal orientation of the aromatic ring and t-butyl groups approximately parallel to the interfacial plane is also consistent with simple geometric calculations carried out using energetically optimized structures created in molecular mechanics software using space filling models and MM2 energy minimization.[38] Using the distances between the t-butyl groups on either side of the IN1076 phenol head group the cross-sectional area was estimated. In the case of IN1010, distances between phenolic head groups of the four "arms" were used to calculate the areas assuming different numbers of contacts with the aqueous subphase. Based on the measured molecular areas, we estimate ~2-3 sterically hindered phenols to be in contact with the subphase.

The spectra of IN1010 (Figure 3.9) are dominated by a moderately strong band centered at 2920 cm^{-1} assigned nominally to the $-CH_2$ asymmetric stretch (d^-). IN1010 does not contain extended alkyl chains, but the surfactant does contain 24 separate methyl groups. The absence of strong intensity assigned to either r^+ or r^- indicates that the different "arms" of the IN1010 are either randomly directed in the

IN1010 monolayer or oriented parallel to the water surface, even when the monolayer is tightly packed and close to collapse. (Both spectra – monolayer and excess – do show weak shoulders at ~2950 cm^{-1} on the high frequency side of the d^- band, and these are assigned to the $-CH_3$ asymmetric stretch, r^-.) The fact that the IN1010 spectrum (pre-collapse) shares many similarities with that of the IN1076 spectrum suggests that the phenolic sub-units with the accompanying t-butyl groups share similar orientations in the two separate monolayers. The largest difference between the two spectra can be attributed to the long alkyl chain in the IN1076 contributing intensity to d^+, a feature that is unlikely to appear in an IN1010 spectrum given the absence of long alkyl segments. Again, structure in the alkyl stretching region does not change significantly with the addition of excess surfactant to the monolayer sample, but the water intensity (above 3100 cm^{-1}) vanishes, indicating that the additional IN1010 significantly influences the water structure underlying the organic film. As with the IN1076 film, the absence of strong vibrational features in the IN1010 spectra and the apparent lack of sensitivity of molecular structure to the amount of surfactant present imply that these surfactants are also unable to form domains having well-defined order.

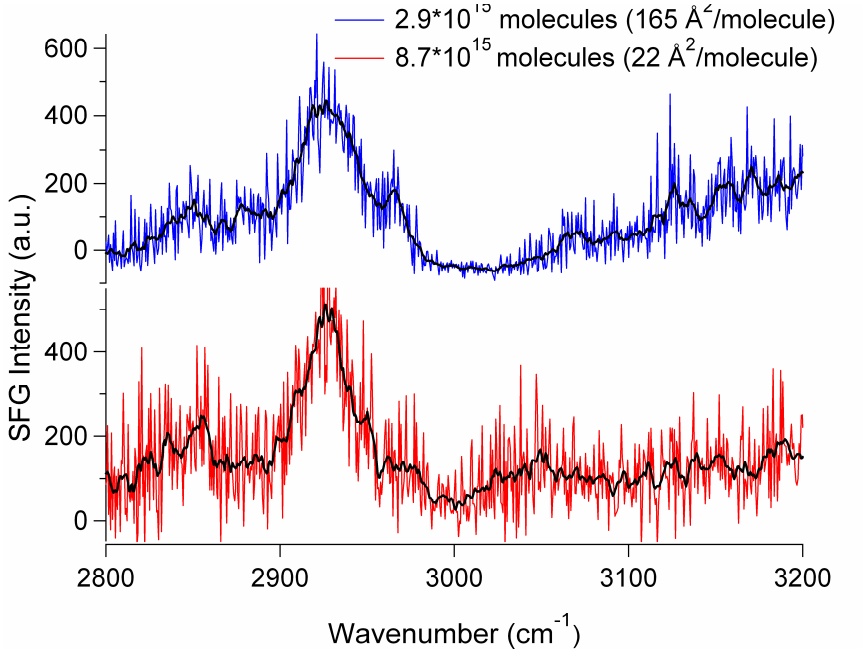

Figure 3.9. SFG spectra of IN1010 films. Spectra were acquired detecting S polarized signal resulting from S polarized visible and P polarized IR light.

3.3 Conclusions

Successive isothermal compressions of IN1076 and IN1010 monolayers adsorbed to the air/water interface exhibit hysteresis that implies a loss of monomers when the surfactants become too tightly packed. Quantitative analysis shows that IN1076 monolayers lose more molecules per compression than do IN1010 monolayers. This difference can be attributed to differences in the molecular structure between the two species. The long hydrophilic tails of IN1076 have more opportunity to interact during full compression. If this phenomenon is irreversible then it will lead to a decrease in the number of molecules in the monolayer when the film is re-expanded. IN1010 has much less conformational freedom behaving more like a sphere, thus fewer monomers are lost between each compression. IN1010 also

has a higher isothermal compressibility, which is exhibited by the higher slope in the -A isotherm.

VSFS shows IN1076 to be disordered at the air/water interface, in monolayer and excess coverage, supporting the idea that the hydrocarbon tails of IN1076 are not well organized. This disorder may be caused by the presence of the bulky t-butyl groups surrounding the phenol. Another worthwhile experiment would then be to investigate the surface activity of long chain alkylphenols such as 4-dodecylphenol. Surface tension measurements of these long chain alkylphenols would simulate the surface activity of IN1076 without the bulky t-butyl groups attached. IN1010 VSFS spectra show a lack of molecular order in the monolayer films as well; however, when excess IN1010 is added, there is a significant change in the subphase as illustrated by the disappearance of intensity above 3100 cm^{-1}.

References

1. Zweifel, H., *Stabilization of Polymeric Materials*. Springer: Heidelberg 1997.

2. Zweifel, H., *Plastics Additives Handbook*. 5th ed.; Hanser: Cincinnati, 2001.

3. Spatafore, R. a. P., L. T. , *Polymer Engineering and Science* **1991,** 31, 1610-1617.

4. Rawls, A. S., Hirt, D. E., Havens, M. R., Roberts, W. P. , Evaluation of surface concentration of erucamide in LLDPE films. *Journal of Vinyl and Additive Technology* **2002,** 8, 130-138.

5. O'Brien, A., Cooper, I. , Practical experience in the use of mathematical models to predict migration of additives from food-contact polymers. *Food Additives and Contaminants* **2002,** 19, Suppliment 63-72.

6. Limm, W., Hollifield, H. C. , Modelling of additive diffusion in polyolefins. *Food Additives and Contaminants* **1996,** 13, 949.

7. Tehrany, E. A., Desobry, S., Fournier, F. , Simple method to calculate partition coefficient of migrant in food simulant/polymer system. *Journal of Food Engineering* **2006,** 77, 135-139.

8. Limm, W., Hollifield. H. C. , Effects of temperature and mixing on polymer adjuvant migration to corn oil and water. *Food Additives and Contaminants* **1995,** 12, 609-624.

9. Olsen, G. W., Burris, J. M., Burlew, M. M., Mandel, J. H., Epidemiologic assessment of worker serum perfluorooctanesulfonate (PFOS) and perfluorooctanoate (PFOA) concentrations and medical surveillance examinations. *Journal of Occupational and Environmental Medicine* **2003,** 45, (3), 260-270.

10. Eilperin, J., Compound in Teflon A 'Likely Carcinogen'. *The Washington Post. Washington, D.C.* Jun 29, 2005, 2005, pg. A.04.

11. Zweifel, H., *Polymer Durability*. ACS: Washington, 1996.

12. Schwetlick, K., *Pure and Applied Chemistry* **1983,** 55, 1634.

13. Schwetlick, K., Konig, T., Ruger, C., Pointeck, J., Habicher, W. D. , *Polymer Degradation and Stability* **1986,** 55, (97).

14. O'Brien, A., Cooper, I., Polymer additive migration into foods -- a direct comparison of experimental data and values calculated from migration models for polypropylene. *Food Additives and Contaminants* **2001,** 18, (4), 343-355.

15. Begley, T., Castle, L., Feigenbaum, A., Franz, R., Hinrichs, K., Lickly, T., Mercea, P., Milana, M., O'Brien, A., Rebre, S., Rijk, R., Pringer, O. , Evaluation of migration models that might be used in support of regulations for food-contact plastics. *Food Additives and Contaminants* **2005,** 22, (1), 73-90.

16. Stoffers, N. H., Stormer, A., Bradley,E.L., Brandsch, R., Cooper, I., Linssen, J. P. H., Franz, R. , Feasibility study for the development of certified reference materials for specific migration testing. Part 1: Initial migrant concentration and specific migration. *Food Additives and Contaminants* **2004,** 21, (12), 1203-1216.

17. Stoffers, N. H., Brandsch, R., Bradley, E. L., Cooper, I., Dekker, M., Stormer, A., Franz, R., Feasibility study for the development of certified reference materials for specific migration testing. Part 2: Estimation of diffusion parameters and comparison of experimental and predicted data. *Food Additives and Contaminants* **2005,** 22, (2), 173-184.

18. Begley, T., Biles, J., Cunningham, C., Pringer, O. , Migration of a UV stabilizer from polyethylene terephthalate (PET) into food simulants. *Food Additives and Contaminants* **2004,** 21, 1007-1014.

19. Limm, W., Begley, T.H., Lickly, T., Hentges, S.G. , Diffusion of limonene in polyethylene. *Food Additives and Contaminants* **2006,** 23, (7), 738-746.

20. Vitrac, O., Mougharbel, A., Feigenbaum, A. , Interfacial mass transport properties with control the migration of packaging constituents into foodstuffs. *Journal of Food Engineering* **2006, ASAP**.

21. Tehrany, E. A., Desobry, S. , Partition coefficients in food/packaging systems: a review. *Food Additives and Contaminants* **2004,** 21, (12), 1186-1202.

22. Helmroth, I. E., Dekker, M., Hankemeier, T., Additive Diffusion from LDPE Slabs into Contacting Solvents as a Function of Solvent Absorption. *Journal of Applied Polymer Science* **2003,** 90, 1609-1617.

23. Helmroth, I. E., Dekker, M., Hankemeier, T., Influence of solvent absorption on the migration of Irganox 1076 from LDPE. *Food Additives and Contaminants* **2002,** 19, 176-183.

24. Dopico-Garcia, M. S., Lopez-Vilarino, J. M., Gonzalez-Rodriguez, M. V. , Effect of temperature and type of food simulant on antioxidant stability. *Journal of Applied Polymer Science* **2006,** 100, 656-663.

25. Pospisil, J., Nespurek, S., Sweifel, H., The role of quinone methides in thermostabilization of hydrocarbon polymers - I. Formation and reactivity of quinone methides. *Polymer Degradation and Stability* **1996,** 54, 7-14.

26. Pospisil, J., Nespurek, S., Sweifel, H., The role of quinone methides in thermostabilization of hydrocarbon polymers - II. Properties and activity mechanisms. *Polymer Degradation and Stability* **1996,** 54, 15-21.

27. Gaines, G. L., Jr., *Insoluble Monolayers at Liquid-Gas Interfaces*. Interscience Publishers: New York, 1966.

28. Grigoriev, D. O. L., M. E.; Michel, M.; Miller, R., Component separation in spread sodium stearoyl lactylate (SSL) monolayers induced by high surface pressure. *Colloids and Surfaces A* **2006,** 286, 57-61.

29. Liang, Y.; Wu, Z.; Wu, S., Monolayer Behavior and LB Film Structure of Poly(2-methoxy-5-(n-hexadecyloxy)-p-phenylene vinylene). *Langmuir* **2001,** 17, 7267-7273.

30. Liou, S. H.; Hsu, W. P.; Lee, Y. L., Monolayer characteristics of stereoregular PMMA at the air/water interface. *Applied Surface Science* **2006,** 252, 4312-4320.

31. Ourisson, G.; Ariga, K.; Yuki, H.; Kikuchi, J.; Dannemuller, O.; Albrecht-Gary, A. M.; Nakatani, Y., Monolayer Studies of Single-Chain Polyprenyl Phosphates. *Langmuir* **2005,** 21, 4578-4583.

32. Gaines, G. L. J., Monolayers of Polymers. *Langmuir* **1991,** 7, 834-839.

33. Esker, A. R., Zhang, L.H., Olsen, C. E., No, K., Yu, H., Static and Dynamic Properties of Calixarene Monolayers at the Air/Water Interface. 1. pH Effects with p-Dioctadecanoylcalix[4]arene. *Langmuir* **1999,** 15, (5), 1716-1724.

34. Zhang, L. H., Esker, A. R., No, K., Yu, H., Static and Dynamic Properties of Calixarene Monolayers at the Air/Water Interface. 2. Effects of Ionic Interactions with p-Dioctadecanoylcalix[4]arene. *Langmuir* **1999,** 15, (5), 1725-1730.

35. MacPhail, R. A., Strauss, H. L., Snyder, R. G., Elliger, C. A., C-H Stretching Modes and the Structure of n-Alkyl Chains 2. Long, All-Trans Chains. *Journal of Physical Chemistry* **1984,** 88, 334-341.

36. Raymond, E. A., Tarbuck, T. L., Richmond, G. L., Isotopic Dilution Studies of the Vapor/Water Interface as Investigated by Vibrational Sum-Frequency Spectroscopy. *Journal of Physical Chemistry B* **2002,** 106, (11), 2817-2820.

37. Can, S. Z., Mago, D. D., Walker R. A., Structure and Organization of Hexadecanol Isomers. *Langmuir* **2006, 22**, 8043-8049.

38. *Chem3D Pro 8.0*, Chem3D Pro 8.0; CambridgeSoft Corporation: Cambridge, MA, 1985-2003.

Chapter 4 Migration of Dichloroethylene Isomers through LDPE: Effects of Migrant Structure

4.1 Introduction

In a continuing effort to protect the purity and safety of the food supplies, regulatory authorities monitor and evaluate the mass transfer of food packaging components into foods so that exposure estimates can be accessed and minimized.[1-7] The safety of migrating food packaging components is generally accessed and migration is minimized. Most models used to predict exposure estimates consider only a migrant's mass when calculating migration properties. However efforts to quantify mass transfer are focusing on molecular structure as a potential metric for predicting the amount of migration from food packaging into food.[8] Correlations between molecular structure and other related properties (such as dipole moments) and mass transfer processes may improve substantially the accuracy of predicted exposure estimates to food packaging components.[8, 9]

Evaluating the risks posed by migrating analytes requires accurate, quantitative exposure estimates that often result from measured or calculated diffusion coefficients. Diffusion coefficients are often determined experimentally through one of two tests. The Moisan test is typically used for open systems with low vapor pressure analytes. In these experiments a concentration gradient is measured after a fixed amount of time in a stack of three film layers in direct contact with one another, with only the middle film initially containing the migrating analyte.[10, 11] The three-layer test is similar to the Moisan type test in that it measures a concentration gradient in a stack of 3 film layers, but the three-layer test can be done in a closed system with either the outer or inner films containing the migrating analyte.[10]

Because both methods rely on analyte migration between solid materials, experiments can take weeks to months to yield definitive results, limiting the ability of these approaches to provide data from large numbers of systems. To save time and resources in the lab, empirical migration models have been developed to predict diffusion coefficients of migrants typically encountered in industrial applications.[12-15]

Related to diffusion is permeability. Permeability is a function of both migrant diffusion as well as migrant solubility in a polymer matrix. Diffusion determines how fast a migrant will move in a film, while solubility determines how much migrant can be accommodated in the film. As the product of these two functions, permeation determines the amount of migrant that filters through the film. If diffusion is fast and solubility low, permeation of the migrant through the film will be low. Also if solubility is high, but diffusion slow, migrant permeation will again be limited. Only when the migrant exhibits a high solubility in the polymer, as well as fast diffusion, will permeation be high. When considering the total amount of material that migrates through a film, permeation studies are ideally suited to conditions when experimental techniques can determine migration rates under steady state conditions.

A feature common to most migration models is the dependence of migration rates on a migrant's mass. To first order, such treatment is reasonable given that a migrant's size will generally scale with mass and heavier migrants will move more slowly in polymer films. However these models necessarily overlook the effects that a migrant's structure can have on transport. These effects will be more pronounced for small molecules having well defined conformers and more clearly distinguishable isomeric structures. Experiments described in this work examine migration of

dichloroethylene (DCE) isomers (Figure 4.1) through single, thin sheets (76.2 m) of low density polyethylene (LDPE) into solutions of Miglyol, a liquid food simulant comprised of caprylic/capric triglycerides (shown in figure 4.2). Because these experiments measure the total amount of migration to the low concentration side of the cell, the relevant quantity to consider is permeation not diffusion. LDPE is considered a "worst case scenario" food contact material in terms of analyte migration because the polymer has a loose chain structure with low tensile strength. This combination of properties allows for faster migration than what would occur through high tensile strength, rigid polymers such as polypropylene or high density polyethylene. Despite being so permeable to migrants, LDPE still enjoys widespread use in food wraps, food storage containers, and sandwich bags. 1,1-dichloroethylene (1,1-DCE), cis-1,2-dichloroethylene (c1,2-DCE) and trans-1,2-dichloroethylene (t1,2-DCE) were chosen as migrants because they have very different molecular and fluid properties despite having the same molecular weight. 1,1-DCE has a relatively low boiling point compared to t1,2-DCE and c1,2-DCE, and both 1,1-DCE and c1,2-DCE have dipole moments where as t1,2-DCE does not. These properties are summarized in Table 2.1. Miglyol 812 was chosen due to it's popularity as a food mimic material.[16-22]

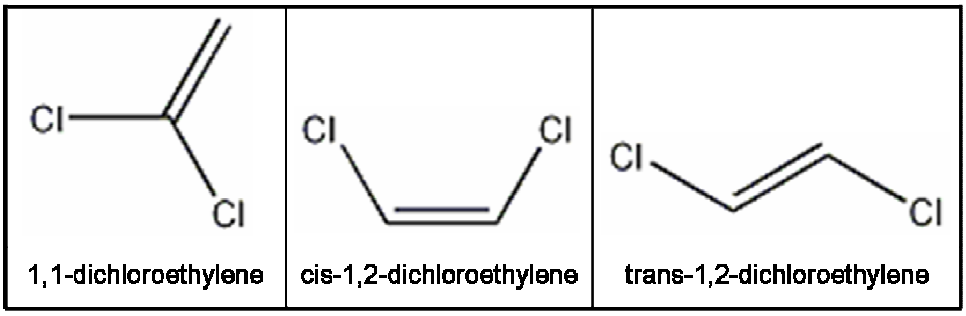

Figure 4.1. Structures of dichloroethylene isomers.

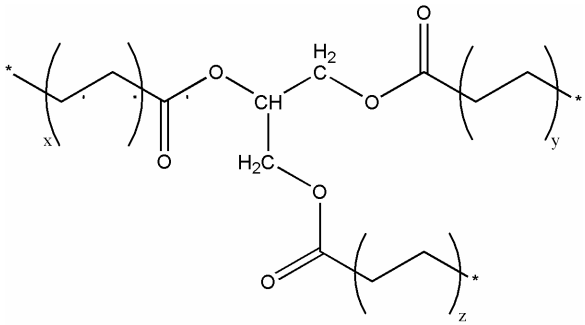

Figure 4.2. Miglyol structure, a caprylic/capric triglyceride x, y, and z have values of 8 or 10.

In addition to serving as model analytes to test the role of molecular structure in migration rates, these isomers are also recognized environmental pollutants. 1,1-DCE is used in refrigerants, food packaging materials and the production of adhesives. Health effects associated with exposure to 1,1-DCE are liver damage and cancer.[23] c1,2-DCE and t1,2-DCE are also used as refrigerants, in the manufacture of artificial pearls, and as solvents for resins. Adverse health effects resulting from exposure include central nervous system depression, as well as long term effects of damage to the liver, circulatory and central nervous systems, with t1,2-DCE being twice as harmful to the central nervous system as c1,2-DCE.[24] Given the differences in toxicity between c1,2-DCE and t1,2-DCE, understanding their transport properties through a food contact polymer is essential for developing successful computational-based methods for estimating migration and, therefore, accurate exposure estimates.

Based on commonly used diffusion models, migration rates of the DCE isomers should be equivalent. Our goal in this work is to test what role, if any, molecular structure plays in analyte transport through food contact polymers.

4.2 Results and Discussion

Data for the saturated permeation experiments were taken over a period of 7-10 hours (depending on temperature). In every experiment migrant appearance on the low concentration side begins to build gradually before eventually assuming a linear dependence on time (Figure 4.3). Linear behavior signifies the onset of steady state migration.[25] Prior to the onset of steady state migration, experiments all show a delay that depended on film composition and thickness. This "lag-time" typically extended over the first ~90 minutes of an experiment. The origin of this delay suggests establishment of a steady state concentration of intermediates somewhere along the migration pathway. We note here that experiments using films already saturated with the appropriate DCE isomer still showed a lag before the onset of steady state migration. (Analysis comparing data from saturated and virgin films are shown in Appendix 1.) This result implies that the lag time's origin may be related to processes occurring outside the film or at the film/liquid interface. Despite the variability in the lag times, the linear dependence of concentration on time after the onset of steady state conditions proved highly reproducible.

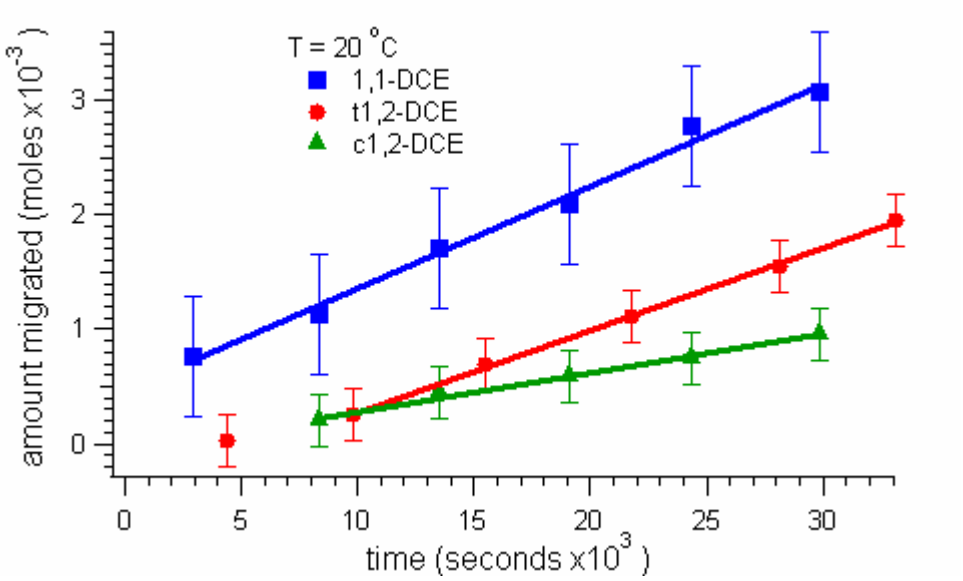

Figure 4.3. Permeation of DCE isomers at 20°C.

The simplest way to measure solute migration in polymers is by determining the diffusion of a gas through a polymer sheet. Steady state diffusion is reached when there is a constant transfer rate across the sheet for all exposed sections and when the concentration change from one side of the film to the other is linear.[26] In the case of gas diffusion, when steady state diffusion is reached, the flux (F) can be described by the diffusion coefficient (D) through the following expression:[25-29]

$$F = -D\frac{dC}{dx} = \frac{D(C_1 - C_2)}{l} \qquad (4.1)$$

where C_1 and C_2 are the surface concentrations (just inside the film surface) on either side of the polymer film, and l is the thickness of the film. In an experiment with gas diffusion where surface concentrations are not known, one can determine the permeability coefficient (P):[25-30]

$$F = \frac{P(p_1 - p_2)}{l} \qquad (4.2)$$

where p_1 and p_2 are the external vapor pressures on either side of the polymer film. From this expression one can determine the permeability coefficients of volatile compounds based on the partial pressures on either side of a diffusion cell. If Henry's law is obeyed, then the surface concentration just within the surface of the film can be related to the external vapor pressure through the solubility constant (S):[25-28, 30]

$$C_i = Sp_i \qquad (i = 1 \text{ or } 2) \tag{4.3}$$

This same solubility constant can be used to relate permeation to diffusion[25-28, 30]

$$P = DS \tag{4.4}$$

The diffusion coefficient is known to correlate with molecular mass and size of the migrant.[8, 9, 11, 31-33] The solubility coefficient depends on the strength of the interactions between the polymer and the penetrating migrant. The stronger the interactions, the more soluble the molecule should be in the polymer, and the higher the solubility coefficient. Similarly, weaker interactions lead to lower solubility within the polymer matrix. Bulk migrant properties such as polarity, density and viscosity will all affect migrant solubility in a given polymer. Thus, based on Equation 4.4, permeation will be affected by interactions between the analyte and the polymer (solubility) in addition to how easily the analyte can move through the polymer (diffusion). Temperature will affect permeation, through changes in both the diffusion and solubility constants.

We now consider the relationships between diffusion, permeation, and solubility of liquids through polymer films. Assuming Fickian behavior and a constant diffusion coefficient, diffusion through a polymer film can be calculated through the time lag method. Under the conditions that the polymer film is free of migrant at the onset of the experiment, and migrant is removed from the low

concentration side of the film –conditions that match exactly those of our experiments – then the amount that passes though the sheet (Q_t) with thickness (l) in time (t) can be described by[26-28, 34]

$$\frac{Q_t}{lC_1} = \frac{Dt}{l} - \frac{1}{6} - \frac{2}{\pi^2} \sum_{n=1}^{\infty} \frac{(-1)^n}{n^2} \exp\left(\frac{-Dn^2\pi^2 t}{l^2} \right) \tag{4.5}$$

where n is the number of sheets in the polymer film (1). As the steady state conditions are approached, and t $\rightarrow \infty$, the exponential terms go to zero, so that a graph of Q_t versus time will have a linear dependence on (t):[27, 28]

$$Q_t = \frac{DC_1}{l}\left(t - \frac{l^2}{6D} \right) \tag{4.6}$$

The x-intercept on the time axis, represents the lag time (L). The lag time is related to the diffusion coefficient based on the lag time equation.[26-28, 34, 35]

$$L = \frac{l^2}{6D} \tag{4.7}$$

In a plot of concentration versus time, L is found by extrapolating to zero concentration. This diffusion-based analysis yielded inconsistent results when applied to our data (Appendix 1). Inconsistencies observed in the lag time data could be due to a combination of interfacial resistance inhibiting DCE transfer across the liquid/polymer interface and a lack of sensitivity of our analytical technique to detect low (<0.8% by volume) concentrations. As mentioned earlier experiments carried out with a film pre-saturated with DCE isomer also exhibited a delay before the onset of steady state migration, similar to experiments carried out with clean LDPE films. When thicker LDPE films (0.102 cm) were used for the migration experiments the observed lag times were consistent. The presence of the delay in

steady state behavior with saturated thin films, and consistent lag times observed with thicker LDPE films supports the idea that interfacial resistance, perhaps related to the processing of the thin LDPE films, is primarily responsible for the initially slow migration rates. What remains consistent for all experiments, however, is the isomer and temperature dependent migration rates following the establishment of steady state migration conditions.

Permeation depends on both diffusion and solubility. Different experimental quantities can be used to describe the permeation based on experiments using liquids as the migrating analyte. Using Equations 4.1-4.4 permeation can be written for liquids where p_1 and p_2 are now described in terms of the bulk concentrations on either side of the film (C_1^{bulk}, C_2^{bulk}):[25, 27, 28]

$$F = P\frac{C_1^{bulk} - C_2^{bulk}}{l} \tag{4.8}$$

The permeation can be described by the slope of the change in concentration versus change in time when the steady state diffusion rate is reached. The permeation coefficient can be calculated using easily measured experimental parameters[25]

$$P = \frac{(slope)(l)}{(A)(\Delta C)} \tag{4.9}$$

where the slope of the line is found in the steady state portion of a plot of change in concentration versus time, A is the cross sectional area of the film exposed to the analyte, and C is the difference in the bulk concentrations on either side of the film at the onset of the experiment. For experiments described in this work, C_2^{bulk} is zero. Note that permeation coefficients have the same units as diffusion coefficients, cm^2/s.

The permeation coefficients for the DCE isomers are reported in Table 4.1. Permeation coefficients were generally on the order of 10^{-8} cm^2/s. These values

compare well with previously reported data describing permeation of various organic liquids in different types of polyethylene.[36] Figure 4.3 shows that 1,1-DCE has the largest permeation coefficient ($7.3*10^{-8}$ cm^2/s at 293K), and c1,2-DCE has the lowest ($2.3*10^{-8}$ cm^2/s at 293K). These results come from using the linear part of the migration profile. The permeation coefficient of t1,2-DCE is approximately twice as large as that of c1,2-DCE. These results show clearly that migration of solvents through polymer films depends sensitively on molecular structure as well as molar mass.

Temp (K)	$P_{1,1\text{-DCE}}$ ($*10^8$)	$P_{t1,2\text{-DCE}}$ ($*10^8$)	$P_{c1,2\text{-DCE}}$ ($*10^8$)
293.1	7.3 ± 1.3	5.1 ± 0.3	2.3 ± 0.2
298.1	13 ± 4	7.2 ± 0.2	3.7 ± 0.4
303.1	N/A	8 ± 2	4.7 ± 0.9
308.1	N/A	14 ± 2	4.8 ± 1
E_P (kJ/mol)	80	47 8	36 10

Table 4.1. Average experimental permeation coefficients of dichloroethylene isomers at different temperatures. No high temperature results are presented for 1,1-DCE due to the low boiling point of the molecule. The final row presents the activation energy of permeation from analyzing the temperature dependent behavior with an Arrhenius model (note that the error for Ep 1,1-DCE is infinite).

Permeation of analytes through a polymer should be sensitive to a number of variables including analyte size and analyte interactions with surroundings. Differences in permeation constants for the DCE isomers reported in Table 4.1, we sought to determine if the observed trends scaled with geometric size. Isomer sizes were calculated using the van der Waals radii of the outer atoms, as well as reported bond lengths and bond angles to determine the molecular radii and are shown in Figure 4.4.[37] Use of van der Waals parameters will introduce some errors to the calculations, but the errors should be systematic and consistent for all three isomers.

Based on these calculations t1,2-DCE has the largest molecular radius of 4.02 Å. 1,1-DCE and c1,2-DCE have similar sizes of 3.49 and 3.47 Å respectively. The calculated size of these molecules suggest that c1,2-DCE and 1,1-DCE should migrate faster through LDPE and t1,2-DCE slower. The observed permeation values, however, show t1,2-DCE permeating about twice as fast as c1,2-DCE.

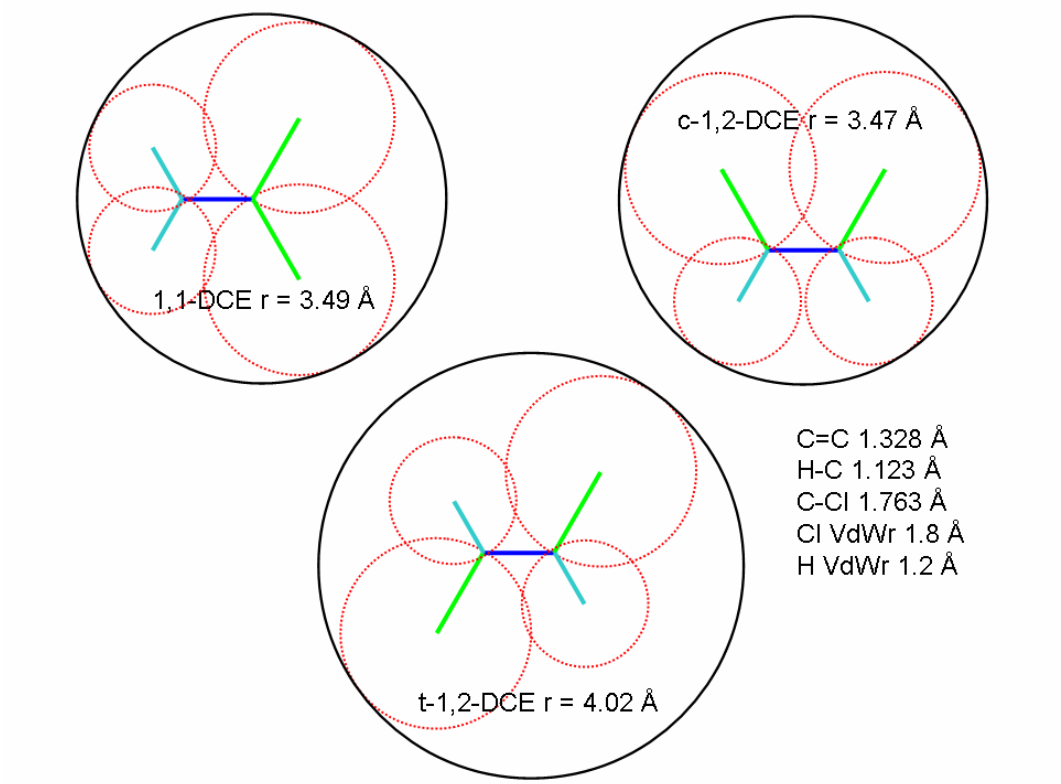

Figure 4.4. Calculated molecular radii from van der Waals radii, bond lengths, and bond angles.

Given that migrant size does not appear to correlate with migration rates (and permeation coefficients) we need to consider what other factors may influence experimental results. One property that differentiates t1,2-DCE from c1,2-DCE is the former's lack of a permanent dipole. The presence of a dipole can affect results in several ways. Dipole pairing between analytes can lead to correlated motion of monomers in solution and a larger effective radius. Dipole-induced dipole

interactions with the LDPE may also slow the migration of c1,2-DCE relative to t1,2-DCE.

Dipole moments and steric factors will also affect other properties for the isomers used in these studies, we note that permeation tracks analyte boiling points. Such correlation may be reasonable given that to a first approximation, a substances boiling point depends on intermolecular forces. Solvating DCE in LDPE will require overcoming these interactions between the monomers within the neat liquid. To further explore the role of intermolecular forces on permeation, we varied temperature to determine if the isomer dependent behavior observed at 20 ^{o}C persisted at higher temperatures.

Migration of 1,1-DCE was studied at 20 and 25 ^{o}C. t1,2-DCE and c1,2-DCE were studied at 20, 25, 30 and 35 ^{o}C. Figure 4.5 shows that permeation of t1,2-DCE increases with increasing temperature. Similar results are observed for all isomers (Figure 4.6) although our studies of 1,1-DCE are limited to only two points due to this migrant's low boiling point. Interestingly, the observed linear dependence of the permeation coefficient on T is different for different isomers. Focusing only on c1,2-DCE and t1,2-DCE, the slope of the temperature behavior of P on T is 1.6×10^{-9} for c1,2-DCE and 5.5×10^{-8} cm^2/(s*K) for t1,2-DCE. In other words, migration of t1,2-DCE, the more biologically active of the two structural isomers, depends more sensitively on temperature.

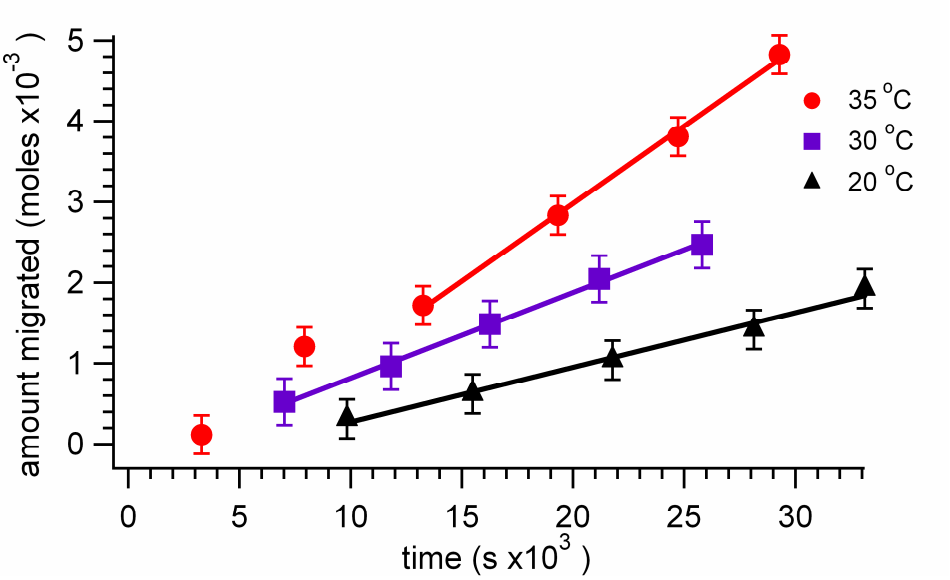

Figure 4.5. Permeation of t1,2-DCE at 20, 30, and 35 °C.

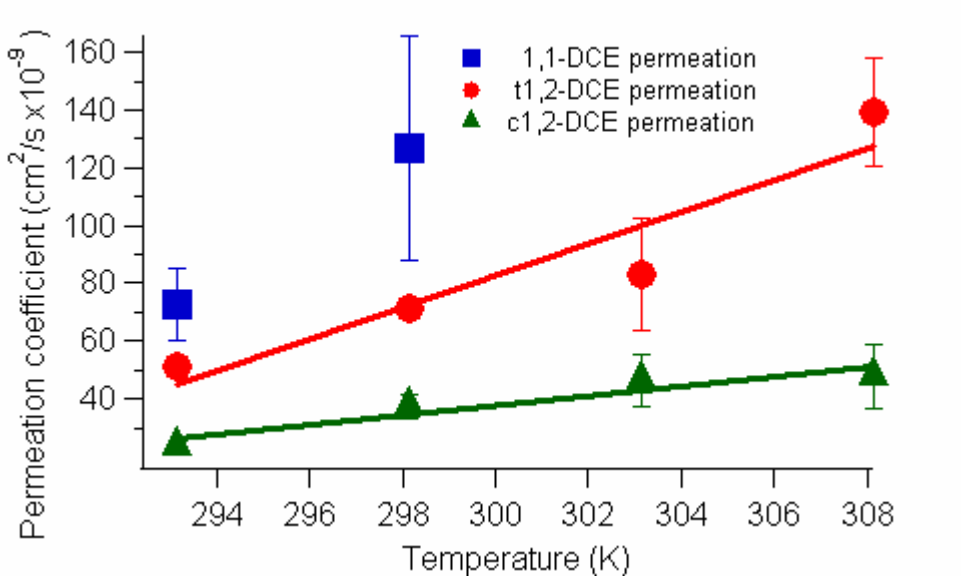

Figure 4.6. Permeation coefficients of DCE isomers with respect to temperature. Large uncertainties of 1,1-DCE at 298K are likely due to the experiment being run close to the boiling point of 1,1-DCE.

Migration of analytes through polymers increases with increasing temperature.[36, 38-42] The isomers investigated each have a different dependence of permeation on temperature. Specifically for the case of c1,2-DCE and t1,2-DCE we can use the permeation coefficients at different temperatures to determine an activation energy for permeation given the following Arrhenius-type equation:[36, 38-40, 43]

$$P = P_0 \exp\left(\frac{-E_P}{RT}\right) \tag{10}$$

where P_0 is the preexponential factor, E_P is the activation energy for permeation, R is the universal gas constant, and T is the temperature. Similar to permeation, the activation energy for permeation will depend on the migrating molecule's interactions with the polymer matrix (solubility), as well as the motion of the molecule through the polymer (diffusion). Figure 4.7 shows a plot of ln P versus 1/T for the DCE isomers. c1,2-DCE, t1,2-DCE, and 1,1-DCE have E_P values of 36, 47, and 80 kJ/mol respectively. These values are comparable to those reported for organic liquids permeating through LLDPE and VLDPE.[36] At the same time, these results show quite clearly that molecular structure plays a significant role in controlling mass transport through LDPE.

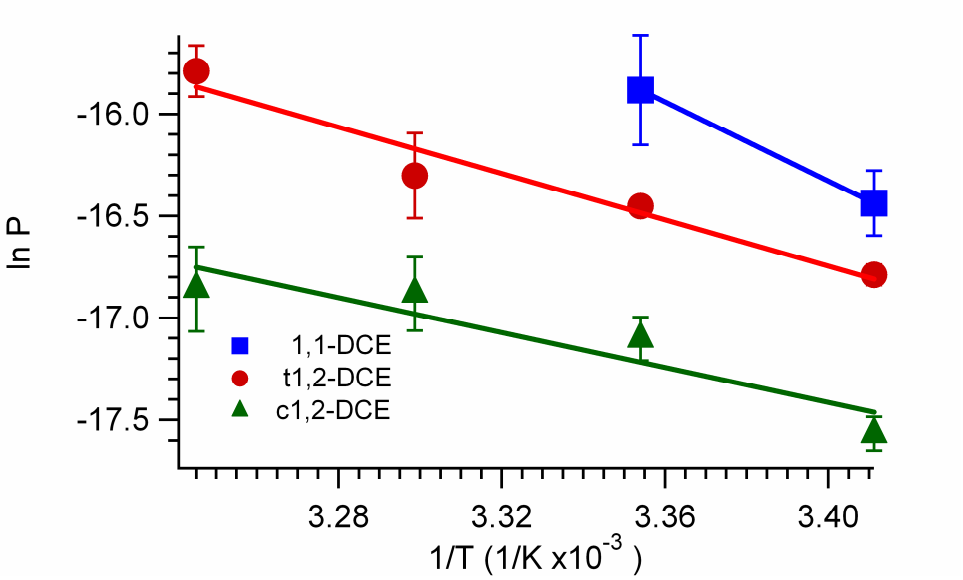

Figure 4.7. Arrhenius plot of ln P vs 1/T for DCE isomers. E_p values reported in Table 4.1.

Interpreting the E_p results presents a challenge given that a number of processes have to occur for DCE to migrate from one side of the polymer film to the other. First, DCE migrants must pass across the $DCE_{(l)}$/LDPE interface, where DCE then becomes solvated and sets up a concentration gradient across the film. This step of the migration process will depend upon the energetics of interphase mass transfer. Next, the migrant must move from one side of the polymer to the other, a step assumed to be governed by diffusion. Finally the migrating analyte must cross a second interface, passing from the LDPE to the Miglyol, which is dependent upon the partitioning of the DCE between the LDPE and Miglyol. Eventually this process reaches a steady state condition defined by a constant concentration gradient across the polymer film and a constant rate of migration. These steps are illustrated schematically in Figure 4.8. In general, activation energies associated with diffusion of small molecules through LDPE are ~30 kJ/mol[36], meaning that the sum of energies associated with both barrier crossings are positive and on the order of ~10 kJ/mol.

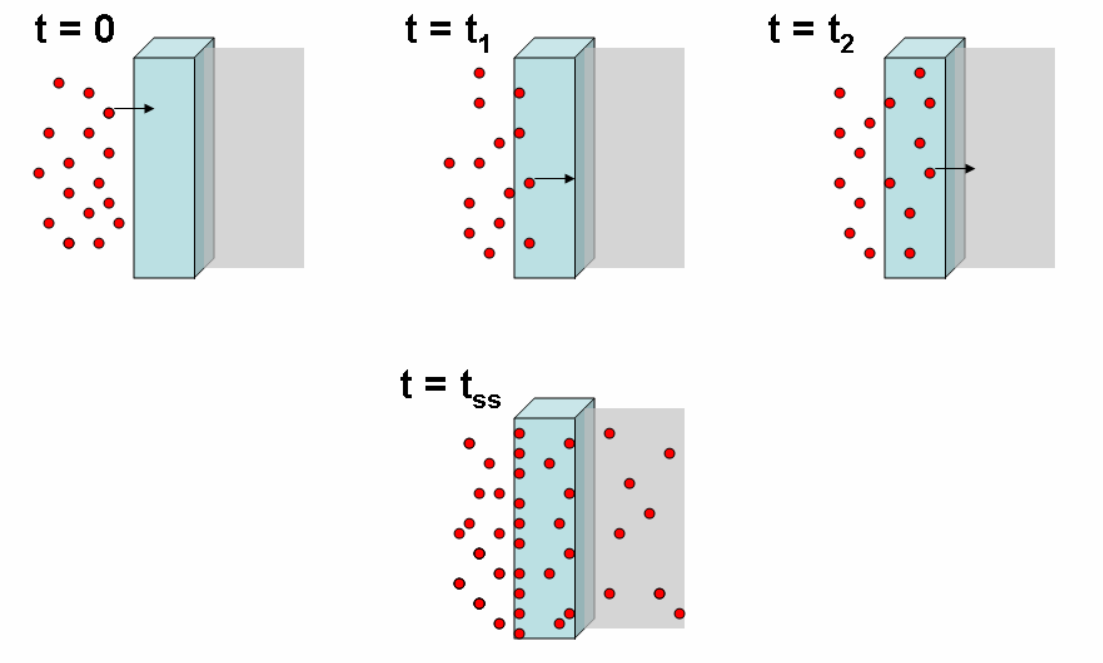

Figure 4.8. Schematic of the steps involved in DCE migration through an LDPE film. t=0 is the onset of the experiment where the DCE has to cross the LDPE barrier. t_1 occurs when the DCE travels across the LDPE film, t_2 is just before the DCE leaves the LDPE film, t_{ss} describes a time after the steady state concentration gradient is established and a constant migration rate is observed.

Taken together the E_p results raise an interesting dilemma. Despite having the slowest migration rates, c1,2-DCE appears to have the smallest permeation activation energy of the three isomers (although similar to t1,2-DCE within experimental error), a result that is not uncommon in temperature dependent diffusion studies.[44] Both permeation and diffusion activation energies have been known to increase with increasing migrant size.[43] This correlation *might* explain the differences in permeation activation energy between c1,2-DCE and t1,2-DCE since t1,2-DCE has a larger molecular volume. However, this correlation fails to account for the observed differences between the similarly sized isomers 1,1-DCE and c1,2-DCE. To reconcile these results, we recall that permeation is a function of both solubility and diffusion. Thus differences in permeation activation energies depend on the temperature dependence of *both* the diffusion coefficient *and* solubility constant for

each isomer. Thermogravametric analysis data (Shown in Figure 2.6) revealed that although all DCE isomers were mostly insoluble in LDPE (• 0.3% by mass), t1,2-DCE and 1,1-DCE were markedly less soluble than c1,2-DCE. LDPE films soaked overnight in c1,2-DCE showed a 0.3% mass loss at a temperature of 120 °C for three hours, while films soaked in either 1,1-DCE or t1,2-DCE showed no measurable (< 0.1%) mass loss. In contrast, LDPE films soaked in isooctane — a known plasticizing agent — showed mass loss of 3% (Figure 4.9). These differences in DCE solubility are similar when one compares the Henry's Law solubility constants for the isomers in water which are 0.27, 0.11, and 0.039 for c1,2-DCE, t1,2-DCE and 1,1-DCE respectively.[45] The solubility of the DCE isomers in water can be related to the solubility in any condensed phase such as LDPE, in the absence of significant entropic disorder, which is unlikely given the similar sizes of the isomers. The differences in solubility could account for the increased energy barrier that t1,2-DCE and 1,1-DCE must overcome to permeate through the polymer matrix. Since solubility studies show less t1,2-DCE, and 1,1-DCE in the polymer compared to c1,2-DCE, we propose that the isomers face a larger barrier to migration into the polymer compared to c1,2-DCE.

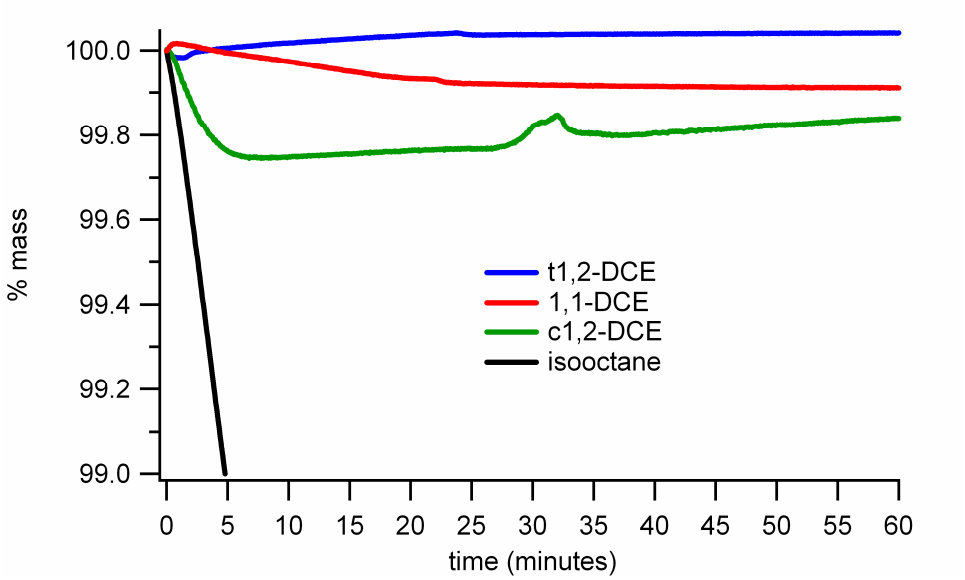

Figure 4.9. TGA analysis of DCE isomers and isooctane.

4.3 Conclusions

The studies described above sought to determine the effects of molecular structure on migration through food contact polymers. Our findings show that structural isomers can migrate at different rates that vary by more than a factor of three, and these differences do not correlate to calculated molecular radii of the isomers but do correlate to the isomer H_{vap} values. These results might be anticipated if one assumes that stronger intermolecular forces will slow migration from one side of the LDPE film to the other. Our findings are specific to the permeation rate of DCE isomers migrating through LDPE into Miglyol but imply a more general phenomenon. Such structural differences in permeability become increasingly important from a public health standpoint when one realizes that different isomers have different biological activity. The use of LDPE in permeation studies represents a worse case scenario since this polymer is a loose chain polymer that can allow facile analyte migration. However, this polymer is still widely used as a food contact polymer, so the concern about the migration behavior is warranted.

Future work with these isomers will focus on the effects of migrant concentrations on permeation rates. Using initial concentrations of ≤1% by volume the migration of t1,2-DCE and c1,2-DCE can be investigated at a single temperature as a function of initial concentration. Through these experiments we will further explore what role *molecular properties* of c1,2-DCE and t1,2-DCE play in migration and if isolated migrants behave similarly to bulk materials.

References

1. Bradley, E. L.; Speck, D. R.; Read, W. A.; Castle, L., Method of test and survey of caprolactam migration into foods packaged in nylon-6. *Food Additives and Contaminants* **2004,** 21, (12), 1179-1185.

2. Lopez-Cervantes, J.; Paserio-Losada, P., Determination of bisphenol A in, and its migration from, PVC stretch film used for food packaging. *Food Additives and Contaminants* **2003,** 20, (6), 596-606.

3. Garde, J. A.; Catala, R.; Gavara, R.; Hernandez, R. J., Characterizing the migration of antioxidants from polypropylene into fatty food simulants. *Food Additives and Contaminants* **2001,** 18, (8), 750-762.

4. Dopico-Garcia, M. S.; Lopez-Vilarino, J. M.; Gonzalez-Rodriguez, M. V., Antioxidant Content of and Migration from Commercial Polyethylene, Polypropylene, and Polyvinyl Chloride Packages. *Journal of Agricultural and Food Chemistry* **2007,** 55, 3225-3231.

5. Matsuga, M.; Kawamura, Y.; Sugita-Konishi, Y.; Hara-Kudo, Y.; Takatori, K.; Tanamoto, K., Migration of formaldehyde and acetaldehyde into mineral water in

polyethylene terephthalate (PET) bottles. *Food Additives and Contaminants* **2006,** 23, (2), 212-218.

6. Haldimann, M.; Blanc, A.; Dudler, V., Exposure to antimony from polyethylene terephthalate (PET) trays used in ready-to-eat meals. *Food Additives and Contaminants* **2007,** 24, (8), 860-868.

7. Limm, W.; Hollifield, H. C., Effects of temperature and mixing on polymer adjuvant migration to corn oil and water. *Food Additives and Contaminants* **1995,** 12, 609-624.

8. Reynier, A.; Dole, P.; Humbel, S.; Feigenbaum, A., Diffusion Coefficients of Additives in Polymers 1. Correlation with Geometric Parameters. *Journal of Applied Polymer Science* **2001,** 82, 2422-2433.

9. Saleem, M.; Asfour, A.-F. A.; Kee, D. D., Diffusion of Organic Penetrants through Low Density Polyethylene (LDPE) Films: Effect of Size and Shape of the Penetrant Molecules. *Journal of Applied Polymer Science* **1989,** 37, 617-625.

10. Feigenbaum, A.; Dole, P.; Aucejo, S.; Dainelli, D.; Garcia, C. D. L. C.; Hankemeier, T.; N'gono, Y.; Papaspyrides, C. D.; Paserio, P.; Pastorelli, S.; Pavlidou, S.; Pennarun, P. Y.; Saillard, P.; Vidal, L.; Vitrac, O.; Voulzatis, Y., Functional barriers: Properties and evaluation. *Food Additives and Contaminants* **2005,** 22, (10), 956-967.

11. Moisan, J. Y., Additive diffusion in polyethylene I. Influence and nature of additives. *European Polymer Journal* **1980,** 16, 979-987.

12. Limm, W.; Hollifield, H. C., Modelling of additive diffusion in polyolefins. *Food Additives and Contaminants* **1996,** 13, 949.

13. Brandsch, J.; Mercea, P.; Ruter, M.; Tosa, V.; Piringer, O., Migration modelling as a tool for quality assurance of food packaging. *Food Additives and Contaminants* **2002,** 19, (Supplement), 29-41.

14. Begley, T. H.; Castle, L.; Feigenbaum, A.; Franz, R.; Hinrichs, K.; Lickley, T.; Mercea, P.; Milana, M.; O'Brien, A.; Rebre, S.; Rijk, R.; Piringer, O., Evaluation of migration models that might be used in support of regulations for food-contact plastics. *Food Additives and Contaminants* **2005,** 22, (1), 73-90.

15. Dole, P.; Voulzatis, Y.; Vitrac, O.; Reynier, A.; Hankemeier, T.; Aucejo, S.; Feigenbaum, A., Modelling of migration from multi-layers and functional barriers: Estimation of parameters. *Food Additives and Contaminants* **2006,** 23, (10), 1038-1052.

16. Begley, T. H.; Hsu, W.; Noonan, G.; Diachenko, G., Migration of fluorochemical paper additives from food-contact paper into foods and food simulants. *Food Additives and Contaminants* **2007,** 25, (3), 384-392.

17. Begley, T. H.; White, K.; Honigfort, P.; Twaroski, M. L.; Neches, R.; Walker, R. A., Perfluorochemicals: Potential sources of and migration from food packaging. *Food Additives and Contaminants* **2005,** 22, (10), 1023-1031.

18. Begley, T. H.; Gay, M. L.; Hollifield, H. C., Determination of the migrants in and migration from nylon food packaging. *Food Additives and Contaminants* **1995,** 12, 671-676.

19. Biles, J. E.; McNeal, T. P.; Begley, T. H.; Hollifield, H. C., Determination of bisphenol A in reusable polycarbonate food-contact plastics and migration to food-simulating liquids. *Journal of Agricultural and Food Chemistry* **1997,** 45, 3541-3544.

20. Brede, C.; Fjeldal, P.; Skjevrak, I.; Herikstad, H., Increased migration levels of bisphenol A from polycarbonate baby bottles after dishwashing, boiling and brushing. *Food Additives and Contaminants* **2003,** 20, 684-689.

21. Franz, R.; Welle, F., Migration measurement and modelling from poly(ethylene terephthalate) (PET) into soft drinks and fruit juices in comparison with food simulants. *Food Additives and Contaminants* **2008,** iFirst.

22. Begley, T. H.; Biles, J. E.; Cunningham, C.; Piringer, O., Migration of a UV stabilizer from polyethylene terephthalate (PET) into food simulants. *Food Additives and Contaminants* **2004,** 21, 1007-1014.

23. Consumer Factsheet on: 1,1-dichloroethylene. http://www.epa.gov/safewater/dwh/c-voc/11-dichl.html (Febuary 28th, 2008),

24. Consumer Factsheet on: 1,2-dichloroethylene. http://www.epa.gov/OGWDW/dwh/c-voc/12-dich2.html (Febuary 28th, 2008),

25. Garbarini, G. R.; Eaton, R. F.; Kwei, T. K.; Tobolsky, A. V., Diffusion and Reverse Osmosis through Polymer Membranes. *Journal of Chemical Education* **1971,** 48, 226.

26. Vergnaud, J. M., *Liquid transport processes in polymeric materials: modeling and industrial applications*. Prentice Hall: Englewood Cliffs, NJ, 1991.

27. Crank, J.; Park, G. S., *Diffusion in Polymers*. Academic Press Inc.: London, 1968.

28. Crank, J., *The Mathematics of Diffusion*. 2nd ed.; Oxford University Press: New York, 1975.

29. Zweifel, H., *Plastics Additives Handbook*. 5th ed.; Hanser: Cincinnati, 2001.

30. *Plastic Packaging Materials for Food: Barrier Function, Mass Transport, Quality Assurance and Legislation*. Wiley-VCH: New York, 2000.

31. Al-Malaika, S.; Goonetileka, M. D. R. J.; Scott, G., Migration of 4-substituted 2-hydroxy benzophenones in low density polyethylene: Part1- Diffusion characteristics. *Polymer Degradation and Stability* **1991,** 32, (2), 231-247.

32. Berens, A. R.; Hopfenberg, H. B., Diffusion of organic vapors at low concentrations in glassy PVC, polystyrene, and PMMA. *Journal of Membrane Science* **1982,** 10, 283-303.

33. Moisan, J. Y., *European Polymer Journal* **1981,** 8, 857-864.

34. Schwope, A. D.; Goydan, R.; Reid, R. C.; Krishnamurthy, S., Sate-of-the-Art Review of Permeation Testing and the Interpretation of Its Results. *American Industrial Hygiene Association Journal* **1988,** 49, (11), 557-565.

35. Piergiovanni, L.; Fava, P.; Schiraldi, A., Study of Diffusion through LDPE film of Di-*n*-butyl phthalate. *Food Additives and Contaminants* **1999,** 16, (8), 353-359.

36. Aminabhavi, T. M.; Naik, H. G., Molegular migration of low sorbing organic liquids into polymeric geomembranes. *Polymer International* **1999,** 48, 373-381.

37. *CRC Handbook of Chemistry and Physics*. 77 ed.; CRC Press, Inc.: New York, 1996.

38. Aminabhavi, T. M.; Phayde, H. T. S., Sorption, Desorption, Resorption, Redesorption, and Diffusion of Haloalkanes into Polymeric Blend of Ethylene-Propylene Random Copolymer and Isotatic Polypropylene. *Journal of Applied Polymer Science* **1995,** 57, 1419-1428.

39. Kariduraganavar, M. Y.; Kulkarni, S. B.; Kulkarni, S. S.; Kittur, A. A., Studies on Molecular Transport of n-Alkanes Through Poly(tetrafluoroethylene-co-propylene) Elastomeric Membrane. *Journal of Applied Polymer Science* **2006,** 101, 2228-2235.

40. Kulkarni, S. B.; Karidurganavar, M. Y.; Aminabhavi, T. M., Sorption, Diffusion, and Permation of Esters, Aldehydes, Ketones, and Aromatic Liquids into Tetrafluoroethylene/Propylene at 30, 40, and 50^{o}C. *Journal of Applied Polymer Science* **2003,** 89, 3201-3209.

41. O'Brien, A.; Cooper, I., Polymer additive migration to foods -- a direct comparison of experimental data and values calculated from migration models for polypropylene. *Food Additives and Contaminants* **2001,** 18, (4), 343-355.

42. Schwarz, T.; Steiner, G.; Koppelmann, J., Measurement of Diffusion of Antioxidants in Isotactic Polypropylene by Isothermal Differential Thermal Analysis. *Journal of Applied Polymer Science* **1989,** 38, 1-7.

43. Harogoppad, S. B.; Aminabhavi, T. M., Diffusion and Sorption of Organic Liquids through Polymer Membranes. 5. Neoprene, Styrene-Butadiene-Rubber, Ethylene-Propylene-Diene Terpolymer, an dNatural Rubber versus Hydrocarbons (C_8-C_{16}). *Macromolecules* **1991,** 21, 2598-2605.

44. Choi, J. O.; Jitsunari, F.; Asakawa, F.; Lee, D. S., Migration of styrene monomer, dimers and trimers from polystyrene to food simulants. *Food Additives and Contaminants* **2005,** 22, (7), 693-699.

45. Gossett, J. M., Measurement of Henry's law constants for C1 and C2 chlorinated hydrocarbons. *Environmental Science and Technology* **1987,** 21, 202-208.

Chapter 5 Migration of Dilute Dichloroethylene Isomer Solutions through LDPE: Effects of Migrant Concentration

5.1 Introduction

In recent years, reports of chemical migration out of and through food contact polymers have raised concerns about the long term health risks from the national food supply.[1-5] One recent example is the migration of Bisphenol-A (BPA), a disruptor of endocrine activity, out of polycarbonate drinking bottles into water or from epoxy can coatings into foods where it is used as a stabilizer.[3, 4] The general population's exposure comes from these polycarbonate bottles and can linings, despite the fact that migration levels of BPA under normal use conditions are below the specific migration limits set by regulators.[3-5] Another example of additive migration is perfluorooctanoic acid (PFOA), a processing aid in the production of polytetrafluroethylene (PTFE) and a contaminant in some fluorochemicals. PFOA has been classified as weakly carcinogenic.[6] The population's exposure to PFOA can come from such substances as non-stick cookware, fast food paper, microwaveable popcorn bags, or carpets and clothing.[7] Given its low reactivity, PFOA accumulates in the body over time. Due to the widespread use of PTFE, elderly Americans have on average a 40 nM concentration of PFOA in their bloodstream.[8] A third, low molecular weight additive to polymers, caprolactam, has also been shown to migrate relatively rapidly from plastics into contact materials.[9] This migrant's long-term biological activity remains poorly characterized, but short term effects of exposure to caprolactam include topical irritation and seizures. With the rising use of new and recycled food contact polymers in food applications, issues related to food safety and

contamination will remain high priorities for consumer groups, manufacturers and public policy makers. These same issues associated with analyte migration out of polymers are also relevant to exigent toxins and contaminants brought into contact externally with these same polymers.

Traditionally, concern for neat liquid migration through polymers has been focused in the area of chemical protective clothing and waste containers.[10-17] The standard ASTM permeation cell used in many experiments is similar to our own migration cells shown in Chapter 2 of this thesis.[12] Aminabhavi et al. investigated the migration parameters of many organic solvents through different polymers such as polypropylene, high density polyethylene, and neoprene.[18-20] In the case of long chain alkanes, migration depends on both the penetrant molecule and the membrane material.[18] A survey of organic liquid migration through various polyethylene membranes revealed that esters had lower migration rates than other organic compounds.[19] Migration studies of short chain chloroalkanes led to the conclusion that diffusion and permeation through copolymer membranes donot correlate with migrant size, a conclusion that is similar to observations in Chapter 4.[20]

Saleem et al. investigated the size and shape effect of molecules migrating through LDPE.[21] One system of particular interest in this study is the migration of xylene isomers through LDPE. The diffusion coefficients of the xylene isomers ranged from $1.567 - 0.940 \times 10^{-12}$ cm^2/s for p-xylene and o-xylene respectively.[21] This difference in migration is markedly smaller than that observed for the neat migration of dichloroethylene isomers discussed in Chapter 4 of this thesis. Importantly, Saleem et al. noted that of the xylene isomers studied, o-xylene has the

smallest diffusion coefficient of the isomers despite having the smallest molar volume of the three isomers. This result is similar to the migration behavior we observe with neat c1,2-DCE migration through LDPE in Chapter 4 where the smaller c1,2-DCE has a smaller permeation coefficient compared to the larger t1,2-DCE.

The differences in permeation coefficients of neat DCE migration through LDPE for c1,2-DCE and t1,2-DCE raises several interesting questions. Permeation depends on both solubility of the analyte in the polymer, as well as the diffusion of the analyte through the polymer. Activation energies of permeation resulting from an Arrhenius treatment of the permeation data showed c1,2-DCE to have a slightly lower barrier to migration compared to t1,2-DCE. Because permeation depends on two properties - diffusion and solubility – interpreting these results requires analysis of how both diffusion and solubility depend on temperature. One plausible explanation of permeation activation energy results observation could be due to the differences in the solubility of c1,2-DCE in LDPE compared to t1,2-DCE. Solubility becomes less of a factor at low concentrations, when there is much less migrant present to be solvated in the polymer matrix. Experiments described in this chapter examine separately the permeation of c1,2-DCE and t1,2-DCE in Miglyol (1% by volume) through LDPE into pure Miglyol. These low concentrations are similar to the concentrations in which additives are added to food contact polymers. Results again show that t1,2-DCE again migrates through the polymer faster than c1,2-DCE. Temperature dependent studies show that the permeation activation energies of both migrants to increase significantly relative to migration from the neat DCE liquid. These permeation activation energies appear to be similar for both low concentration

isomers to within experimental uncertainty. These results suggest strongly that when solubility is not limiting, migration is controlled by an interfacial resistance associated with the migrant passing across the solution/polymer interface.

5.2 Results and Discussion

The migration rates of c1,2-DCE and t1,2-DCE solutions in Miglyol migrating through LDPE into pure Miglyol will be discussed in terms of permeation. Permeation (P) is a function of both diffusion (D) and solubility (S).[22-26]

$$P = DS \tag{5.1}$$

Diffusion is a measure of how fast an analyte moves through a polymer. Solubility defines a migrant's solubility is in a polymer matrix and is usually expressed in terms of mole or weight percent. Permeability measures how much analyte has gone through a polymer, the quantity measured in our experiments. Therefore, if diffusion is slow but solubility is high, permeation will be slow; if diffusion is fast – but solubility low, permeation will still be slow. Fast permeation is a function of higher solubility of the analyte in the polymer and fast diffusion of the analyte through the polymer.

When considering the diffusion of a gas through a polymer film after steady state diffusion is reached, the flux (F) can be described by the diffusion coefficient (D) through the following expression:[23-27]

$$F = -D\frac{dC}{dx} = \frac{D(C_1 - C_2)}{l} \tag{5.2}$$

where C_1 and C_2 are the surface concentrations (just inside the film surface) on either side of the polymer film, and l is the thickness of the film. Since C_1 and C_2 are not

easily determined, a direct measurement of diffusion through a film is often hard to determine experimentally. An more accessible quantity to measure is the permeation which can be determined with the vapor pressures on either side of the polymer film.[22-27]

$$F = \frac{P(p_1 - p_2)}{l} \tag{5.3}$$

where p_1 and p_2 are the external vapor pressures on either side of the film. If Henry's law is obeyed, C_i is related through p_i through the solubility constant mentioned in Equation 5.1.[22-26]

$$C_i = Sp_i \qquad (i = 1 \text{ or } 2) \tag{5.4}$$

Similar considerations apply for liquids migrating through a polymer film. In the case of liquid migration, p_1 and p_2 are now described in terms of the bulk concentrations on either side of the film, C_1^{bulk} and C_2^{bulk}:[23-25]

$$F = P\frac{C_1^{bulk} - C_2^{bulk}}{l} \tag{5.5}$$

By monitoring the change in concentration on the low concentration side of the film, P can be found experimentally. Using the slope of the change in concentration versus change in time once steady state diffusion is reached P can be found by:[25]

$$P = \frac{(slope)(l)}{(A_{cs})(\Delta C)} \tag{5.6}$$

where A_{cs} is the cross sectional area of the film exposed to the analyte, and ΔC is the difference in the bulk concentrations on either side of the film at the onset of the experiment (for the experiments described in this work C_2^{bulk} is zero).

Dilute permeation experiments used solutions of 1% (by volume) DCE in Miglyol as the donor compound. Measurements were taken over a period of 3-4 hours depending on temperature. The permeation rates for c1,2-DCE and t1,2-DCE at 25 ^{o}C are shown in Figure 5.1. Since the migration rate is used to determine the permeation coefficient (Equation 5.6) t1,2-DCE has a larger permeation coefficient than c1,2-DCE at 1% by volume concentrations.

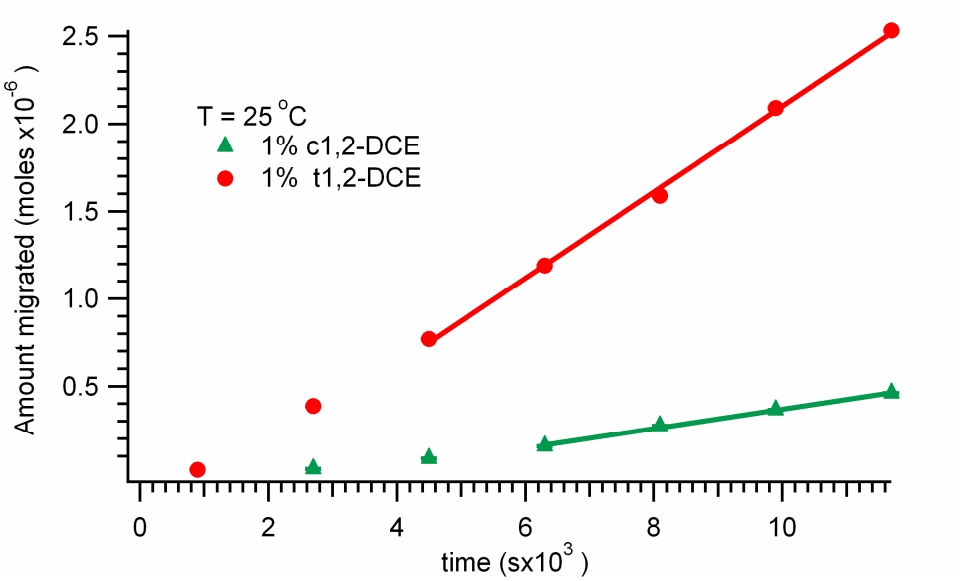

Figure 5.1. Permeation of 1% (by volume DCE in Miglyol) c1,2-DCE and t1,2-DCE at 25 ^{o}C.

Permeation of migrants through polymers should be sensitive to many variables including analyte size and interactions with surroundings. Given differences in permeation constants for t1,2-DCE versus c1,2-DCE one might imagine that the different migration rates might be a function of the sizes of the analytes. Isomer sizes were calculated using the van der Waals radii of the outer atoms, as well as reported bond lengths and bond angles to determine the molecular radii.[28] Use of the van der Waals parameters will introduce some errors, but the errors should be systematic and consistent for both isomers. As reported in Chapter 4

these calculations show t1,2-DCE to have a larger molecular radius of 4.02 Å that is ~15% larger than that of c1,2-DCE (3.47 Å). Based on these molecular radii calculations, any size based model used to describe permeation would predict t1,2-DCE to permeate more slowly, contrary to experimental results.

Since single temperature, dilute migration results demonstrate that migrant size does not correlate with the permeation coefficients, we need to consider what other factors may influence the experimental results. One property that differentiates the two isomers is the presence of a dipole for c1,2-DCE (1.85D) and lack of one for t1,2-DCE. This dipole of c1,2-DCE can affect permeation in several ways. Dipole pairing between analytes, or pairing between the analyte and the Miglyol solvent can lead to correlated motion of monomers in solution and a larger effective radius. Dipole-induced dipole interactions with the LDPE may also slow the migration of c1,2-DCE relative to t1,2-DCE. To help develop a clearer understanding of the migrant properties that affect diffusion, we investigated permeation of 1%v/v DCE in Miglyol at different temperatures, to see if the same behavior persisted.

Migration studies using solutions of 1% by volume c1,2-DCE and t1,2-DCE in Miglyol migration cells were carried out at 20, 25, and 30 ^{o}C. Results are shown in Figure 5.2. Permeation coefficients for c1,2-DCE and t1,2-DCE are shown in Table 5.1. Typically, permeation increases with increasing temperature. Similar to observations at 25 ^{o}C, t1,2-DCE permeates ~ 4 times faster than c1,2-DCE at all temperatures. Figure 5.2a and b illustrate the rates of migration at 20 and 30 ^{o}C. Comparing the slopes of the lines in Figure 5.2c, one observes that t1,2-DCE permeation depends more sensitively on temperature than c1,2-DCE (2.4×10^{-9} and

5.2×10^{-10} $cm^2/s*K$ respectively) as expected considering the rates of migration shown at different temperatures. An important point to note is that isomer dependent differences in permeation coefficients for dilute migration are larger than the differences reported in Table 4.1 for neat permeation. c1,2-DCE dilute permeation decreases by a full order of magnitude. t1,2-DCE permeation decreases by a factor of ~2. The temperature dependence of the permeation rates motivates the need to determine permeation activation energies.

Temp (K)	$\mathbf{P_{c\text{-}1,2\text{-}DCE}}$ **(*10^9)**	$\mathbf{P_{t\text{-}1,2\text{-}DCE}}$ **(*10^9)**
293.1	1.0 ± 0.2	4 ± 1
298.1	3.8 ± 1.0	17 ± 4
303.1	6.2 ± 0.6	28 ± 6
$\mathbf{E_P}$ **(kJ/mol)**	136 ± 35	147 ± 38

Table 5.1. Permeation coefficients of 1% by volume solutions of t1,2-DCE and c1,2-DCE in Miglyol. The last column shows the calculated permeation activation energies.

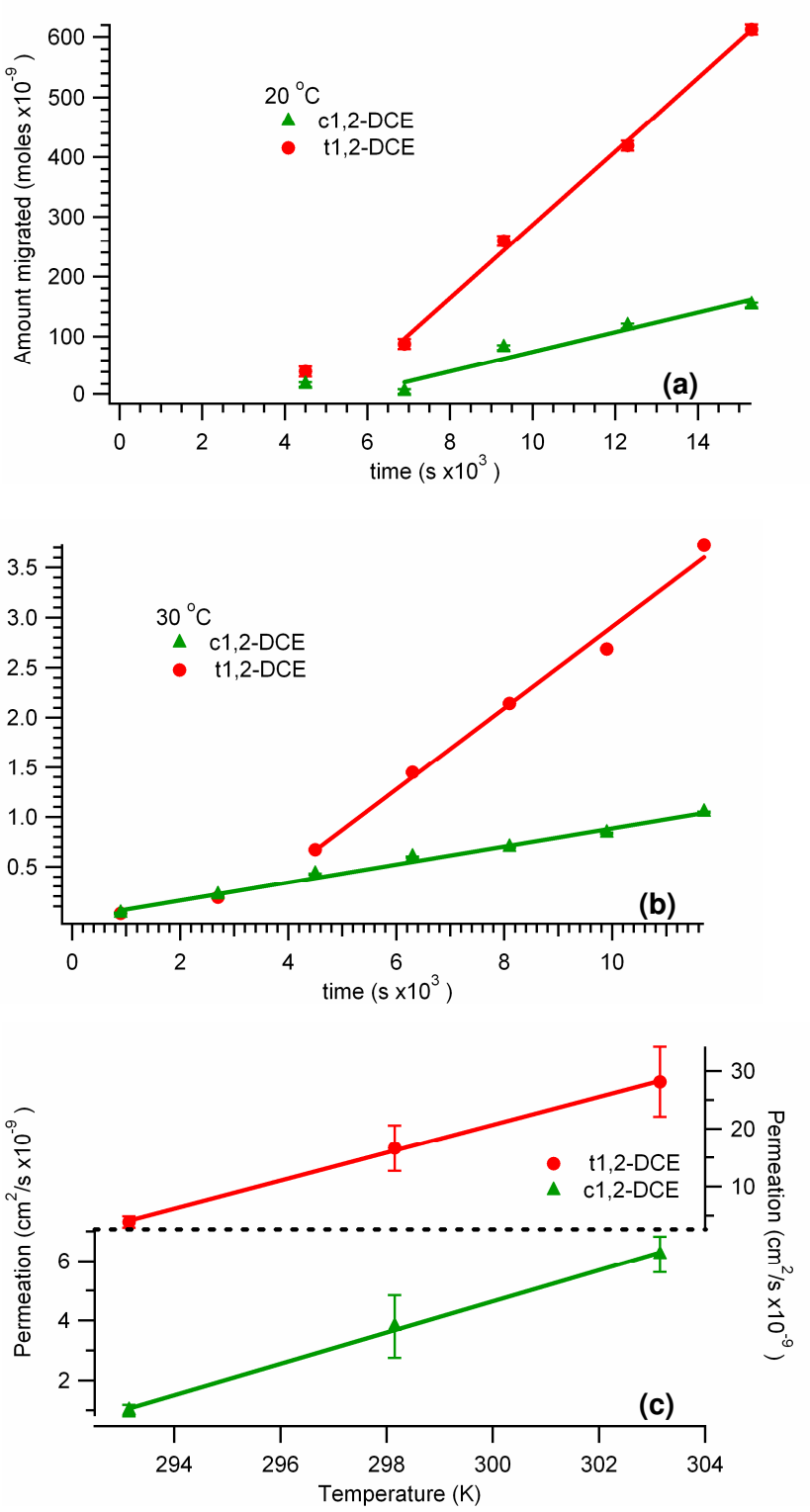

Figure 5.2. 1% by volume DCE permeation at different temperatures. (a) Permeation rate for DCE at 20 °C (b) permeation rate at 30 °C (c) permeation coefficient as a function of temperature.

An Arrhenius treatment of the data would determine a permeation activation energy by using the following Arrhenius-type equation:[18, 19, 29-31]

$$P = P_0 \exp\left(\frac{-E_P}{RT}\right) \tag{5.7}$$

where P_0 is the preexponential factor, E_P is the activation energy for permeation, R is the universal gas constant, and T is the temperature. Similar to permeation, the activation energy for permeation will depend on the migrating molecule's interactions with the polymer matrix (solubility), as well as the motion of the molecule through the polymer (diffusion). In addition to these quantities that directly impact permeation, other interactions can have secondary effects on permeation. These interactions include (but are not limited to), DCE/Miglyol interactions in solution, dipole-dipole, and the formation of a barrier layer by the Miglyol at the LDPE/solution interface. Such a barrier may not impede passage of DCE across the interface, but could slow the rate at which the DCE can approach the polymer surface. Figure 5.3 shows a plot of ln P versus 1/T for the 1% v/v DCE isomers in Miglyol solutions. The E_P values for c1,2-DCE and t1,2-DCE are 136 24 and 147 38 kJ/mol respectively, and are reported in Table 5.1. Again, the results for t1,2-DCE is slightly larger than that of c1,2-DCE but these values should be viewed as indistinguishable given experimental uncertainties. These numbers represent a significant increase compared to the E_P values for the neat permeation experiments of c1,2-DCE and t1,2-DCE (36 and 47 kJ/mol respectively). The increase in activation energies could be a product of the lower concentrations in bulk solutions. Fewer DCE molecules will necessarily lead to diminished permeation rates. Furthermore, the solubility contribution to permeation will reflect the *partitioning* of DCE between

LDPE and Miglyol, rather than the total amount of DCE accommodated by LDPE in contact with a neat DCE solvent.

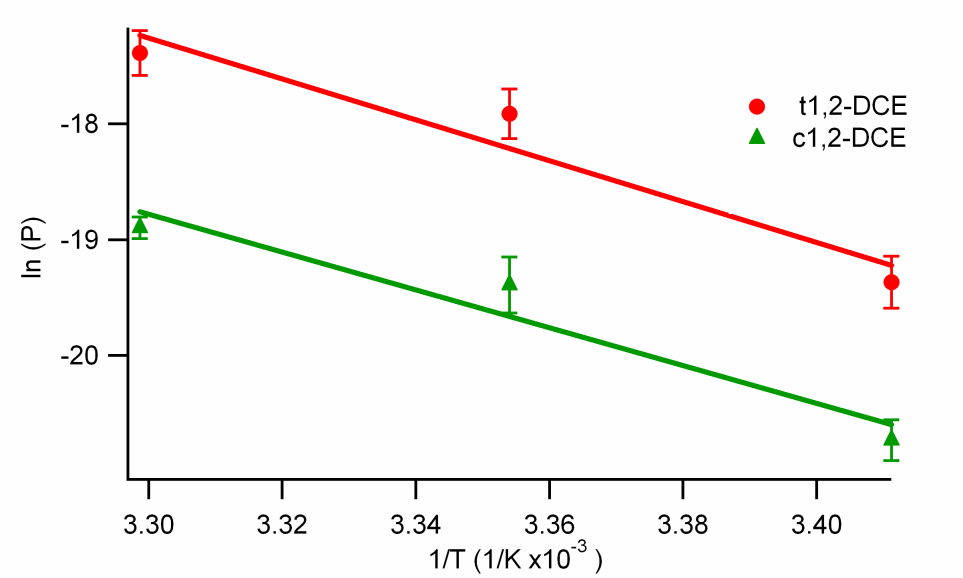

Figure 5.3. Arrhenius plot of ln P vs 1/T for 1% v/v t1,2-DCE and c1,2-DCE in Miglyol.

Experiments comparing the effects of migrant concentration on permeation (Chapters 4 and 5) illustrate clearly that conditions outside the polymer film will affect significantly not only the absolute permeation rates, but also the temperature dependence of analyte migration. From the reported data one concludes that permeation coefficients for DCE from the dilute solutions are smaller (compared to neat), and that permeation activation energies are larger. For a given composition (neat or 1%), t1,2-DCE always permeates through LDPE faster than c1,2-DCE.

These high and low concentration experiments are identical except for the composition of the donor side of the cell (Figure 5.4). Slower permeation coefficients are likely a function of the lower concentrations used. Equation 5.6 used to calculate the permeation coefficient from steady state migration rates predict that smaller

differences in concentration should lead to slower permeation. The C value in the case of the dilute solutions of DCE in Miglyol will be 1% not 100%. This contribution to the permeation would predict that permeation coefficients should decrease by a factor of 100, were the concentration gradients the sole driving force responsible for permeation. However the observed decrease in the steady-state slopes used to calculate permeation coefficients is ~ 400 times smaller for the dilute migration than neat. The temperature dependence of these rates is responsible for E_P values that are significantly larger than those calculated for migration across LDPE from neat DCE solutions.

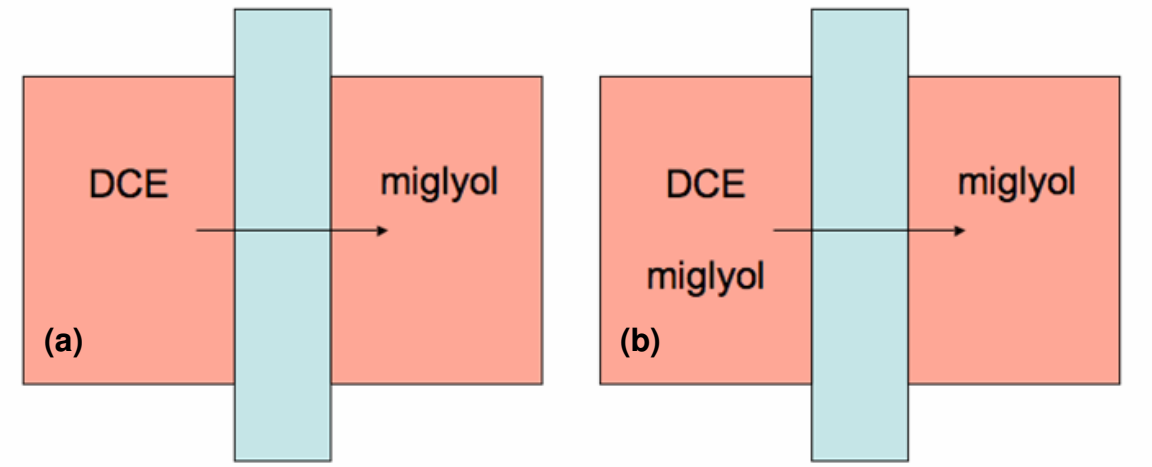

Figure 5.4. Comparison of the donor side of the migration cells in (a) neat and (b) dilute DCE migration experiments

Permeation depends on diffusion and solubility. Permeation and diffusion are both activated processes. If we consider the solubility to be the partitioning constant of the DCE between Miglyol and LDPE one can derive the following relationship from Equation 5.7:

$$P_0 \exp\left(\frac{-E_P}{RT}\right) = D_0 \exp\left(\frac{-E_D}{RT}\right)\exp\left(\frac{-\Delta G_{part}}{RT}\right) \qquad (5.8)$$

where E_D is the diffusion activation energy, and ΔG_{part} is the free energy of partitioning of DCE between LDPE and Miglyol. Assuming that P_0 and D_0 do not exhibit a temperature dependence, and are dependent on properties of the polymer and migrant molecule, we can simplify the expression to

$$E_P = E_D + \Delta G_{part} \tag{5.9}$$

E_P values have already been determined experimentally for neat and dilute migration through LDPE. Using standard models for migration, we can estimate diffusion coefficients at the temperature range used in experiments to estimate a E_D.[7, 22, 32, 33] Thus, with quantities for both the activation energies, we can determine ΔG_{part}, which allows us to calculate a partitioning constant of the DCE between Miglyol and LDPE. In the absence of other competing factors, this analysis predicts differences in partitioning constants of ~600 for c1,2-DCE versus t1,2-DCE (with the c1,2-DCE being more soluble in LDPE than t1,2-DCE). This last result agrees qualitatively with the results from TGA experiments described in Chapter 2.

5.3 Conclusions

The studies described above sought to determine the effects of dilute concentrations on migration of isomers through food contact polymers. The permeation coefficients of c1,2-DCE and t1,2-DCE were still different, with t1,2-DCE having larger permeation coefficient, similar to observations with migration of neat DCE. Given that the neat and dilute DCE experiments are equivalent in every way except for the composition of the initial migrant solution, these results suggest that the limiting quantity controlling permeation is migrant solubility in the polymer film. When little migrant is available to pass through the LDPE, permeation slows

but the non polar migrant, t1,2-DCE, still passes through the film ~ 4 times faster than the more polar c1,2-DCE. This is most likely due to the lack of intermolecular attractive forces for t1,2-DCE (dipole moment and polarizabillity). The large differences in permeation of c1,2-DCE and t1,2-DCE illustrate how differently two molecules with equivalent masses can migrate. Migration models that only consider molecular weight of migrating analytes are ignoring important "chemical details" that impact migration. As shown in the work of Chapters 4 and 5 of this thesis, "chemical details" significantly impact migration rates.

References

1. Begley, T. H.; Hsu, W.; Noonan, G.; Diachenko, G., Migration of fluorochemical paper additives from food-contact paper into foods and food simulants. *Food Additives and Contaminants* **2007,** 25, (3), 384-392.

2. Bradley, E. L.; Read, W. A.; Castle, L., Investigation into the migration potential of coating materials from cookware products. *Food Additives and Contaminants* **2007,** 24, (3), 326-335.

3. Maragou, N. C.; Makri, A.; Lampi, E. N.; Thomaidis, N. S.; Koupparis, M. A., Migration of bisphenol A from polycarbonate baby bottles under real use conditions. *Food Additives and Contaminants* **2008,** 25, (3), 373-383.

4. Munguia-Lopez, E. M.; Gerardo-Lugo, S.; Peralta, E.; Bulmen, S.; Soto-Valdez, H., Migration of bisphenol A (BPA) from can coatings into a fatty food simulant and tuna fish. *Food Additives and Contaminants* **2005,** 22, (9), 892-898.

5. Lopez-Cervantes, J.; Paserio-Losada, P., Determination of bisphenol A in, and its migration from, PVC stretch film used for food packaging. *Food Additives and Contaminants* **2003,** 20, (6), 596-606.

6. Gerald. L. Kennedy, J.; Butenhoff, J. L.; Olsen, G. W.; O'Connor, J. C.; Seacat, A. M.; Perkins, R. G.; Biegel, L. B.; Murphy, S. R.; Farrar, D. G., The Toxicology of Perfluorooctanoate. *Critical Reveiws in Toxicology* **2004,** 34, (4), 351-384.

7. Begley, T. H.; Castle, L.; Feigenbaum, A.; Franz, R.; Hinrichs, K.; Lickly, T.; Mercea, P.; Milana, M.; O'Brien, A.; Rebre, S.; Rijk, R.; Piringer, O., Evaluation of migration models that might be used in support of regulations for food-contact plastics. *Food Additives and Contaminants* **2005,** 22, (1), 73-90.

8. Olsen, G. W.; Burris, J. M.; Burlew, M. M.; Mandel, J. H., Epidemiologic assessment of worker serum perfluorooctanesulfonate (PFOS) and perfluorooctanoate (PFOA) concentrations and medical surveillance examinations. *Journal of Occupational and Environmental Medicine* **2003,** 45, (3), 260-270.

9. Stoffers, N. H.; Stormer, A.; Bradley, E. L.; Brandsch, R.; Cooper, I.; Linssen, J. P. H.; Franz, R., Feasibility study for the development of certified reference materials for specific migration testing. Part 1: Initial migrant concentration and specific migration. *Food Additives and Contaminants* **2004,** 21, (12), 1203-1216.

10. O'Callaghan, K.; Fredericks, P. M.; Bromwich, D., Evaulation of Chemical Protective Clothing by FT-IR/ATR Spectroscopy. *Applied Spectroscopy* **2001,** 55, (5), 555-562.

11. Schwope, A. D.; Goydan, R.; Reid, R. C.; Krishnamurthy, S., Sate-of-the-Art Review of Permeation Testing and the Interpretation of Its Results. *American Industrial Hygiene Association Journal* **1988,** 49, (11), 557-565.

12. Britton, L. N.; Ashman, R. B.; Aminabhavi, T. M.; Cassidy, P. E., Permeation and Diffusion of Enviornmental Pollutants through Flexible Polymers. *Journal of Applied Polymer Science* **1989,** 38, 227-236.

13. Chao, K. P.; Hsu, Y. P.; Chen, S. Y., Permeation of aromatic solvent mixtures through nitrile protective gloves. *Journal of Hazardous Materials* **2008,** 153, (3), 1059-1066.

14. Lind, M. L.; Johnsson, S.; Meding, B.; Bowman, A., Permeability of hair dye compounds p-phenylenediamine, toluene-2,5-diaminesulfate and resorcinol through protective gloves in hairdressing. *Annals of Ocupational Hygiene* **2007,** 51, (5), 479-485.

15. Makela, E. A.; Vainiatlo, S.; Peltonen, K., The permeability of surgical gloves to seven chemicals commonly used in hospitals. *Annals of Occupational Hygiene* **2003**.

16. Chao, K. P.; Lee, P. H.; Wu, M. J., Organic solvents permeation through protective nitrile gloves. *Journal of Hazardous Materials* **2003,** 99, (2), 191-201.

17. Daugherty, M. L.; Watson, A. P.; Tuan, V. D., Currently available permeability and breakthrough data characterizing chemical warfare agents and their simulants in civilian protective clothing materials. *Journal of Hazardous Materials* **1992,** 30, (3), 243-267.

18. Harogoppad, S. B.; Aminabhavi, T. M., Diffusion and Sorption of Organic Liquids through Polymer Membranes. 5. Neoprene, Styrene-Butadiene-Rubber, Ethylene-Propylene-Diene Terpolymer, an dNatural Rubber versus Hydrocarbons (C_8-C_{16}). *Macromolecules* **1991,** 21, 2598-2605.

19. Aminabhavi, T. M.; Naik, H. G., Molegular migration of low sorbing organic liquids into polymeric geomembranes. *Polymer International* **1999,** 48, 373-381.

20. Aminabhavi, T. M.; Harlapur, S. F.; Balundgi, R. H.; Ortego, J. D., An investigation of the long-term sorption kinetics and diffusion anomalies of chloroalkanes into tetrafluoroethylene/propylene copolymer membranes at 30, 45, and 60^{o}C. *Polymer* **1998,** 39, (5), 1067-1074.

21. Saleem, M.; Asfour, A.-F. A.; Kee, D. D., Diffusion of Organic Penetrants through Low Density Polyethylene (LDPE) Films: Effect of Size and Shape of the Penetrant Molecules. *Journal of Applied Polymer Science* **1989,** 37, 617-625.

22. *Plastic Packaging Materials for Food: Barrier Function, Mass Transport, Quality Assurance and Legislation*. Wiley-VCH: New York, 2000.

23. Crank, J., *The Mathematics of Diffusion*. 2nd ed.; Oxford University Press: New York, 1975.

24. Crank, J.; Park, G. S., *Diffusion in Polymers*. Academic Press Inc.: London, 1968.

25. Garbarini, G. R.; Eaton, R. F.; Kwei, T. K.; Tobolsky, A. V., Diffusion and Reverse Osmosis through Polymer Membranes. *Journal of Chemical Education* **1971,** 48, 226.

26. Vergnaud, J. M., *Liquid transport processes in polymeric materials: modeling and industrial applications*. Prentice Hall: Englewood Cliffs, NJ, 1991.

27. Zweifel, H., *Plastics Additives Handbook*. 5th ed.; Hanser: Cincinnati, 2001.

28. *CRC Handbook of Chemistry and Physics*. 77 ed.; CRC Press, Inc.: New York, 1996.

29. Aminabhavi, T. M.; Phayde, H. T. S., Sorption, Desorption, Resorption, Redesorption, and Diffusion of Haloalkanes into Polymeric Blend of Ethylene-Propylene Random Copolymer and Isotatic Polypropylene. *Journal of Applied Polymer Science* **1995,** 57, 1419-1428.

30. Kariduraganavar, M. Y.; Kulkarni, S. B.; Kulkarni, S. S.; Kittur, A. A., Studies on Molecular Transport of n-Alkanes Through Poly(tetrafluoroethylene-co-propylene) Elastomeric Membrane. *Journal of Applied Polymer Science* **2006,** 101, 2228-2235.

31. Kulkarni, S. B.; Karidurganavar, M. Y.; Aminabhavi, T. M., Sorption, Diffusion, and Permation of Esters, Aldehydes, Ketones, and Aromatic Liquids into Tetrafluoroethylene/Propylene at 30, 40, and 50^{o}C. *Journal of Applied Polymer Science* **2003,** 89, 3201-3209.

32. Brandsch, J.; Mercea, P.; Ruter, M.; Tosa, V.; Piringer, O., Migration modelling as a tool for quality assurance of food packaging. *Food Additives and Contaminants* **2002,** 19, (Supplement), 29-41.

33. Stoffers, N. H.; Brandsch, R.; Bradley, E. L.; Cooper, I.; Dekker, M.; Stormer, A.; Franz, R., Feasibility study for the development of certified reference materials for specific migration testing. Part 2: Estimation of diffusion parameters and

comparison of experimental and predicted data. *Food Additives and Contaminants* **2005,** 22, (2), 173-184.

Chapter 6 Summary and Future Directions

6.1 Summary

Research performed for this project characterized interactions that could lead to analyte migration from or through food contact polymers. Through the use of a variety of experimental techniques, we were able to simulate conditions where migration from food contact polymers would be possible. Measurements at the air/water interface were able to simulate conditions in which surface concentrations of additives would be increased due to migration and adsorption at the polymer/aqueous interface. Consequences for additive adsorption to the interface include decreased antioxidant activity in the polymer itself and changed packaging surface properties. Direct migration of neat and dilute DCE solutions through commonly available LDPE polymers into a fatty food simulant (Miglyol) was also investigated to determine the role played by chemical structure in mass transport through polymers.

6.1.1 Surface Activity

Isothermal compressions of IN1010 and IN1076 are irreversible after film collapse. Successive compressions of these molecules at the air/water interface exhibit an unusual hysteresis, where the lift off area decreases by a uniform amount. The decreasing lift off area indicates a loss of molecules at the air/water interface possibly through aggregation. Quantitative analysis of these isotherms show a larger loss of molecules to the IN1076 monolayers compared to IN1010, on a per molecule basis. The irreversible loss of molecules is a function of molecular structure. IN1076 is composed of a sterically hindered phenol attached to a C_{18} chain; IN1010 has 4

sterically hindered phenols extending from a central carbon. The long chain on IN1076 provides the opportunity for more interaction during a full compression, and the opportunity for chain entanglement and subsequently fewer free monomers when the film is re-expanded. The branched structure of IN1010 imparts to this additive much less intramolecular structural freedom. The sphere-like structure of IN1010 suggests weaker intermolecular interactions and the loss of fewer molecules between each compression. Complementary studies using vibrational sum frequency spectroscopy – a surface specific technique capable of recording vibrational spectra – show IN1076 to be disordered both at full monolayer coverage as well as with excess coverage, implying that the IN1076 hydrocarbon tails are not well organized. Spectra of IN1010 also show disorder in the monolayer films. Spectra also show a significant change in the subphase, as illustrated in a disappearance of intensity above 3100 cm^{-1}. This observation implies that full monolayers of IN1010 create disorder in the adjacent water layers whereas IN1076 leaves interfacial water structure largely unperturbed. These findings imply that IN1076 and IN1010 can both form aggregates spontaneously at high surface coverage and that these aggregates are highly disorganized. Consequences of increased interfacial aggregation are additive blooming, decreased antioxidant activity, and non uniform diffusion.

6.1.2 Neat Migration Studies

Migration experiments investigated the permeation of neat DCE isomers passing through LDPE into Miglyol at various temperatures. 1,1-DCE migrates with the fastest rate, while c1,2-DCE migrates slowest. Permeation coefficients were calculated from the migration data. Permeation comparisons at a single temperature

illustrate that molecular structure has a large effect on migration rates. Permeation coefficients did not correlate with molecular size, since 1,1-DCE (the fastest migrant) and c1,2-DCE (the slowest migrant) are approximately equivalent in size, and t1,2-DCE is ~15% larger (with an intermediate migration rate). Trends in the migration data for the isomers were consistent over a range of temperatures. The temperature dependences indicated that migration is an activated process. Permeation activation energies were calculated using an Arrhenius treatment of the temperature dependent migration data. 1,1-DCE had the largest E_P of 80 kJ/mol, t1,2-DCE and c1,2-DCE had energies of 47 8 kJ/mol and 36 10 kJ/mol respectively. Differences in the permeation activation energy are attributed to differences in solubility of the isomers in LDPE, with c1,2-DCE having the highest solubility. Solubility effects on permeation warrant an investigation of permeation from solutions containing low concentrations of DCE through LDPE into Miglyol. Typical empirical models used to estimate migration from food contact polymers only consider the molar mass of the migrant. Results from experiments investigating migration of different DCE isomers show considerable differences in migration rates due to molecular structure.

6.1.3 Dilute Migration Studies

Migration experiments with 1% by volume solutions of c1,2-DCE and t1,2-DCE in Miglyol through LDPE were performed at various temperatures. Permeation coefficients for dilute solutions decreased compared to those of neat DCE permeating through LDPE. t1,2-DCE permeated at a faster rate than c1,2-DCE. Permeation increased as a function of temperature. An Arrhenius treatment of

temperature dependent permeation coefficients yielded activation energies of 136 35 and 147 38 kJ/mol for c1,2-DCE and t1,2-DCE respectively. The increased activation energies (relative to those calculated from the bulk DCE data) could likely be caused by the decrease in concentration, which would decrease the number of molecules in direct contact with the polymer film, thus decreasing the amount of permeation that is able to occur.

6.2 Future Directions

6.2.1 Surface Activity

The surface activity of IN1010 and IN1076 can be continued with a new addition to our Langmuir trough. Recently, a dipper was purchased which has the ability to make Langmuir-Blodgett films. One particular study of interest is to observe films deposed on glass slides using Polarization Modulation Infrared Reflection-Absorption Spectroscopy (PM-IRRAS). The goal of these experiments would be to determine if there is a systematic increase in IR intensity as a function of monolayer compression. Preliminary studies of films made manually suggest that such studies are feasible (Appendix 2), but will require careful control of monolayer preparation.

Using three new molecules, 2,2-bis(4-hydroxyphenyl)propane (bisphenol A, BPA), bis(2-hydroxyphenyl)methane (bisphenol F, BPF), and polychlorinated biphenols (PCBs), surface tension measurements at the air/water interface can reveal whether or not these molecules show a tendency to aggregate at interfaces. BPA and BPF are common additives to food contact materials including polycarbonate drinking bottles as well as epoxy can coatings.[1, 2] PCB is a chemical regulated by the

EPA that was used in many applications including coolant for transistors, caulking and fluorescent lights.[3] Structures and molar masses of these compounds are shown in Figure 6.1. These molecules are good candidates for surface tension measurements at the air/water interface since they have low water solubilities, and amphiphilic character. Since BPA and BPF are of lower molecular weights than IN1076 (531 g/mol) they may be less constrained in the polymer matrix meaning that they will likely be much more mobile. The surface activity of PCB would be of interest due to concerns of contamination of food contact polymers exposed to PCB.

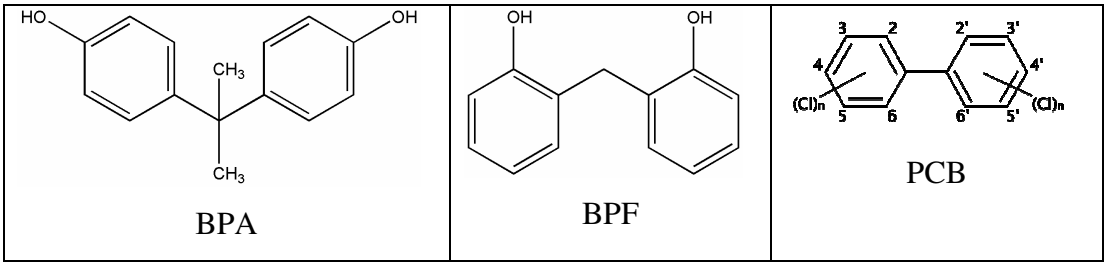

Figure 6.1. BPA, BPF, PCB structures

6.2.2 Permeation Experiments

Continuation of dilute migration experiments is of paramount interest. This work has shown large differences between the permeation of neat DCE through LDPE, and the permeation of DCE from dilute (1% by volume) solutions through LDPE. One quantity of interest is the large differences in the permeation activation energies. A study that determined E_p for solutions having systematically varied DCE concentrations might provide insight into different steps in the permeation process. Migration data from solutions containing amounts of c1,2-DCE point to an initial spike in migration rate before the establishment of slower permeation.

Other experiments of interest include replacing the membrane material with polypropylene, nylon, PET, and other thin polymer films and revisiting neat DCE permeation. LDPE is known as a worst case scenario for migration, so it is possible that the differences in the DCE isomer permeation are magnified. Such studies would test the generality of the findings presented in this work, namely that permeation depends on chemical structure as well as molar mass.

Finally, changing the migrant used for permeation would further improve understanding of the molecular factors responsible for permeation. The three molecules discussed above, BPA, BPF, and PCB, could form the basis of an interesting comparison given their similar sizes and chemical composition. These experiments would also be relevant in terms of comparing experimental migration rates with those predicted through the use of empirical models.[4-7] Research carried out for this thesis made important advances highlighting the role played by molecular structure in determining permeation through thin polymer films. Discoveries regarding solute polarity and solubility suggest a number of other projects that could clarify fundamental underpinnings to mass transport through polymer films and assist policy makers in formulating well-informed regulations.

References

1. Maragou, N. C.; Makri, A.; Lampi, E. N.; Thomaidis, N. S.; Koupparis, M. A., Migration of bisphenol A from polycarbonate baby bottles under real use conditions. *Food Additives and Contaminants* **2008,** 25, (3), 373-383.

2. Munguia-Lopez, E. M.; Gerardo-Lugo, S.; Peralta, E.; Bulmen, S.; Soto-Valdez, H., Migration of bisphenol A (BPA) from can coatings into a fatty food simulant and tuna fish. *Food Additives and Contaminants* **2005,** 22, (9), 892-898.

3. Basic Information: Polychlorinated Biphenyl. http://www.epa.gov/pcbs/pubs/about.htm (August 9, 2008),

4. *Plastic Packaging Materials for Food: Barrier Function, Mass Transport, Quality Assurance and Legislation*. Wiley-VCH: New York, 2000.

5. Begley, T. H.; Castle, L.; Feigenbaum, A.; Franz, R.; Hinrichs, K.; Lickley, T.; Mercea, P.; Milana, M.; O'Brien, A.; Rebre, S.; Rijk, R.; Piringer, O., Evaluation of migration models that might be used in support of regulations for food-contact plastics. *Food Additives and Contaminants* **2005,** 22, (1), 73-90.

6. Brandsch, J.; Mercea, P.; Ruter, M.; Tosa, V.; Piringer, O., Migration modelling as a tool for quality assurance of food packaging. *Food Additives and Contaminants* **2002,** 19, (Supplement), 29-41.

7. Stoffers, N. H.; Stormer, A.; Bradley, E. L.; Brandsch, R.; Cooper, I.; Linssen, J. P. H.; Franz, R., Feasibility study for the development of certified reference materials for specific migration testing. Part 1: Initial migrant concentration and specific migration. *Food Additives and Contaminants* **2004,** 21, (12), 1203-1216.

Appendix 1 Migration though a Saturated LDPE Film

One question that arose during the experiments described in Chapter 4 – migration of DCE isomers from the neat liquid through LDPE and into Miglyol – was whether or not the time lag before observed migration was due to the polymer film first needing to saturate *or* a barrier associated with DCE passing across the DCE/polymer and/or polymer/Miglyol interface. To address this issue, we carried out migration experiments using films that had already been saturated with DCE. Figure A.1.1 compares migration of 1,1-DCE through a normal film and a film pre-saturated with 1,1-DCE. The saturated film had soaked in pure 1,1-DCE overnight in a closed vial. Migration with each film exhibits a delay in the onset of the steady-state as shown by the linear fits at later points in the experiment. The initial measurements for the pre-saturated films exhibit a migration rate slightly faster than the steady state and more overall migration occurs through the pre-saturated film, but the original delay in the onset of detectable migration is present for both films.

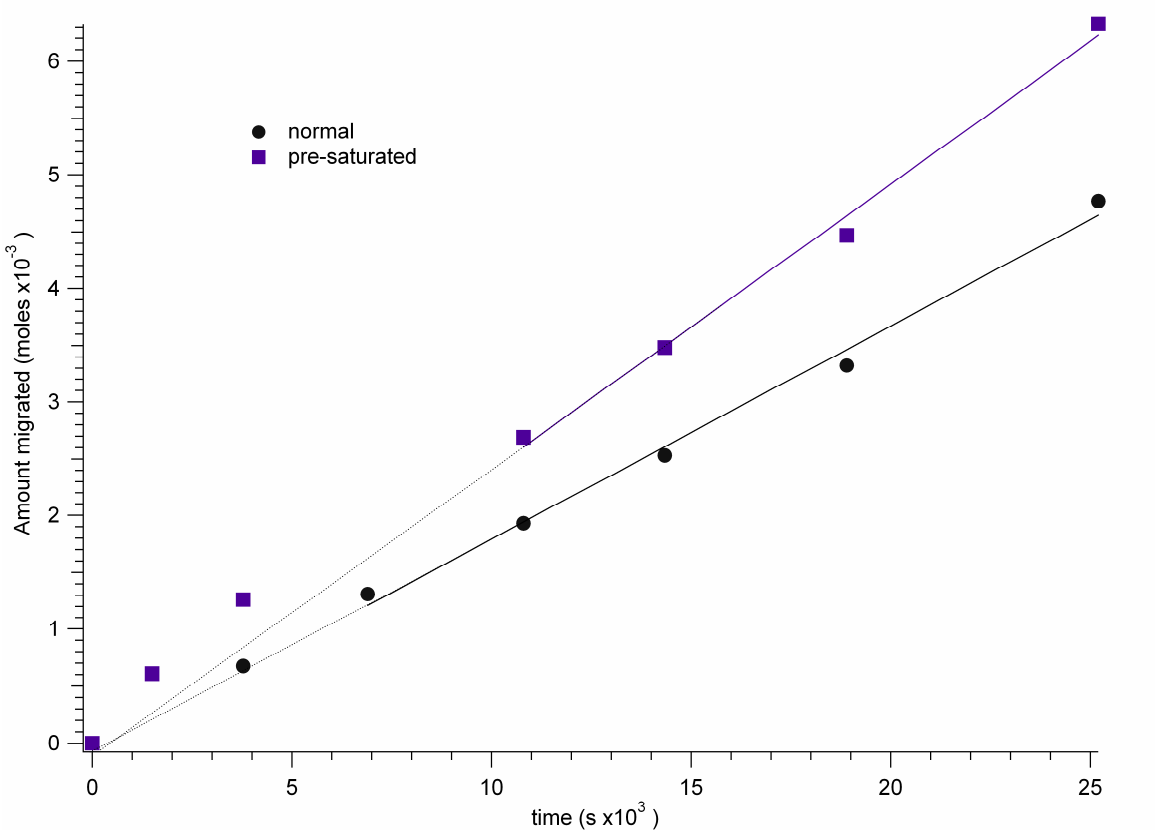

Figure A.1.1. Migration profile of neat 1,1-DCE migrating through LDPE at 20 °C.

A second issue that arose from the migration studies is the influence of film thickness on both the permeability. Experiments using thick films were set up similarly to the neat migration experiments described in Chapter 2, only with the thin (76.2 μm) LDPE film replaced by a thicker (1.02 mm) LDPE film. Thick LDPE permeation experiments were run at 20, 25, and 30°C with neat t1,2-DCE as the donor compound. Migration profiles are shown in Figure A.1.2. Diffusion and Permeation coefficients are summarized in Table A.1.1. Using thick LDPE films, consistent lag times are able to be determined from the migration profile. When using thin LDPE films, lag time analysis yielded inconsistent results as shown in Figure A.1.3. Inconsistencies in the lag time calculation could be a combination of

lack of sensitivity in analytical technique or an interfacial resistance. Notice the diffusion of c1,2-DCE decreases as temperature increases.

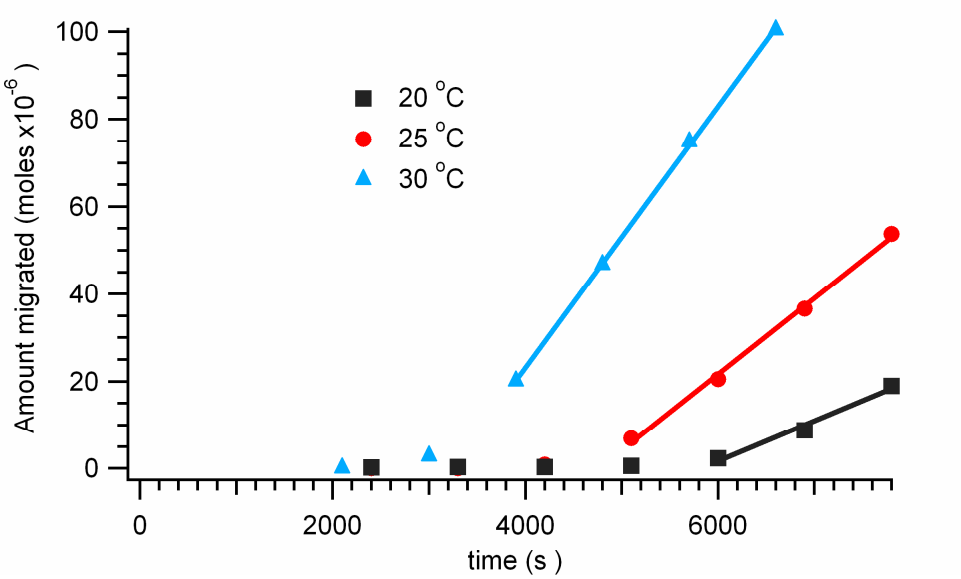

Figure A.1.2. Migration profile of neat t1,2-DCE through thick LDPE (1.02mm) at 20, 25, and 30 °C.

Analyte	Temp (K)	P (cm^2/s *10^8)	D (cm^2/s *10^9)
t1,2-DCE	293.1	7.30	4.87
t1,2-DCE	298.1	17.2	5.89
t1,2-DCE	303.1	32.8	8.16

Table A.1.1. Permeation and diffusion coefficients of t1,2-DCE migration through thick LDPE (1.02mm) at different temperatures.

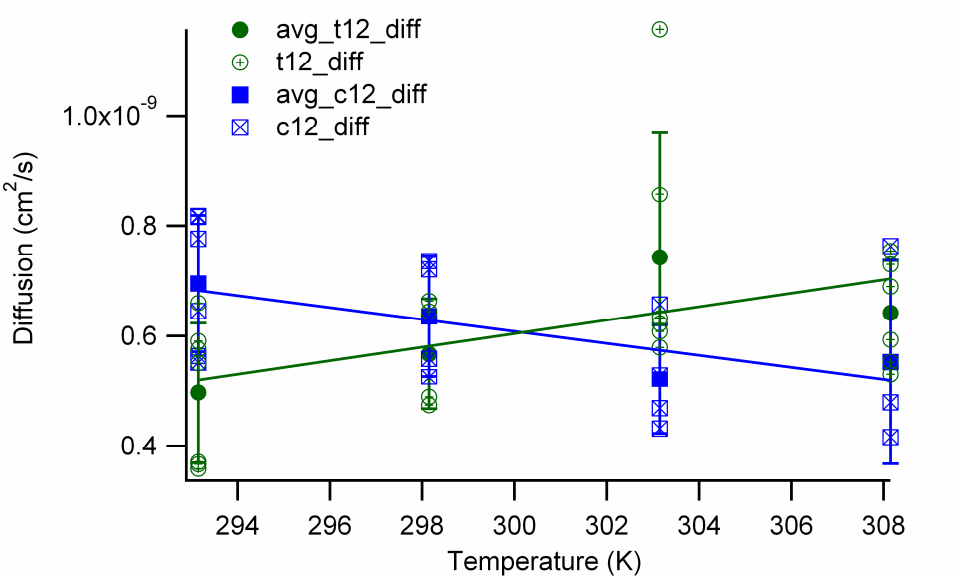

Figure A.1.3. Lag time analysis results for t1,2-DCE and c1,2-DCE migration through thin LDPE (72.6 μm).

Appendix 2 PM-IRRAS of IN1076 Langmuir-Blodgett Film

An enduring question from the studies of antioxidant additive behavior at aqueous vapor interfaces was whether or not the aggregates assumed to form during repeated compressions of the films grew monotonically. To investigate further the properties of IN1076 films formed by repeated compressions, we attempted to deposit these films onto clean silica surfaces and then probe these films spectroscopically. Figure A.2.1 shows PM-IRRAS spectra of IN1076 monolayers after varying numbers of compressions. Films were prepared by making the required number of compressions on the IN1076 monolayer using the trough, then depositing the films at the compressed state onto a glass slide. As illustrated above, the intensity increases as compressions increase. The new addition of a dipper to the trough would provide consistent deposition of the monolayers on the glass slde, and hopefully reproducibility in PM-IRRAS measurements.

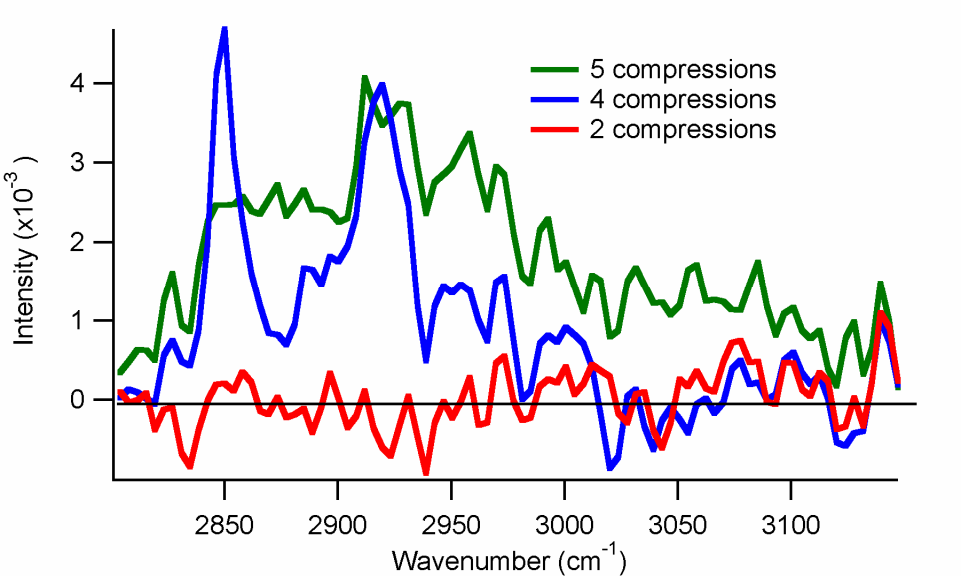

Figure A.2.1. PM-IRRAS spectra of films formed by repeated compressions of IN1076.

Appendix 3 Preliminary Migration Studies

Preliminary migration studies were executed using certified reference polymers (CRMs) obtained from Europe.[1] Studies focused on two materials, CRM1 and CRM5, their properties are summarized in Table A.3.1. Both films contained IN1076 and Irgafos 168 (IF168). Extraction experiments were set up by cutting pieces of the CRMs into 1 cm × 2 cm pieces of the polymers and weighing samples before they were left to soak in a known volume of extraction liquid for a specified period of time at room temperature (~23 ^{o}C). Typically isooctane was used as an extraction liquid.

	Polymer	IN1076 (mg/kg)	IF168 (mg/kg)
CRM1	LDPE	601	536
CRM5	PP	1392	1538

Table A.3.1. Summary of CRMs.

Initially, the concentration of additives that had migrated out of the polymer was monitored periodically using UV/Vis spectroscopy to quantify the concentration of additive in solution. Since IN1076 and IF168 have similar λ_{max} values (~ 280 nm), UV/Vis data only quantified the total amount of migration of additives from the polymer. The absorbance peak was integrated and normalized according to the surface area of the samples, since migration from the polymer will depend on the area exposed to the extracting liquid. Figure A.3.1 shows an extraction experiment that extended over two weeks. Comparing total amount of migration at late times, CRM5 lost more additive than CRM1, which is expected according to the concentration of the additives in the polymer. The behavior at earlier times however, suggested that CRM1 lost additives to solution more quickly than CRM5.

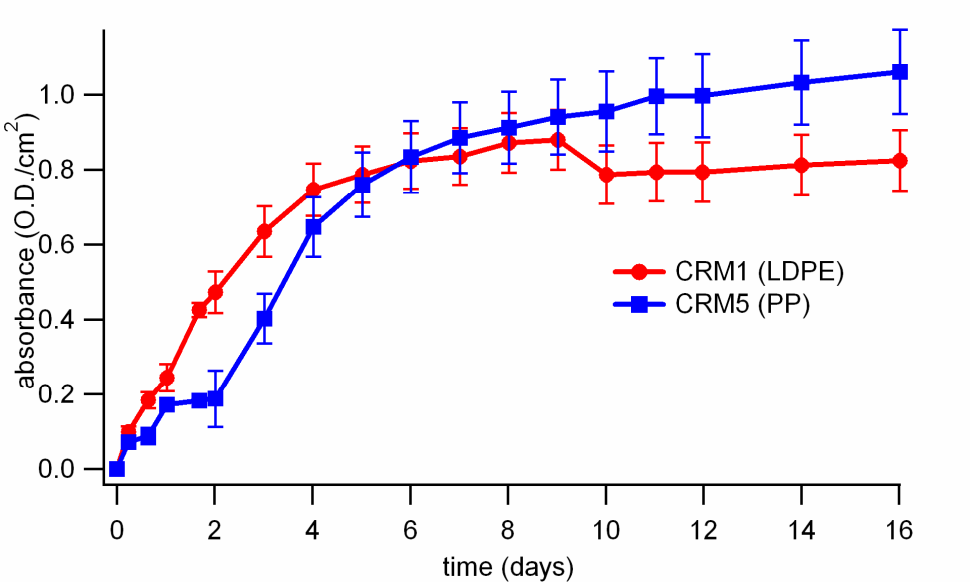

Figure A.3.1. CRM additive loss over two weeks.

Additional short time extractions were carried out to determine if CRM1 was losing more additives than CRM5 at early times. The results are shown in Figure A.3.2. At early times, CRM1 is losing more antioxidant additive than CRM5. However, detection is limited to total amount of migration using UV/Vis. Thus, we decided to take a closer look at the time dependent migration through a "freeze frame" extraction experiment with high performance liquid chromatography to separate IN1076 from IF168 and mass spectrometry detection (HPLC-MSD). A schematic of the freeze frame extraction experiment is shown in Figure A.3.3.

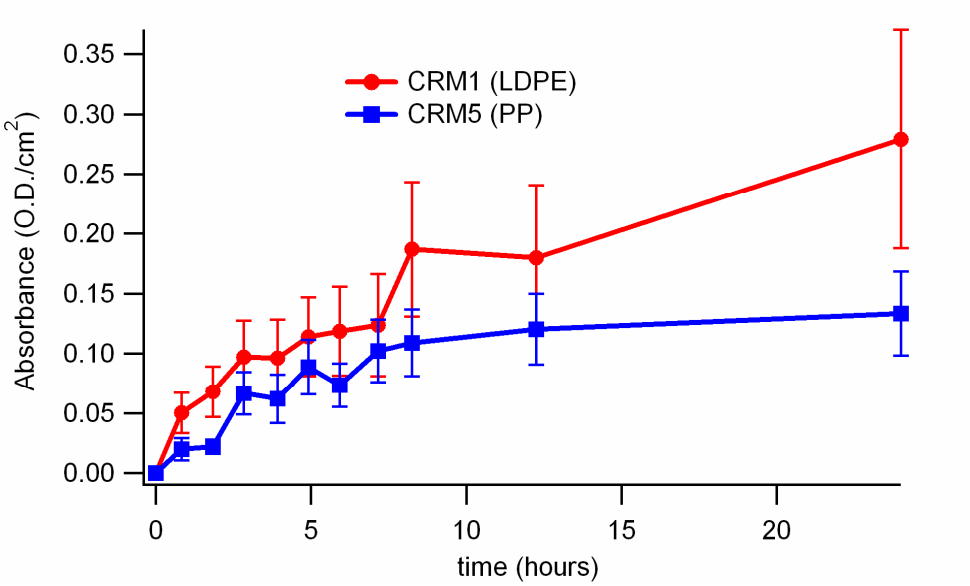

Figure A.3.2. CRM extraction over 24 hours.

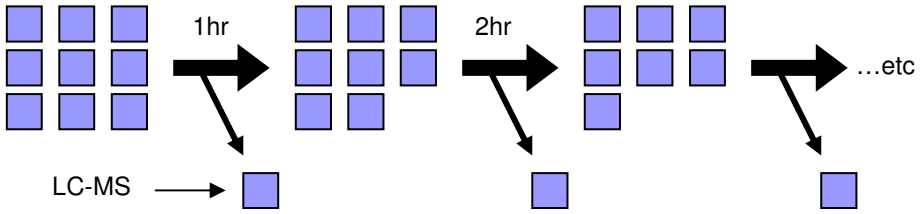

Figure A.3.3. Schematic for freeze frame extraction experiments.

Samples used for the "freeze frame" were weighed and measured, and dropped into a known volume of isooctane. After a specific amount of time, the sample was removed and the extraction liquid saved for later testing via HPLC-MSD. Quantities of IN1076 and IF168 were determined through a Beer's law analysis. Migrant amounts at specific times were normalized based on the surface area of the film used in that sample. Figure A.3.4 shows migration of IN1076 and IF168 from CRM1 and CRM5.

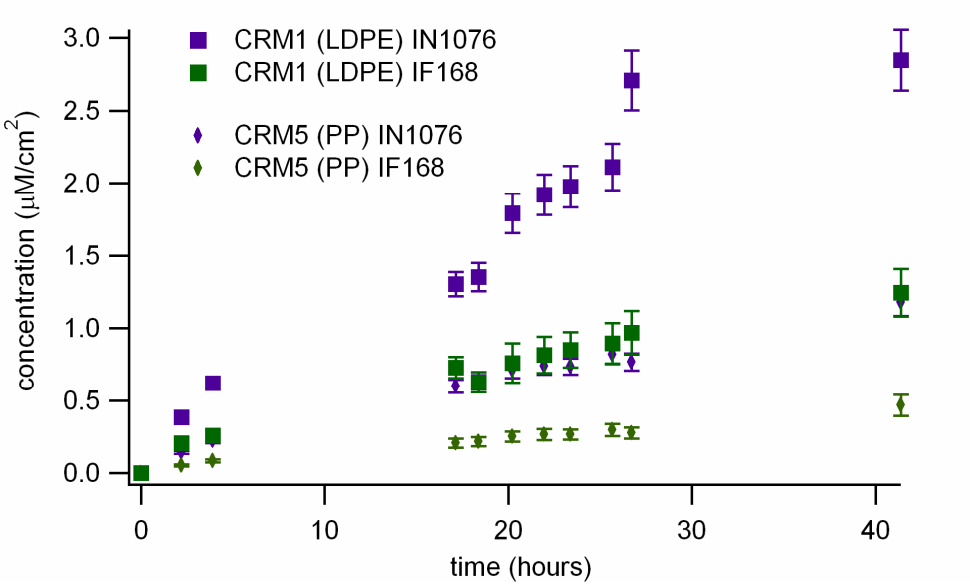

Figure A.3.4 Migration of IN1076 and IF168 from CRM1 and CRM5.

Based on Figure A.3.4 it seemed that in both CRMs, IN1076 was migrating out faster than IF168. Since migration can be correlated to molecular mass this may seem obvious since IN1076 is 531g/mol and IF168 is 646.9 g/mol. To gain a clearer understanding of the migration rates as a function of migrant mass, we compared the ratio of migration (IN1076/IF168) to an absolute ratio (dotted lines) of IN1076/IF168 from a complete extraction of the polymers, shown in Figure A.3.5.

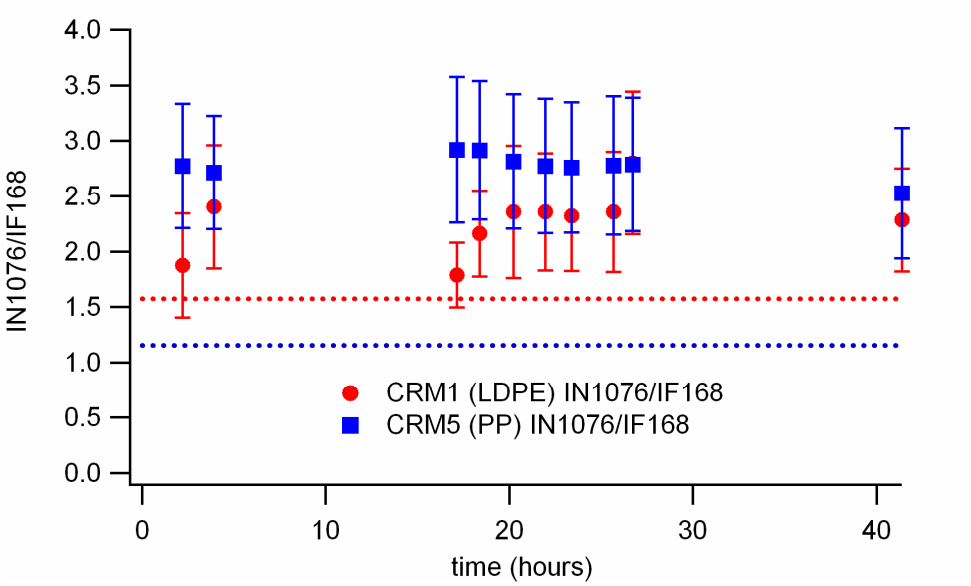

Figure A.3.5. Ratio of migration (IN1076/IF168) from CRM1 and CRM5 compared to an absolute ratio determined from a full extraction of additives from CRMs.

Through the use of a popular migration model we can predict the diffusion of both IN1010 and IF168 from LDPE and PP.[2, 3] The migration of IN1076 from PP was predicted, and compared to the measured values, shown in Figure A.3.5. More IN1076 migration was predicted based on the model compared to the observed experimental IN1076 migration, which is expected since these models are used to set specific migration limits for exposure.[3] We note here the only migrant dependent property used in the empirical models is the molar mass. Time was later spent on the effects of molecular properties on migration.

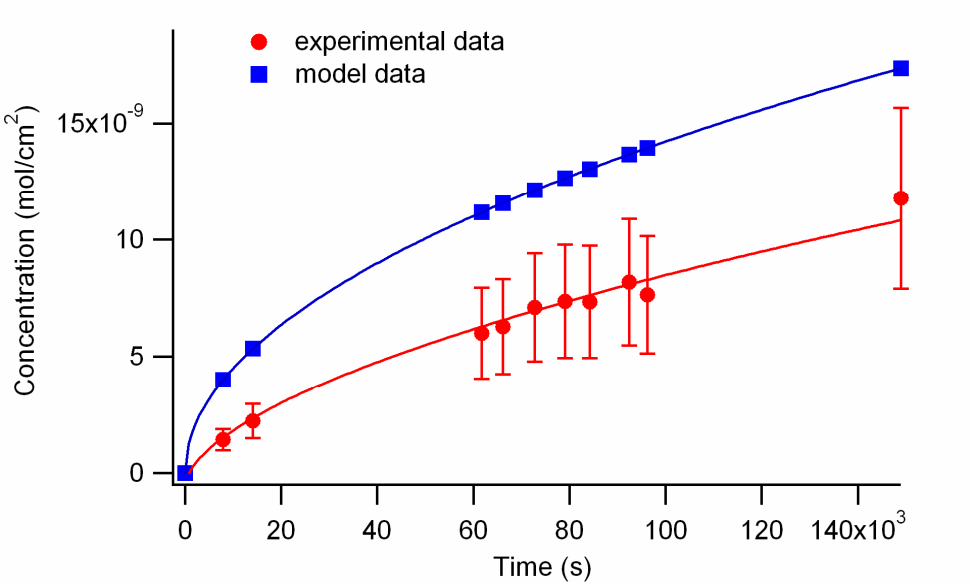

Figure A.3.6. IN1076 estimated migration compared to the experimental migration from CRM5 (PP).

References

1. Stoffers, N. H.; Stormer, A.; Bradley, E. L.; Brandsch, R.; Cooper, I.; Linssen, J. P. H.; Franz, R., Feasibility study for the development of certified reference materials for specific migration testing. Part 1: Initial migrant concentration and specific migration. *Food Additives and Contaminants* **2004**, 21, (12), 1203-1216.

2. Limm, W.; Hollifield, H. C., Effects of temperature and mixing on polymer adjuvant migration to corn oil and water. *Food Additives and Contaminants* **1995**, 12, 609-624.

3. Begley, T.; Castle, L.; Feigenbaum, A.; Franz, R.; Hinrichs, K.; Lickly, T.; Mercea, P.; Milana, M.; O'Brien, A.; Rebre, S.; Rijk, R.; Pringer, O., Evaluation of migration models that might be used in support of regulations for food-contact plastics. *Food Additives and Contaminants* **2005**, 22, (1), 73-90.

References

1. Municipal Solid Waste (MSW): Recycling. (July 14, 2008),

2. Eilperin, J., Compound in Teflon A 'Likely Carcinogen'. *The Washington Post. Washington, D.C.* Jun 29, 2005, 2005, p A.04.

3. Grossman, E., Chemicals May Play Role in Rise in Obesity. *The Washington Post* March 12, 2007, 2007, p A06.

4. Eliperin, J., Harmful Teflon Chemical To Be Eliminated by 2015. *Washington Post* January 26, 2006, p A01.

5. Mishori, R., The Plastics Revolution: It Changed Our World. But Are We Trading Convenience for Safety? *The Wahsington Post* April 22, 2008, 2008, p HE01.

6. Zweifel, H., *Plastics Additives Handbook*. 5th ed.; Hanser: Cincinnati, 2001.

7. Zweifel, H. In *Polymer Durability*, American Chemical Society, Washington, 1996; R. L. Clough, K. T. G., N. C. Billingham, Ed. Washington, 1996.

8. Schwetlick, K., *Pure and Applied Chemistry* **1983,** 55, 1634.

9. Schwetlick, K.; Konig, T.; Ruger, C.; Pointeck, J.; Habicher, W. D., *Polymer Degradation and Stability* **1986,** 55, (97).

10. *Plastic Packaging Materials for Food: Barrier Function, Mass Transport, Quality Assurance and Legislation*. Wiley-VCH: New York, 2000.

11. Mao, G.; Desai, J.; Flach, C. R.; Mendelsohn, R., Structural characterization of the monolayer-multilayer transition in a pulmonary surfactant model: IR studies of films transferred at continuously varying surface pressures. *Langmuir* **2008,** 24, (5), 2025-2034.

12. Sakai, K.; Umezawa, S.; Tamura, M.; Takamatsu, Y.; Tsuchiya, K.; Torigoe, K.; Ohkubo, T.; Yoshimura, T.; Esumi, K.; sakai, H.; Abe, M., Adsorption and micellization behavior of novel gluconamide-type gemini surfactants. *Journal of Colloid and Interface Science* **2008,** 318, 440-448.

13. Kosaka, O.; Iida, S.; Sehgal, P.; Doe, H., Solubilization of endocrine disruptors in micellar media. *Colloid Polymer Science* **2008,** 286, 545-551.

14. Kosaka, O.; Sehgal, P.; Doe, H., Behavior of cationic surfactants micellar solution solubilizing an endocrine disruptor bisphenol A. *Food Hydrocolloids* **2008,** 22, (1), 144-149.

15. Bradley, E. L.; Read, W. A.; Castle, L., Investigation into the migration potential of coating materials from cookware products. *Food Additives and Contaminants* **2007,** 24, (3), 326-335.

16. Bradley, E. L.; Speck, D. R.; Read, W. A.; Castle, L., Method of test and survey of caprolactam migration into foods packaged in nylon-6. *Food Additives and Contaminants* **2004,** 21, (12), 1179-1185.

17. Choi, J. O.; Jitsunari, F.; Asakawa, F.; Lee, D. S., Migration of styrene monomer, dimers and trimers from polystyrene to food simulants. *Food Additives and Contaminants* **2005,** 22, (7), 693-699.

18. Garde, J. A.; Catala, R.; Gavara, R.; Hernandez, R. J., Characterizing the migration of antioxidants from polypropylene into fatty food simulants. *Food Additives and Contaminants* **2001,** 18, (8), 750-762.

19. Limm, W.; Begley, T. H.; Lickly, T.; Hentges, S. G., Diffusion of limonene in polyethylene. *Food Additives and Contaminants* **2006,** 23, (7), 738-746.

20. O'Brien, A.; Cooper, I., Polymer additive migration to foods -- a direct comparison of experimental data and values calculated from migration models for polypropylene. *Food Additives and Contaminants* **2001,** 18, (4), 343-355.

21. Begley, T., Biles, J., Cunningham, C., Pringer, O. , Migration of a UV stabilizer from polyethylene terephthalate (PET) into food simulants. *Food Additives and Contaminants* **2004,** 21, 1007-1014.

22. Dopico-Garcia, M. S., Lopez-Vilarino, J. M., Gonzalez-Rodriguez, M. V. , Effect of temperature and type of food simulant on antioxidant stability. *Journal of Applied Polymer Science* **2006,** 100, 656-663.

23. Helmroth, I. E., Dekker, M., Hankemeier, T., Additive Diffusion from LDPE Slabs into Contacting Solvents as a Function of Solvent Absorption. *Journal of Applied Polymer Science* **2003,** 90, 1609-1617.

24. Limm, W., Hollifield. H. C. , Effects of temperature and mixing on polymer adjuvant migration to corn oil and water. *Food Additives and Contaminants* **1995,** 12, 609-624.

25. Vitrac, O., Mougharbel, A., Feigenbaum, A. , Interfacial mass transport properties wich control the migration of packaging constituents into foodstuffs. *Journal of Food Engineering* **2007, 79**, (3), 1048-1064.

26. O'Brien, A.; Cooper, I., Polymer additive migration into foods -- a direct comparison of experimental data and values calculated from migration models for polypropylene. *Food Additives and Contaminants* **2001,** 18, (4), 343-355.

27. Lundback, M.; Hedenqvist, M. S.; Mattozzi, A.; Geede, U. W., Migration of phenolic antioxidants from linear and branched polyethylene. *Polymer Degradation and Stability* **2006,** 91, 1571-1580.

28. Rawls, A. S.; Hirt, D. E.; Havens, M. R.; Roberts, W. P., Evaluation of surface concentration of erucamide in LLDPE films. *Journal of Vinyl and Additive Technology* **2002,** 8, 130-138.

29. Spatafore, R.; Pearson, L. T., *Polymer Engineering and Science* **1991,** 31, 1610-1617.

30. Schwope, A. D.; Goydan, R.; Reid, R. C.; Krishnamurthy, S., Sate-of-the-Art Review of Permeation Testing and the Interpretation of Its Results. *American Industrial Hygiene Association Journal* **1988,** 49, (11), 557-565.

31. O'Callaghan, K.; Fredericks, P. M.; Bromwich, D., Evaulation of Chemical Protective Clothing by FT-IR/ATR Spectroscopy. *Applied Spectroscopy* **2001,** 55, (5), 555-562.

32. Britton, L. N.; Ashman, R. B.; Aminabhavi, T. M.; Cassidy, P. E., Permeation and Diffusion of Enviornmental Pollutants through Flexible Polymers. *Journal of Applied Polymer Science* **1989,** 38, 227-236.

33. Saleem, M.; Asfour, A.-F. A.; Kee, D. D., Diffusion of Organic Penetrants through Low Density Polyethylene (LDPE) Films: Effect of Size and Shape of the Penetrant Molecules. *Journal of Applied Polymer Science* **1989,** 37, 617-625.

34. Begley, T. H.; Castle, L.; Feigenbaum, A.; Franz, R.; Hinrichs, K.; Lickley, T.; Mercea, P.; Milana, M.; O'Brien, A.; Rebre, S.; Rijk, R.; Piringer, O., Evaluation

of migration models that might be used in support of regulations for food-contact plastics. *Food Additives and Contaminants* **2005,** 22, (1), 73-90.

35. Brandsch, J.; Mercea, P.; Ruter, M.; Tosa, V.; Piringer, O., Migration modelling as a tool for quality assurance of food packaging. *Food Additives and Contaminants* **2002,** 19, (Supplement), 29-41.

36. Stoffers, N. H.; Brandsch, R.; Bradley, E. L.; Cooper, I.; Dekker, M.; Stormer, A.; Franz, R., Feasibility study for the development of certified reference materials for specific migration testing: Part 2: Estimation of diffusion parameters and comparison of experimental and predicted data. *Food Additives and Contaminants* **2005,** 22, (2), 173-184.

37. Begley, T. H.; Hsu, W.; Noonan, G.; Diachenko, G., Migration of fluorochemical paper additives from food-contact paper into foods and food simulants. *Food Additives and Contaminants* **2007,** 25, (3), 384-392.

38. Begley, T. H.; White, K.; Honigfort, P.; Twaroski, M. L.; Neches, R.; Walker, R. A., Perfluorochemicals: Potential sources of and migration from food packaging. *Food Additives and Contaminants* **2005,** 22, (10), 1023-1031.

39. Begley, T. H.; Gay, M. L.; Hollifield, H. C., Determination of the migrants in and migration from nylon food packaging. *Food Additives and Contaminants* **1995,** 12, 671-676.

40. Biles, J. E.; McNeal, T. P.; Begley, T. H.; Hollifield, H. C., Determination of bisphenol A in reusable polycarbonate food-contact plastics and migration to food-simulating liquids. *Journal of Agricultural and Food Chemistry* **1997,** 45, 3541-3544.

41. Brede, C.; Fjeldal, P.; Skjevrak, I.; Herikstad, H., Increased migration levels of bisphenol A from polycarbonate baby bottles after dishwashing, boiling and brushing. *Food Additives and Contaminants* **2003,** 20, 684-689.

42. Franz, R.; Welle, F., Migration measurement and modelling from poly(ethylene terephthalate) (PET) into soft drinks and fruit juices in comparison with food simulants. *Food Additives and Contaminants* **2008,** iFirst.

43. Begley, T. H.; Biles, J. E.; Cunningham, C.; Piringer, O., Migration of a UV stabilizer from polyethylene terephthalate (PET) into food simulants. *Food Additives and Contaminants* **2004,** 21, 1007-1014.

44. Consumer Factsheet on: 1,2-dichloroethylene. http://www.epa.gov/OGWDW/dwh/c-voc/12-dich2.html (Febuary 28th, 2008),

45. Consumer Factsheet on: 1,1-dichloroethylene. http://www.epa.gov/safewater/dwh/c-voc/11-dichl.html (Febuary 28th, 2008),

46. Huang, J.-C.; Liu, H.; Liu, Y., Diffusion in Polymers with Concentration Dependent Diffusivity. *International Journal of Polymeric Material* **2001,** 49, 15-24.

47. Grossman, R. B., *The Art of Writing Reasonable Organic Reaction Mechanisms*. Second ed.; Springer: New York, 2003.

48. Esenturk, O.; Walker, R. A., Surface Structure at hexadecane and Halo-hexadecane Liquid/Vapor Interfaces. *Journal of Physical Chemistry B* **2004,** 108, (30), 10631-10635.

49. Richter, L. J.; Petralli-Mallow, T. P.; Stephenson, J. C., Vibrationally resolved sum-frequency generation with broad-bandwidth inf rared pulses *Optics Letters* **1998,** 23, 1594-1596.

50. Richmond, G. L., Molecular bonding and interactions at aqueous surfaces as probed by vibrational sum frequency spectroscopy. *Chemical Reviews* **2002,** 102, (8), 2693-2724.

51. Can, S. Z.; Mago, D. D.; Walker, R. A., Structure and Organization of Hexadecanol Isomers. *Langmuir* **2006, 22**, 8043-8049.

52. Can, S. Molecular Structure and Organization in Organic Monolayers at Aqueous/Vapor Interfaces. PhD, University of Maryland, College Park, 2008.

53. *CRC Handbook of Chemistry and Physics*. 77 ed.; CRC Press, Inc.: New York, 1996.

54. Beyer, H.; Walter, W., *Organic Chemistry: A Comprehensive Degree Text and Source Book*. Albion Publishers: Chichester, 1997.

55. Howe, J. A.; Flygare, W. H., Strong Field Stark Effect. *The Journal of Chemical Physics* **1962,** 36, (3), 650-652.

56. *Lange's Handbook of Chemistry*. 15 ed.; McGraw-Hill, Inc.: New York, 1999.

57. Zweifel, H., *Stabilization of Polymeric Materials*. Springer: Heidelberg 1997.

58. Spatafore, R. a. P., L. T. , *Polymer Engineering and Science* **1991,** 31, 1610-1617.

59. Rawls, A. S., Hirt, D. E., Havens, M. R., Roberts, W. P. , Evaluation of surface concentration of erucamide in LLDPE films. *Journal of Vinyl and Additive Technology* **2002,** 8, 130-138.

60. O'Brien, A., Cooper, I. , Practical experience in the use of mathematical models to predict migration of additives from food-contact polymers. *Food Additives and Contaminants* **2002,** 19, Suppliment 63-72.

61. Limm, W., Hollifield, H. C. , Modelling of additive diffusion in polyolefins. *Food Additives and Contaminants* **1996,** 13, 949.

62. Tehrany, E. A., Desobry, S., Fournier, F. , Simple method to calculate partition coefficient of migrant in food simulant/polymer system. *Journal of Food Engineering* **2006,** 77, 135-139.

63. Olsen, G. W., Burris, J. M., Burlew, M. M., Mandel, J. H., Epidemiologic assessment of worker serum perfluorooctanesulfonate (PFOS) and perfluorooctanoate (PFOA) concentrations and medical surveillance examinations. *Journal of Occupational and Environmental Medicine* **2003,** 45, (3), 260-270.

64. Eilperin, J., Compound in Teflon A 'Likely Carcinogen'. *The Washington Post. Washington, D.C.* Jun 29, 2005, 2005, p pg. A.04.

65. Zweifel, H., *Polymer Durability*. ACS: Washington, 1996.

66. Schwetlick, K., Konig, T., Ruger, C., Pointeck, J., Habicher, W. D. , *Polymer Degradation and Stability* **1986,** 55, (97).

67. O'Brien, A., Cooper, I., Polymer additive migration into foods -- a direct comparison of experimental data and values calculated from migration models for polypropylene. *Food Additives and Contaminants* **2001,** 18, (4), 343-355.

68. Begley, T., Castle, L., Feigenbaum, A., Franz, R., Hinrichs, K., Lickly, T., Mercea, P., Milana, M., O'Brien, A., Rebre, S., Rijk, R., Pringer, O. , Evaluation of

migration models that might be used in support of regulations for food-contact plastics. *Food Additives and Contaminants* **2005,** 22, (1), 73-90.

69. Stoffers, N. H., Stormer, A., Bradley,E.L., Brandsch, R., Cooper, I., Linssen, J. P. H., Franz, R. , Feasibility study for the development of certified reference materials for specific migration testing. Part 1: Initial migrant concentration and specific migration. *Food Additives and Contaminants* **2004,** 21, (12), 1203-1216.

70. Stoffers, N. H., Brandsch, R., Bradley, E. L., Cooper, I., Dekker, M., Stormer, A., Franz, R., Feasibility study for the development of certified reference materials for specific migration testing. Part 2: Estimation of diffusion parameters and comparison of experimental and predicted data. *Food Additives and Contaminants* **2005,** 22, (2), 173-184.

71. Limm, W., Begley, T.H., Lickly, T., Hentges, S.G. , Diffusion of limonene in polyethylene. *Food Additives and Contaminants* **2006,** 23, (7), 738-746.

72. Vitrac, O., Mougharbel, A., Feigenbaum, A. , Interfacial mass transport properties with control the migration of packaging constituents into foodstuffs. *Journal of Food Engineering* **2006, ASAP**.

73. Tehrany, E. A., Desobry, S. , Partition coefficients in food/packaging systems: a review. *Food Additives and Contaminants* **2004,** 21, (12), 1186-1202.

74. Helmroth, I. E., Dekker, M., Hankemeier, T., Influence of solvent absorption on the migration of Irganox 1076 from LDPE. *Food Additives and Contaminants* **2002,** 19, 176-183.

75. Pospisil, J., Nespurek, S., Sweifel, H., The role of quinone methides in thermostabilization of hydrocarbon polymers - I. Formation and reactivity of quinone methides. *Polymer Degradation and Stability* **1996,** 54, 7-14.

76. Pospisil, J., Nespurek, S., Sweifel, H., The role of quinone methides in thermostabilization of hydrocarbon polymers - II. Properties and activity mechanisms. *Polymer Degradation and Stability* **1996,** 54, 15-21.

77. Gaines, G. L., Jr., *Insoluble Monolayers at Liquid-Gas Interfaces*. Interscience Publishers: New York, 1966.

78. Grigoriev, D. O. L., M. E.; Michel, M.; Miller, R., Component separation in spread sodium stearoyl lactylate (SSL) monolayers induced by high surface pressure. *Colloids and Surfaces A* **2006,** 286, 57-61.

79. Liang, Y.; Wu, Z.; Wu, S., Monolayer Behavior and LB Film Structure of Poly(2-methoxy-5-(n-hexadecyloxy)-p-phenylene vinylene). *Langmuir* **2001,** 17, 7267-7273.

80. Liou, S. H.; Hsu, W. P.; Lee, Y. L., Monolayer characteristics of stereoregular PMMA at the air/water interface. *Applied Surface Science* **2006,** 252, 4312-4320.

81. Ourisson, G.; Ariga, K.; Yuki, H.; Kikuchi, J.; Dannemuller, O.; Albrecht-Gary, A. M.; Nakatani, Y., Monolayer Studies of Single-Chain Polyprenyl Phosphates. *Langmuir* **2005,** 21, 4578-4583.

82. Gaines, G. L. J., Monolayers of Polymers. *Langmuir* **1991,** 7, 834-839.

83. Esker, A. R., Zhang, L.H., Olsen, C. E., No, K., Yu, H., Static and Dynamic Properties of Calixarene Monolayers at the Air/Water Interface. 1. pH Effects with p-Dioctadecanoylcalix[4]arene. *Langmuir* **1999,** 15, (5), 1716-1724.

84. Zhang, L. H., Esker, A. R., No, K., Yu, H., Static and Dynamic Properties of Calixarene Monolayers at the Air/Water Interface. 2. Effects of Ionic Interactions with p-Dioctadecanoylcalix[4]arene. *Langmuir* **1999,** 15, (5), 1725-1730.

85. MacPhail, R. A., Strauss, H. L., Snyder, R. G., Elliger, C. A., C-H Stretching Modes and the Structure of n-Alkyl Chains 2. Long, All-Trans Chains. *Journal of Physical Chemistry* **1984,** 88, 334-341.

86. Raymond, E. A., Tarbuck, T. L., Richmond, G. L., Isotopic Dilution Studies of the Vapor/Water Interface as Investigated by Vibrational Sum-Frequency Spectroscopy. *Journal of Physical Chemistry B* **2002,** 106, (11), 2817-2820.

87. Can, S. Z., Mago, D. D., Walker R. A., Structure and Organization of Hexadecanol Isomers. *Langmuir* **2006, 22**, 8043-8049.

88. *Chem3D Pro 8.0*, Chem3D Pro 8.0; CambridgeSoft Corporation: Cambridge, MA, 1985-2003.

89. Lopez-Cervantes, J.; Paserio-Losada, P., Determination of bisphenol A in, and its migration from, PVC stretch film used for food packaging. *Food Additives and Contaminants* **2003,** 20, (6), 596-606.

90. Dopico-Garcia, M. S.; Lopez-Vilarino, J. M.; Gonzalez-Rodriguez, M. V., Antioxidant Content of and Migration from Commercial Polyethylene, Polypropylene, and Polyvinyl Chloride Packages. *Journal of Agricultural and Food Chemistry* **2007,** 55, 3225-3231.

91. Matsuga, M.; Kawamura, Y.; Sugita-Konishi, Y.; Hara-Kudo, Y.; Takatori, K.; Tanamoto, K., Migration of formaldehyde and acetaldehyde into mineral water in

polyethylene terephthalate (PET) bottles. *Food Additives and Contaminants* **2006,** 23, (2), 212-218.

92. Haldimann, M.; Blanc, A.; Dudler, V., Exposure to antimony from polyethylene terephthalate (PET) trays used in ready-to-eat meals. *Food Additives and Contaminants* **2007,** 24, (8), 860-868.

93. Limm, W.; Hollifield, H. C., Effects of temperature and mixing on polymer adjuvant migration to corn oil and water. *Food Additives and Contaminants* **1995,** 12, 609-624.

94. Reynier, A.; Dole, P.; Humbel, S.; Feigenbaum, A., Diffusion Coefficients of Additives in Polymers 1. Correlation with Geometric Parameters. *Journal of Applied Polymer Science* **2001,** 82, 2422-2433.

95. Feigenbaum, A.; Dole, P.; Aucejo, S.; Dainelli, D.; Garcia, C. D. L. C.; Hankemeier, T.; N'gono, Y.; Papaspyrides, C. D.; Paserio, P.; Pastorelli, S.; Pavlidou, S.; Pennarun, P. Y.; Saillard, P.; Vidal, L.; Vitrac, O.; Voulzatis, Y., Functional barriers: Properties and evaluation. *Food Additives and Contaminants* **2005,** 22, (10), 956-967.

96. Moisan, J. Y., Additive diffusion in polyethylene I. Influence and nature of additives. *European Polymer Journal* **1980,** 16, 979-987.

97. Limm, W.; Hollifield, H. C., Modelling of additive diffusion in polyolefins. *Food Additives and Contaminants* **1996,** 13, 949.

98. Dole, P.; Voulzatis, Y.; Vitrac, O.; Reynier, A.; Hankemeier, T.; Aucejo, S.; Feigenbaum, A., Modelling of migration from multi-layers and functional barriers:

Estimation of parameters. *Food Additives and Contaminants* **2006,** 23, (10), 1038-1052.

99. Garbarini, G. R.; Eaton, R. F.; Kwei, T. K.; Tobolsky, A. V., Diffusion and Reverse Osmosis through Polymer Membranes. *Journal of Chemical Education* **1971,** 48, 226.

100. Vergnaud, J. M., *Liquid transport processes in polymeric materials: modeling and industrial applications*. Prentice Hall: Englewood Cliffs, NJ, 1991.

101. Crank, J.; Park, G. S., *Diffusion in Polymers*. Academic Press Inc.: London, 1968.

102. Crank, J., *The Mathematics of Diffusion*. 2nd ed.; Oxford University Press: New York, 1975.

103. Al-Malaika, S.; Goonetileka, M. D. R. J.; Scott, G., Migration of 4-substituted 2-hydroxy benzophenones in low density polyethylene: Part1- Diffusion characteristics. *Polymer Degradation and Stability* **1991,** 32, (2), 231-247.

104. Berens, A. R.; Hopfenberg, H. B., Diffusion of organic vapors at low concentrations in glassy PVC, polystyrene, and PMMA. *Journal of Membrane Science* **1982,** 10, 283-303.

105. Moisan, J. Y., *European Polymer Journal* **1981,** 8, 857-864.

106. Piergiovanni, L.; Fava, P.; Schiraldi, A., Study of Diffusion through LDPE film of Di-*n*-butyl phthalate. *Food Additives and Contaminants* **1999,** 16, (8), 353-359.

107. Aminabhavi, T. M.; Naik, H. G., Molegular migration of low sorbing organic liquids into polymeric geomembranes. *Polymer International* **1999,** 48, 373-381.

108. Aminabhavi, T. M.; Phayde, H. T. S., Sorption, Desorption, Resorption, Redesorption, and Diffusion of Haloalkanes into Polymeric Blend of Ethylene-Propylene Random Copolymer and Isotatic Polypropylene. *Journal of Applied Polymer Science* **1995,** 57, 1419-1428.

109. Kariduraganavar, M. Y.; Kulkarni, S. B.; Kulkarni, S. S.; Kittur, A. A., Studies on Molecular Transport of n-Alkanes Through Poly(tetrafluoroethylene-co-propylene) Elastomeric Membrane. *Journal of Applied Polymer Science* **2006,** 101, 2228-2235.

110. Kulkarni, S. B.; Karidurganavar, M. Y.; Aminabhavi, T. M., Sorption, Diffusion, and Permation of Esters, Aldehydes, Ketones, and Aromatic Liquids into Tetrafluoroethylene/Propylene at 30, 40, and 50^{o}C. *Journal of Applied Polymer Science* **2003,** 89, 3201-3209.

111. Schwarz, T.; Steiner, G.; Koppelmann, J., Measurement of Diffusion of Antioxidants in Isotactic Polypropylene by Isothermal Differential Thermal Analysis. *Journal of Applied Polymer Science* **1989,** 38, 1-7.

112. Harogoppad, S. B.; Aminabhavi, T. M., Diffusion and Sorption of Organic Liquids through Polymer Membranes. 5. Neoprene, Styrene-Butadiene-Rubber, Ethylene-Propylene-Diene Terpolymer, an dNatural Rubber versus Hydrocarbons (C_8-C_{16}). *Macromolecules* **1991,** 21, 2598-2605.

113. Gossett, J. M., Measurement of Henry's law constants for C1 and C2 chlorinated hydrocarbons. *Environmental Science and Technology* **1987,** 21, 202-208.

114. Maragou, N. C.; Makri, A.; Lampi, E. N.; Thomaidis, N. S.; Koupparis, M. A., Migration of bisphenol A from polycarbonate baby bottles under real use conditions. *Food Additives and Contaminants* **2008,** 25, (3), 373-383.

115. Munguia-Lopez, E. M.; Gerardo-Lugo, S.; Peralta, E.; Bulmen, S.; Soto-Valdez, H., Migration of bisphenol A (BPA) from can coatings into a fatty food simulant and tuna fish. *Food Additives and Contaminants* **2005,** 22, (9), 892-898.

116. Gerald. L. Kennedy, J.; Butenhoff, J. L.; Olsen, G. W.; O'Connor, J. C.; Seacat, A. M.; Perkins, R. G.; Biegel, L. B.; Murphy, S. R.; Farrar, D. G., The Toxicology of Perfluorooctanoate. *Critical Reveiws in Toxicology* **2004,** 34, (4), 351-384.

117. Begley, T. H.; Castle, L.; Feigenbaum, A.; Franz, R.; Hinrichs, K.; Lickly, T.; Mercea, P.; Milana, M.; O'Brien, A.; Rebre, S.; Rijk, R.; Piringer, O., Evaluation of migration models that might be used in support of regulations for food-contact plastics. *Food Additives and Contaminants* **2005,** 22, (1), 73-90.

118. Olsen, G. W.; Burris, J. M.; Burlew, M. M.; Mandel, J. H., Epidemiologic assessment of worker serum perfluorooctanesulfonate (PFOS) and perfluorooctanoate (PFOA) concentrations and medical surveillance examinations. *Journal of Occupational and Environmental Medicine* **2003,** 45, (3), 260-270.

119. Stoffers, N. H.; Stormer, A.; Bradley, E. L.; Brandsch, R.; Cooper, I.; Linssen, J. P. H.; Franz, R., Feasibility study for the development of certified reference materials for specific migration testing. Part 1: Initial migrant concentration and specific migration. *Food Additives and Contaminants* **2004,** 21, (12), 1203-1216.

120. Chao, K. P.; Hsu, Y. P.; Chen, S. Y., Permeation of aromatic solvent mixtures through nitrile protective gloves. *Journal of Hazardous Materials* **2008,** 153, (3), 1059-1066.

121. Lind, M. L.; Johnsson, S.; Meding, B.; Bowman, A., Permeability of hair dye compounds p-phenylenediamine, toluene-2,5-diaminesulfate and resorcinol through protective gloves in hairdressing. *Annals of Ocupational Hygiene* **2007,** 51, (5), 479-485.

122. Makela, E. A.; Vainiatlo, S.; Peltonen, K., The permeability of surgical gloves to seven chemicals commonly used in hospitals. *Annals of Occupational Hygiene* **2003**.

123. Chao, K. P.; Lee, P. H.; Wu, M. J., Organic solvents permeation through protective nitrile gloves. *Journal of Hazardous Materials* **2003,** 99, (2), 191-201.

124. Daugherty, M. L.; Watson, A. P.; Tuan, V. D., Currently available permeability and breakthrough data characterizing chemical warfare agents and their simulants in civilian protective clothing materials. *Journal of Hazardous Materials* **1992,** 30, (3), 243-267.

125. Aminabhavi, T. M.; Harlapur, S. F.; Balundgi, R. H.; Ortego, J. D., An investigation of the long-term sorption kinetics and diffusion anomalies of chloroalkanes into tetrafluoroethylene/propylene copolymer membranes at 30, 45, and 60^{o}C. *Polymer* **1998,** 39, (5), 1067-1074.

126. Stoffers, N. H.; Brandsch, R.; Bradley, E. L.; Cooper, I.; Dekker, M.; Stormer, A.; Franz, R., Feasibility study for the development of certified reference materials for specific migration testing. Part 2: Estimation of diffusion parameters and

comparison of experimental and predicted data. *Food Additives and Contaminants* **2005,** 22, (2), 173-184.

127. Basic Information: Polychlorinated Biphenyl. http://www.epa.gov/pcbs/pubs/about.htm (August 9),

128. Begley, T.; Castle, L.; Feigenbaum, A.; Franz, R.; Hinrichs, K.; Lickly, T.; Mercea, P.; Milana, M.; O'Brien, A.; Rebre, S.; Rijk, R.; Pringer, O., Evaluation of migration models that might be used in support of regulations for food-contact plastics. *Food Additives and Contaminants* **2005,** 22, (1), 73-90.